2023

Volume : 5
Issue : 2

Ikonion Journal of MATHEMATICS

https://dergipark.org.tr/ikjm
ISSN: 2687-6531

Volume : 5
Issue : 2

2023
https://dergipark.org.tr/en/pub/ikjm

IKONION

JOURNAL OF MATHEMATICS

ISSN: 2687-6531

CONTENTS

Ikonion Journal of Mathematics
https://dergipark.org.tr/tr/pub/ikjm
Research Article
Open Access
https://doi.org/10.54286/ikjm.1319223

ISSN: 2687-6531

A Note on The Maximum Circle Inverses of Lines in The Maximum Plane

Süheyla Ekmekçi [1*]

Keywords:
Image of the line under inversion ,
Inversion in maximum circle,
Maximum distance.

Abstract — In this study, the images of lines under inversion in maximum circle are analytically examined. It is observed that the image of line not passing through the center of the inversion is not a maximum circle, but the closed curve containing at least one parabola arc. Some properties regarding the images of lines are introduced. Then, the images of line segments are examined according to the positions of their end points. In addition, it is seen that the inversion in maximum circle transforms the pencil of parallel lines (except line passing the center) to the set of the closed curves passing the center of inversion. Also, the images of the concurrent lines under inversion with respect to a maximum circle are considered and the results are presented.

Subject Classification (2020): 51B20; 51F99; 51K99.

1. Introduction and Preliminaries

In the real plane and space, the distance between two points is measured in various ways using different distance functions. The most well-known distance functions include the Euclidean distance, the maximum distance, the taxicab distance. The analytical planes equipped with these distance functions are the non-Euclidean geometries. There have been many studies that contributed to the literature in non-Euclidean planes and spaces, [1-4,6,12,21]. Maximum distance, also known as the Chebyshev distance or L_∞-distance (the limit of the L_p-distances when $p \to \infty$), is a way of measuring the distance between any two points. In analytical plane, the maximum distance between two points $A_1 = (x_1, y_1)$ and $A_2 = (x_2, y_2)$ is given by $d_M(A_1, A_2) = \max\{|x_1 - y_1|, |x_2 - y_2|\}$. Its simple formula and intuitive interpretation make it a useful tool in computer science and engineering applications, especially when dealing with problems that involve movement in a grid or lattice.

Inversion in a circle is a geometric transformation such that a point in analytical plane invert another point. Apollonoius of Perga introduced the inversion in circle in his work with the title "Plane Loci". In the 1830s, Steiner studied the inversion in circle, systematically. Many researchers have studied the inversions in circle and contributed to them development since then, [7]. Moreover, inversion maps in an elipse, a sphere, an ellipsoid, parallel lines, central cones, star shape sets were defined and introduced, [8],[11],[18-20]. Besides, inversions with respect to a circle and a sphere in some non-Euclidean geometries such as the taxicab geometry, the Chinese Checkers geometry, the maximum

* sekmekci@ogu.edu.tr
[1] Department of Mathematics and Computer Science, Faculty of Science, Eskişehir Osmangazi University, Eskişehir, Turkey.
Article History: Received: 23.06.2023 — Accepted: 21.08.2023 — Published: 05.09.2023

geometry were defined and their basic properties were given, [5], [9], [10], [14-17], [22]. In this article, the images of lines under inversion in maximum circle have been analytically examined. It has been observed that the image of line not passing through the center of the inversion is not a maximum circle, but the closed curve. Properties regarding their images as the position of lines have been introduced. Then, the images of line segments have been examined according to the fact that the end points of them lie in the regions determined by the separator lines passing through the center of inversion. In addition, it has been seen that the inversion in maximum circle transforms the pencil of parallel lines (except line passing the center) to the set of the closed curves passing the center of inversion. Furthermore, the images of the concurrent lines under inversion with respect to a maximum circle have been examined and the results were presented.

In sequel, the some definitions, concepts and theorems required for this study are summarized as the following:

Definition 1.1. Let A_1 and A_2 be two points whose coordinates are (x_1, y_1) and (x_2, y_2) in analytical plane, respectively. The maximum distance between these points is

$$d_M(A_1, A_2) = \max\{|x_1 - y_1|, |x_2 - y_2|\}.$$

It is clear by definition 1.1 that the maximum distance between these points is equal to the greatest of the lengths of the line segments parallel to the coordinates axes in the right triangle with the hypotenuse A_1A_2.

The maximum plane is the analytical plane endowed with the maximum distance and symbolized by $\mathbb{R}^2_{\mathbf{M}}$. The maximum plane closely resembles the Euclidean plane with the exception of its distance measurement. While the points and lines of the maximum plane are the same as the Euclidean plane, and the angles are measured the same way as the Euclidean plane, the defining characteristic lies in its distance function. Krause classified lines depending on their slope as the following definition:

Definition 1.2. Let m be the slope of the line l in maximum plane. The line l is called the steep line, the gradual line and the separator line in the cases of $| m |>1$, $| m |<1$ and $| m |=1$, respectively. In the special cases that the line l is parallel to x-axis or y-axis, l is named as the horizontal line or the vertical line, respectively,[13].

A circle is a set of points that are equidistant from a given point. Since the maximum distance used to measure this equidistance is different from the Euclidean distance, a circle in maximum plane has a different shape than in Euclidean geometry.

Definition 1.3. The set of all points on the maximum plane which are the given r maximum distance from the given point $M = (m_1, m_2)$ is called the maximum circle centered at $M = (m_1, m_2)$ and radius r.

It is seen by definition 1.3 that the maximum circle centered at the point $M = (m_1, m_2)$ and radius r is the set

$$\mathcal{C} = \{(x, y): \max\{|x - m_1|, |y - m_2| = r\}.$$

As particular case, the maximum unit circle is

$$\mathcal{C} = \{(x, y): \max\{|x|, |y| = 1\},$$

that is the square.

Every Euclidean translation preserves the maximum distance. So, it is an isometry in the maximum plane. Reflections in the coordinate axes and the separator lines through the origin and rotations about the origin by integer multiples of $\frac{\pi}{2}$ are isometries in maximum plane, [21].

2. The Inversion in the Maximum Circle

Let C be the maximum circle centered at the point O and radius r in $\mathbb{R}^2_{\mathrm{M}}$. The inversion in the maximum circle C is

$$I_C: \mathbb{R}^2_{\mathbf{M}} \backslash \{O\} \to \mathbb{R}^2_{\mathbf{M}} \backslash \{O\}$$
$$X \to I_C(X) = X'$$

where the point X' is on the ray $\overrightarrow{OX}$ and $d_M(O,X).\, d_M(O,X') = r^2$. C is called the circle of the maximum circle inversion; O is called the center of the maximum circle inversion; r is called the radius of the maximum circle inversion; and the point X' is called the maximum circle inverse of the point X with respect to I_C. For any point X different from O in the maximum plane, the maximum circle inversion map has the property ${I_C}^2(X) = X$.

Theorem 2.1. The maximum circle inversion maps the point (except the inversion center) inside of the maximum inversion circle to the point outside of it, and vice versa, [9,10,22].

Teorem 2.2. Let C be the maximum circle with centered at the point $O = (0,0)$ and radius r. If the points $P = (x, y)$ and $P' = (x', y')$ are a pair of the maximum circle inverse points by I_C , then the following equality between the coordinates of P and P' are obtained

$$(x', y') = \frac{r^2}{(max\{|x|, |y|\})^2}(x , y),$$

[9,10,22].

Corollary 2.3. Let C be the maximum circle with centered at the point $O = (a, b)$ and radius r. For every point P different from O, if the points $P = (x, y)$ and $P' = (x', y')$ are a pair of the maximum circle inverse points with respect to I_C , then the following equalities between the coordinates of P and P' are obtained

$$x' = a + \frac{r^2(x-a)}{(max\{|x-a|, |y-b|\})^2}$$
$$y' = b + \frac{r^2(y-b)}{(max\{|x-a|, |y-b|\})^2},$$

[9,10,22].

Since translations are isometries in maximum plane, no generality is lost to take the center of maximum circle inversion at origin. Therefore, throughout this study, the center O is the origin unless otherwise stated.

2.1. Images of the Lines Under the Inversion in the Maximum Circle

In this section, the images of the lines under the inversion in the maximum circle are discussed analytically and the results are presented. The inversion in a Euclidean circle leaves fixed lines passing through the inversion center, while it tranforms lines not passing through the inversion center to circles passing through the inversion center. While similar results are obtained for the image of the line passing through the center of the maximum circle inversion, it has been observed that the images of the lines not passing through the center have different shapes and properties depending on their positions. These properties are given in the following theorems.

Theorem 2.1.1. The inversion in the maximum circle maps the lines passing through the center of inversion to themselves, [9, 10, 22].

Theorem 2.1.2. The inversion in maximum circle maps a line not passing through the center of the inversion to the closed curve passing through the center of the maximum inversion.

Proof. Suppose that $I_{\mathcal{C}}$ and ℓ are the inversion in the maximum circle $\mathcal{C}$ centered at $O=(0,0)$ with the radius r and the line with the equation $ax+by+c=0$ where $a,b,c\in\mathbb{R}$ and $a^2+b^2\neq 0, c\neq 0$, respectively. $I_{\mathcal{C}}$ maps the point $X=(x,y)$ on the line ℓ to the maximum inverse point $X'=(x',y')$ satisfying the equation

$$ax'+by'+\frac{c}{\mathrm{r}^2}(\max\{|\mathrm{x}'|,|\mathrm{y}'|\})^2=0.$$

This means that the image is the closed curve consisting the union of two parabola arcs with equations $ax'+by'+\frac{c}{r^2}(x')^2=0$ for $|x'|>|y'|$ and $ax'+by'+\frac{c}{r^2}(y')^2=0$ for $|\mathrm{x}'|\leq|\mathrm{y}'|$. They are not maximum pabola arcs. It is seen that the both of arcs pass through O and the line $ax'+by'=0$ is tangent to them at O. Since the directrices of two parabolas have the equations $y=\frac{(a^2+b^2)r^2}{4bc}$ and $x=\frac{(a^2+b^2)r^2}{4ac}$, parabola arcs are on two orthogonal parabolas whose vertices are $\mathrm{T}=(\lambda,\lambda\frac{m}{2})$ and $\mathrm{S}=(\frac{\beta}{2m},\beta)$ where m is the slope of ℓ, $\lambda=-\frac{a\mathrm{r}^2}{2\mathrm{c}}$ and $\beta=-\frac{b\mathrm{r}^2}{2\mathrm{c}}$, (Fig.1 (a)). In addition, in cases of $|m|<2$, $|m|>\frac{1}{2}$ and $m\in\left[-2,-\frac{1}{2}\right]\cup\left[\frac{1}{2},2\right]$, only the vertex T , only the vertex S and both vertices lie on the image, respectively. If the line ℓ does not intersect $\mathcal{C}$, $d_M(O,X)>r$ for every point X on ℓ. From Theorem 2.1, $d_M(O,X')<r$ where the point X' is the maximum circle inverse of the point X. And, the image of ℓ is in interior of $\mathcal{C}$. Thus, $I_{\mathcal{C}}$ maps the line ℓ not intersecting the inversion circle to the closed curve not intersecting the inversion circle.

In the case of $a=0$ or $b=0$, the line ℓ is parallel to the coordinate axis. Suppose that $a=0$. Then $I_{\mathcal{C}}$ maps the point $X=(x,y)$ on the line ℓ to the maximum inverse point $X'=(x',y')$ satisfying the equation

$$by'+\frac{c}{\mathrm{r}^2}(\max\{|\mathrm{x}'|,|\mathrm{y}'|\})^2=0.$$

This means that the image is the closed curve consisting the union of the line segment and the parabola arc. The the parabola arc is on the parabola whose vertex is the point O, whose directrix is the line with $y=\frac{br^2}{4c}$, and whose axis of symmetry is the y- axis. So, it is observed that $I_{\mathcal{C}}(\ell)$ pass through O and the x-axis is tangent to $I_{\mathcal{C}}(\ell)$ at O. Note that the parabola arc is symmetric about the axis of symmetry. Also, it is seen that the line segment in the image $I_{\mathcal{C}}(\ell)$, the directrix and the line ℓ are parallel, (Fig.1 (b)). If the line ℓ meet $\mathcal{C}$, then $I_{\mathcal{C}}$ leaves the intersection points fixed. In special cases for $a=\pm1, b=\pm1$, line ℓ is a separator line. $I_{\mathcal{C}}$ transforms the separator line ℓ with the equation $x+y+c=0$ to the closed curve with the equation

$$x'+y'+\frac{c}{r^2}(max\{|x'|,|y'|\})^2=0.$$

It states that the image $I_{\mathcal{C}}(\ell)$ consists of two parabola arcs such that they are on two orthogonal parabolas passing through the center of the maximum inversion. Since the reflection in the separator line $y' = x'$ through the inversion center maps each of the parabola arcs to the other, the image is symmetric about the line $y' = x'$. If the separator line ℓ does not meet the inversion circle, then the image is interior of the inversion circle. In the other case, the intersection points are invariant under I_C.

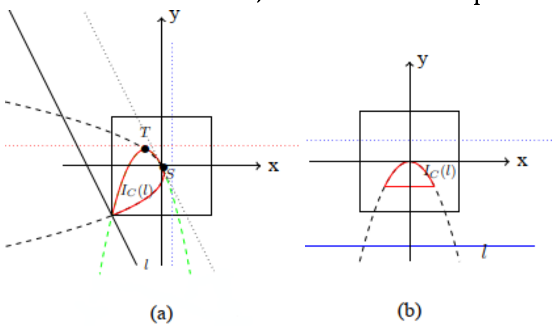

Figure 1. The maximum circle inverse of the line ℓ

Also, the following results are immediately obtained from the proof of the Theorem 2.1.2.

Corollary 2.1.3. The inversion in maximum circle maps a gradual or steep line not passing through the center of the inversion to the closed curve having the following properties:
i) It passes through the center of the maximum inversion,
ii) It consists of two parabola arcs on two orthogonal parabolas, also it pass through two vertices of them when the slope of the given line is in $\left[-2,-\frac{1}{2}\right] \cup \left[\frac{1}{2},2\right]$,
iii) Its tangent at the center of inversion is the line through the center parallel to the given line.

Corollary 2.1.4. The inversion in maximum circle maps a horizontal or vertical line not passing through the center of the inversion to the closed curve having the following properties:
i) It passes through the center of the maximum inversion,
ii) It consists of the line segment and the parabola arc,
iii) The coordinate axis parallel to the given line is tangent to it at the center of inversion
iv) It is symmetric about the coordinate axis perpendicular to the given line,
v) The line segment in the image, the directrix of the parabola containing the parabola arc and the given line are parallel.

Corollary 2.1.5. The inversion in maximum circle maps the seperator line not passing through the center of inversion to the closed curve having the following properties:
i) It passes through the center of the maximum inversion,
ii) It consists of two parabola arcs on two orthogonal parabolas,
iii) It is symmetric about the separator line through the center of the maximum inversion,
iv) The separator line passing through the center of inversion parallel to the given separator line is tangent to it.

2.2. The Line Segments Under the Inversion in the Maximum Circle

Let A and B be two distinct points in the maximum plane. It will be that the image of the line segment joining points A and B under the inversion in maximum circle is on the image of the line passing through points A and B. If the completion of the line segment AB passes through the center of maximum circle inversion, then the line AB inverts to itself. Therefore, the image $A'B'$ lie on the line AB. If the completion of the line segment AB does not pass through the center of maximum circle inversion, then its image is the closed curve passing through the inversion center. The inverse points A' and B' are the intersection points where the rays OA and OB meet this curve. The image of the line segment AB is the curve segment between points A' and B' such that it does not include the point O. The image $A'B'$ has different shapes depending on the position the points A and B. The classification of the images can be given by using the regions formed by the separator lines through the point O as the following:

a) Let the end points of the line segment AB be in the same region. If AB is on the line perpendicular to the coordinate axis in this region, the image $A'B'$ is a line segment. In the remain cases, the image $A'B'$ is a parabola arc, (Fig.2).

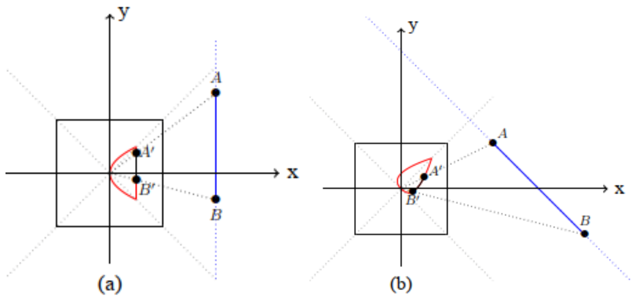

Figure 2. The maximum circle inverse of a line segment when its end points lie on same region.

b) Let the end points of the line segment AB be in two different neighboring regions. If AB is on the line parallel to the coordinate axes, then the image $A'B'$ consists of a line segment parallel to AB and a parabola arc. In the other cases, the image $A'B'$ consists of two parabola arcs, (Fig.3).

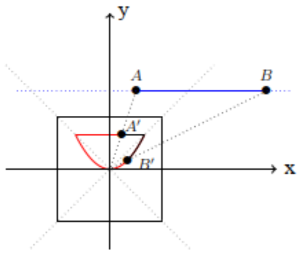

Figure 3. The maximum circle inverse of a line segment when its end points lie on neighboring regions.

c) Let the end points of the line segment AB be in two alternate regions. If AB is on the line parallel to the coordinate axis, then the image $A'B'$ is formed a line segment parallel to AB and two parabola arc. In the other cases, the image $A'B'$ consists of three parabola arcs, (Fig.4).

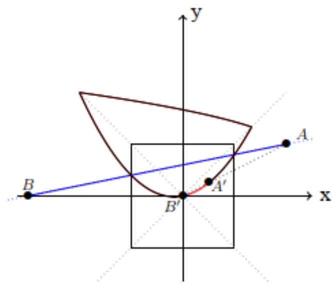

Figure 4. The maximum circle inverse of a line segment when its end points lie on alternate regions.

2.3. Images of Parallel Lines Under the Inversion in the Maximum Circle

In this section, the image of the pencil of all lines parallel to the given line is investigated. Suppose that I_C and ℓ_0 are the inversion in the maximum circle C with the center $O = (0,0)$ and radius r and the line through O with the equation $ax + by = 0$ where $a^2 + b^2 \neq 0$, respectively. The pencil of all lines parallel to the line ℓ_0 is the set $\{\ell : \ell \parallel \ell_0\}$, where ℓ has the line with equation $ax + by + c = 0$, c ∈ ℝ. The image of this pencil under I_C is the set of inverses of all lines parallel to the line ℓ_0. It is clear from theorem 2.1.2 that the maximum circle inversion maps lines in pencil (except ℓ_0) to the closed curves through the inversion center O such that the line ℓ_0 is tangent to them at the inversion center. The set of these closed curves forms the image of the pencil under I_C. In the case that $a \neq 0$ and $b \neq 0$, it is known from theorem 2.1.2 and corollary 2.1.3 that every closed curve in the image of the pencil is the union of two parabola arcs through O and tangent to ℓ_0 at the point O. Additionally, each curve in the image is on two orthogonal parabolas where their vertices are on the lines $y = -\frac{a}{2b}x$ and $y = -\frac{2a}{b}x$, (Fig 5 (a)). In the case that $a = 0$ or $b = 0$, it is seen from theorem 2.1.2 and corollary 2.1.4 that every closed curve in the image of the pencil is the union of a parabola arc and a line segment parallel to ℓ_0. Also, all curves contain the vertex O and are symmetric about the coordinate axis. And, the line ℓ_0 is tangent to them at the point O, (Fig 5 (b)).

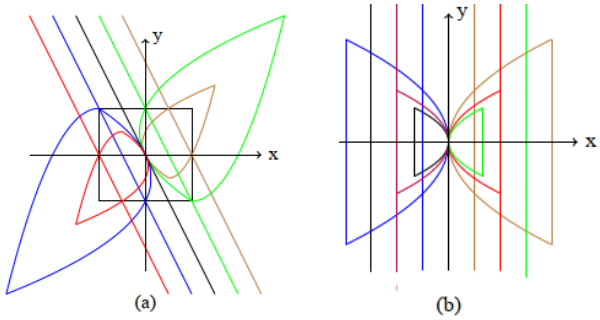

Figure 5. Images of parallel lines under the maximum circle inversion.

2.4. Images of Concurrent Lines Under the Inversion in the Maximum Circle

In this part, it is examined how their images behave when an inversion transform is applied to concurrent lines. Concurrent lines are lines that intersect at a point. It is observed that image of concurrent lines under the maximum circle inversion can vary depending on lines and the inversion circle. Also, it is well known that inversion in a Euclidean circle preserves the angles between intersecting lines. By considering inversion in maximum circle, this property is examined as the following.

Theorem 2.4.1. The angle between the two intersecting lines is the same as the angle between their maximum circle inverses at the center of maximum circle inversion.

Proof. Let θ be the angle between the intersecting lines ℓ_1 and ℓ_2 at the point N. Suppose that I_C is the inversion in the maximum circle C with the center $O = (0,0)$, the radius r. If the lines ℓ_1 and ℓ_2 pass through the inversion center, then the intersection point of ℓ_1 and ℓ_2 must be $N = O$. Since $I_C(\ell_1) = \ell_1$ and $I_C(\ell_2) = \ell_2$, angle between the images is θ. In the case that only the line ℓ_1 passes through the inversion center, then $I_C(\ell_1) = \ell_1$ and $I_C(\ell_2)$ is the closed curve whose tangent at the inversion center is parallel to ℓ_2. So, angle between $I_C(\ell_1)$ and $I_C(\ell_2)$ is θ. If ℓ_1 and ℓ_2 do not pass through the inversion center, then $I_C(\ell_1)$ and $I_C(\ell_2)$ are two closed curves through the inversion center such that tangents of $I_C(\ell_1)$ and $I_C(\ell_2)$ at the inversion center are parallel to ℓ_1 and ℓ_2, respectively. Thus, angle between $I_C(\ell_1)$ and $I_C(\ell_2)$ at the inversion center is θ.

Corollary 2.4.2. The maximum circle inverses of two orthogonal lines are orthogonal at the inversion center.

Now, considering the set of concurrent lines. This set is also called the pencil of concurrent lines. The properties regarding the image of this pencil under the maximum circle inversion are introduced in the following corollary.

Corollary 2.4.3. Let N be a point in the maximum plane. The maximum circle inverse of the pencil of concurrent lines at the point N has in the following properties:

i) If the point N is the inversion center, then I_C leaves the pencil fixed.

ii) If the point N is on the maximum inversion circle, then I_C maps all lines in the pencil, except the line ON, to closed curves passing through point N and the inversion center O, (Fig 6 (a)).

iii) If the point N is not on the maximum inversion circle, then I_C maps all lines in the pencil, except the line ON, to closed curves passing through the inversion center O and the inverse N' of N, (Fig 6 (b)).

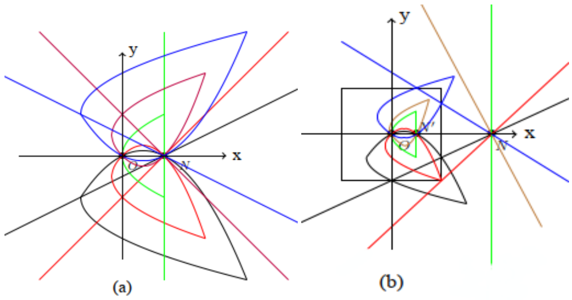

Figure 6. Images of concurrent lines under the maximum circle inversion

3. Conclusion

In this study, the focus was on the examination of the images of lines under inversion in a maximum circle. Through a detailed analytical analysis, several observations were made. It was found that when a line does not pass through the center of inversion, its image does not form a maximum circle but instead becomes a closed curve containing at least one parabolic arc. The study also introduced various properties related to the images of lines under maximum circle inversion. Furthermore, the investigation extended to the examination of line segments and their images, considering the positions of their endpoints. This analysis provided valuable insights into how the inversion in a maximum circle affects the geometric configuration consisting line segments. Another finding was that the inversion in a maximum circle transforms a pencil of parallel lines (excluding the line passing through the center of inversion) into a set of closed curves that all pass through the center of inversion. Additionally, it was examined the images of concurrent lines under inversion with respect to a maximum circle and results were obtained. These findings provide to our understanding of how parallel and concurrent lines are affected by inversion. Consequently, it is thought that the results obtained in this study contribute to the literature including the subject of inversion in non-Euclidean geometry.

Author Contributions

The author read and approved the final version of the manuscript.

Conflicts of Interest

The author declares no conflict of interest.

References

[1] Akça, Z., Kaya, R. (1997) On the taxicab trigonometry. Jour. of Inst. of Math. & Comp. Sci.(Math. Ser.), 10(3), 151-159.

[2] Akça, Z., Kaya R. (2004) On the distance formulae in three dimensional taxicab space. Hadronic J., 27(5): 521–532.

[3] Akça, Z., Nazli, S. (2022) On the versions in the Plane $\mathbb{R}^2_{\pi 3}$ of some Euclidean theorems. New Trends in Mathematical Sciences, 10(1), 20-27.

[4] Akça, Z., Çalış, C. (2021) On the Voronoi Diagram and Taxicab Plane. Erzincan University Journal of Science and Technology, 14(1), 175-181.

[5] Bayar, A., Ekmekçi, S. (2014) On circular inversions in taxicab plane. J. Adv. Res. Pure Math, 6(4), 33-39.

[6] Bayar, A., Ekmekçi, S., Öztürk, İ. (2015) On Complex Numbers and Taxicab Plane. Mathematical Sciences and Applications E-Notes, 3(1), 58-64.

[7] Blair, D. E. (2000) Inversion Theory and Conformal Mapping. Student Mathematical Library, American Math. Society, 9.

[8] Childress, N. (1965) Inversion with Respect to the Central Conics. Mathematics Magazine, 38(3):147-149.

[9] Cırık, Y. (2022) Maksimum Metrik ile Donatılmış Düzlemde ve Uzayda İnversiyonlar. MSc thesis, Eskişehir Osmangazi University, Institute of Science and Technology, Turkey.

[10] Cırık, Y., Ekmekçi, S. (2022) On the Maksimum Spherical Inversions. Erzincan University, Journal of Science and Technology, 15(1):360-371.

[11] Gdawiec, K. (2014) Star-shaped set inversion fractals. Fractals, 22(4): 1450009-1-1450009-17.

[12] Kaya R., Akça Z., Özcan M., Günaltılı, İ. (2000) General equation for taxicab conics and their classification. Mitt. Math. Ges. Hamburg, 19(0): 135–148.

[13] Krause, E. F. (1975) Taxicab Geometry. Addison –Wesley Publishing Company, Menlo Park, California.

[14] Nickel, J.A. (1995) A Budget of Inversion. Mathematical and Computer Modelling, 21(6): 87-93.

[15] Pekzorlu, A., Bayar, A. (2020) On The Chinese Checkers Spherical Invesions in Three Dimensional Chinese Checker Space. Communications Faculty of Sciences University of Ankara Series A1: Mathematics and Statistics, 69(2): 1498-1507.

[16] Pekzorlu, A., Bayar, A. (2020) Taxicab Spherical Invesions in Taxicab Space. Journal of Mahani Mathematical Research Center, 9(1): 45-54.

[17] Pekzorlu, A., Bayar, A. (2022) On the Chinese Checkers Circular Inversions in the Chinese Checkers Plane. Hagia Sophia Journal of Geometry, 4(2): 28–34.

[18] Ramirez, J.L. (2014) Inversions in an Ellipse. Forum Geometricorum,14:107–115.

[19] Ramirez, J.L., Rubiano, G.N. (2014) A Geometrical Construction of Inverse Points with Respect to An Ellipse. International Journal of Mathematical Education in Science and Technology, 45(8): 1254-1259.

[20] Ramirez, J.L., Rubiano, G.N., Zlobec, B. J. (2015) A Generating fractal patterns by using p-circle inversion. Fractals, 23(4):1550047-1-1550047-13.

[21] Salihova, S. (2006) Maksimum Metriğinin Geometrisi Üzerine. Doctoral dissertation, Eskişehir Osmangazi University, Institute of Science and Technology, Turkey.

[22] Yüca, G., Can, Z. (2020) On the Circular Inversion in Maximum Plane. Ikonion Journal Of Mathematics, 2(2):26-34.

Ikonion Journal of Mathematics
https://dergipark.org.tr/tr/pub/ikjm
Research Article
Open Access
https://doi.org/10.54286/ikjm.1227629

ISSN: 2687-6531

A New Hybrid Block Method via Combined Hermite Polynomials and Exponential Functions as Basis Function

Hycienth O. Orapine * [1], John Zira Donald [2], Ali A. Baidu [1], Joshua O. Oladele [3]

Keywords:
Basis function, Collocation, Exponential function, Hermite polynomials, Hybrid block method, Interpolation, Ordinary Differential Equations.

Abstract — The development and implementation of a hybrid block method of order nine for first-order initial value problems (IVPs) of ordinary differential equations (ODEs) that are stiff or oscillatory in nature are presented in this paper. The hybrid block method was created using continuous collocation and interpolation techniques by combining Hermite polynomials and exponential functions as the basis function to produce a continuous implicit linear multistep method (LMM). The method's properties were studied and proven to be consistent, convergent, and zero-stable with an A-stable region of absolute stability, making it a suitable approach for stiff and oscillatory ODEs. The application of a combined basis in the generation of LMMs is an approach that should be widely adopted. The technique shows that continuous LMMs can be derived from a combination of any polynomials and exponential functions through an interpolation and collocation approach. On two sampled stiff and oscillatory problems, the new integrator was tested. The numerical findings demonstrate that our hybrid block integrator is computationally efficient and outperforms previous methods of similar derivations in stability and accuracy of results.

Subject Classification (2020): 65L04, 65L05, 65L6, 65L20.

1. Introduction

We investigate a numerical solution to first-order initial value problems (IVPs) of the ordinary differential equations (ODEs) that may exhibit stiffness or oscillatory behaviour given by

$$y' = f\big(t, y(t)\big), \qquad y(t_0) = y_0, \quad \forall \ \mathrm{a} \le \mathrm{t} \le \mathrm{b}, \tag{1.0}$$

where t_0 is the initial point, y_0 is the solution at t_0, and f is assumed to be continuous and satisfy the Lipchitz theorem for the existence and uniqueness of the solution.

The problem (1.0) frequently arises in studying dynamic systems and electrical networks [4]. According to [10], equation (1.0) is used to simulate population growth, particle trajectory, simple harmonic motion, beam deflection, and other phenomena. Notably, mixture models, the basic Susceptible, Infection, and Recovery (SIR) models, and other related models may all be formulated as problems of the form (1.0).

*hycienthorapine@naub.edu.ng (Corresponding Author);
[1] Department of Mathematics, Nigerian Army University Biu, Borno State, Nigeria;
[2] Department of Mathematics, Adamawa State University Mubi-Nigeria;
[3] Air Force Institute of Technology, Kaduna-Nigeria.
Article History: Received: 09.01.2023 — Accepted: 11.07.2023 — Published: 12.09.2023

The solutions of nonlinear, stiff, and oscillatory problems of ODEs such as (1.0) are often highly unstable [11].

Definition 1.1 [8]. A differential equation is considered to be stiff if $\mathrm{Re}\left(\xi_j\right) < 0,\ j = 1, 2, \ldots, m$, here ξ is the Eigenvalue of the given differential equation.

Definition 1.2 [13]. A differential equation with at least one oscillating solution is said to be oscillatory. If a nontrivial solution (function) of an ODE converges not to a finite limit (or diverges), it is said to be oscillating. (i.e. if the function has an infinity of results).

To deal with this class of problems, researchers have historically focused on developing efficient, stable, and high-order linear multistep methods (LMMs). Because LMMs do not start on their own, they require initial values from one-step methods like Euler's method and the Runge-Kutta family of methods. Ref. [11] gives the k-step generalized LMM as

$$\sum_{j=0}^{k} \alpha_j y_{n+j} = h \sum_{j=0}^{k} \beta_j f_{n+j}, \qquad \alpha_0 + \beta_0 \neq 0, \qquad \alpha_k = 1, \tag{1.1}$$

where α_j *and* β_j are uniquely determined, $h =$ step length, such that $t_{k+n} - t_k = nh$.

According to [11], existing LMMs for solving ODEs may be derived using approaches such as Taylor's series, numerical integration, determining the order of the LMM, and the interpolation approach, all of which are major discrete schemes constrained by assuming the order of convergence.

Ref. [1] and [11] reported that several researchers have shifted to employing the continuous collocation and interpolation process, resulting in the emergence of continuous LMMs of the form

$$y(t) = \sum_{j=0}^{k} \alpha_j(t) y_{n+j} + h \sum_{j=0}^{k} \beta_j(t) f_{n+j}, \tag{1.2}$$

where $\alpha_j(t)$ and $\beta_j(t)$ are continuous functions of t that should be differentiable at least once.

The continuous collocation and interpolation approach is a milestone in numerical analysis and computation for it is widely used. In this study consequently, we will derive continuous LMM and implement it in block form to eliminate its non-self-starting drawback.

Scholars have used continuous collocation technique to derive LMMs using a variety of single basis functions, including power series, Lagrange polynomials, Chebychev polynomials, Legendre polynomials, Hermite polynomials, and exponential functions among others.

It is established that the efficiency of these methods depends mainly on the basis functions chosen and the problem to be solved [2], [9], and [11]. Consequently, in search of a method with better efficiency and stability properties, [13] introduced a combined basis function for the derivation of LMM for the problem (1.0) of the form

$$y(t) = \sum_{j=0}^{r+n-1} a_j t^j + a_{r+n} \sum_{j=0}^{r+n} \frac{\alpha^j t^j}{j!}, \tag{1.3}$$

this combines power series and exponential functions. We improve upon this in terms of the methodology of the derivation, and the order and stability of the method.

In this paper, therefore, we proposed a different combined basis function, which is Hermite polynomials and exponential functions for the derivation of LMM to generate a higher order and efficiently stable hybrid block method for the solution of problem (1.0).

2. Methodology

The collocation procedure for continuous LMM in equation (1.2) intended for ODEs such as equation (1.0) is in general based on a basic idea: identify a function of a defined form that exactly satisfies the differential equation at a given set of points. The approximation function must also meet some additional conditions placed by the nature of the problem under consideration.

In this study, we concatenate Probabilist's Hermite polynomials and exponential functions to be an approximate solution to the problem (1.0) in the form

$$y(t) = \sum_{r=0}^{k} a_r H_r(t) + \sum_{r=k+1}^{m} \sum_{j=0}^{r} a_r \frac{\beta^j t^j}{j!}, \quad m = i + c\,. \tag{1.4}$$

Equation (1.4) is called the *basis function* and is continuously differentiable. where c denotes the number of collocation points, i is the number of interpolation points and $\beta \in \mathbb{R}$.

The coefficients $a_r \in \mathbb{R},\ r = 0, 1, \dots, m$ of the series (1.4), are determined over the interval of integration $[a, b]$, for $a = t_0 < t_1 < \cdots < t_N = b$, with a constant step size h given by $h = t_{n+1} - t_n;\ n = 0, 1, \dots, N-1$. $H_r(t)$ are the Probabilist's Hermite polynomials generated by the formula

$$H_n(t) = (-1)^n e^{\left(\frac{t^2}{2}\right)} \frac{d^n}{dt^n} e^{\left(-\frac{t^2}{2}\right)} = \left(1 - \frac{d}{dt}\right)^n \cdot 1, \tag{1.5}$$

and whose recursive relation is

$$H_{n+1}(t) = tH_n(t) - H_n'(t)\,. \tag{1.6}$$

The first ten probabilist's Hermite polynomials are:

$$H_0 = 1, \quad H_1 = t, \quad H_2 = t^2 - 1, \quad H_3 = t^3 - 3t, \quad H_4 = t^4 - 6t^2 + 3$$

$$H_5 = t^5 - 10t^3 + 15t, \quad H_6 = t^6 - 15t^4 + 45t^2 - 15, \quad H_7 = t^7 - 21t^5 + 105t^3 - 105t$$

$$H_8 = t^8 - 28t^6 + 210t^4 - 420t^2 - 105, \quad H_9 = t^9 - 36t^7 + 378t^5 - 1260t^3 - 945t$$

Now, obtaining the first derivative of (1.4) we have

$$y'(t) = \sum_{r=1}^{k} a_r H_r'(t) + \sum_{r=k+1}^{m} \sum_{j=1}^{r} a_r \frac{\beta^j t^{j-1}}{(j-1)!}, \quad m = i + c. \tag{1.7}$$

Interpolating equation (1.4) at $t = t_n$ and collocating equation (1.7) at $t = t_{n+c},\ c \in \mathbb{R};$ a system of nonlinear equations is produced, which is compactly expressed in the form

$$\left.\begin{aligned} y_n &= \sum_{r=0}^{k} a_r H_r(t_n) + \sum_{r=k+1}^{m} \sum_{j=0}^{r} a_r \frac{\beta^j t_n^j}{j!}, \\ f_{n+c} &= \sum_{r=1}^{k} a_r H_r'(t_{n+c}) + \sum_{r=k+1}^{m} \sum_{j=1}^{r} a_r \frac{\beta^j t_{n+c}^{j-1}}{(j-1)!}\ . \end{aligned}\right\} \quad (1.8)$$

The unknown constants a_r in equation (1.8) are determined using standard methods like Gaussian elimination or matrices inversion method and substituted into equation (1.4). Thus, applying the transformation $x = \frac{t-t_n}{h}$ and algebraic manipulation on equation (1.4), a hybrid continuous LMM of the form in equation (1.2) is obtained for different values of m, and it is implemented in block form.

3. Derivation of Hybrid block Method

The approximate solution to the problem (1.0) is the equation (1.4) where $m = 9$, i.e.

$$y(t) = a_0 + a_1 t + a_2(t^2 - 1) + a_3(t^3 - 3t) + a_4(t^4 - 6t^2 + 3) + a_5(t^5 - 10t^3 + 15t) \quad + a_6 \sum_{j=0}^{6} \frac{\beta^j t^j}{j!}$$

$$+ a_7 \sum_{j=0}^{7} \frac{\beta^j t^j}{j!} + a_8 \sum_{j=0}^{8} \frac{\beta^j t^j}{j!} + a_9 \sum_{j=0}^{9} \frac{\beta^j t^j}{j!}\ . \quad (1.9)$$

Taking the first derivative of equation (1.9) and substituting in equation (1.0) gives

$$f(t, y) = a_1 + 2a_2 t + 3a_3(t^2 - 1) + 4a_4(t^3 - 3t) + 5a_5(t^4 - 6t^2 + 3) + a_6 \sum_{j=1}^{6} \frac{\beta^j t^{j-1}}{(j-1)!}$$

$$+ a_7 \sum_{j=1}^{7} \frac{\beta^j t^{j-1}}{(j-1)!} + a_8 \sum_{j=1}^{8} \frac{\beta^j t^{j-1}}{(j-1)!} + a_9 \sum_{j=1}^{9} \frac{\beta^j t^{j-1}}{(j-1)!}\ . \quad (1.10)$$

Now, interpolating equation (1.9) at point $t_{n+i},\ i = 0$ and collocating equation (1.10) at point $t_{n+c},\ c = 0, \frac{1}{8}, \frac{1}{4}, \frac{3}{8}, \frac{1}{2}, \frac{5}{8}, \frac{3}{4}, \frac{7}{8}$ and 1, the following nonlinear system of equations is obtained

$$B \cdot A = U, \quad (1.11)$$

where

$$A = (a_0, a_1, a_2, a_3, a_4, a_5, a_6, a_7, a_8, a_9)^T,$$

$U = \left(y_n,\ f_n,\ f_{n+\frac{1}{8}},\ f_{n+\frac{1}{4}},\ f_{n+\frac{3}{8}},\ f_{n+\frac{1}{2}}, f_{n+\frac{5}{8}},\ f_{n+\frac{3}{4}}, f_{n+\frac{7}{8}},\ f_{n+1}\right)^T$ and

$$B=\begin{bmatrix}
1 & t_n & (t_n^2-1) & (t_n^3-3t_n) & (t_n^4-6t_n^2+3) & (t_n^5-10t_n^3+15t_n) & \sum_{j=0}^{6}\frac{\beta^j t_n^j}{j!} & \sum_{j=0}^{7}\frac{\beta^j t_n^j}{j!} & \sum_{j=0}^{8}\frac{\beta^j t_n^j}{j!} & \sum_{j=0}^{9}\frac{\beta^j t_n^j}{j!}\\
0 & 1 & 2t_n & 3(t_n^2-1) & 4(t_n^3-3t_n) & 5(t_n^4-6t_n^2+3) & \sum_{j=1}^{6}\frac{\beta^j t_n^{j-1}}{(j-1)!} & \sum_{j=1}^{7}\frac{\beta^j t_n^{j-1}}{(j-1)!} & \sum_{j=1}^{8}\frac{\beta^j t_n^{j-1}}{(j-1)!} & \sum_{j=1}^{9}\frac{\beta^j t_n^{j-1}}{(j-1)!}\\
0 & 1 & 2t_{n+\frac{1}{8}} & 3\left(t_{n+\frac{1}{8}}^2-1\right) & 4\left(t_{n+\frac{1}{8}}^3-3t_{n+\frac{1}{8}}\right) & 5(t_{n+\frac{1}{8}}^4-6t_{n+\frac{1}{8}}^2+3) & \sum_{j=1}^{6}\frac{\beta^j t_{n+1/8}^{j-1}}{(j-1)!} & \sum_{j=1}^{7}\frac{\beta^j t_{n+1/8}^{j-1}}{(j-1)!} & \sum_{j=1}^{8}\frac{\beta^j t_{n+1/8}^{j-1}}{(j-1)!} & \sum_{j=1}^{9}\frac{\beta^j t_{n+1/8}^{j-1}}{(j-1)!}\\
0 & 1 & 2t_{n+\frac{1}{4}} & 3\left(t_{n+\frac{1}{4}}^2-1\right) & 4\left(t_{n+\frac{1}{4}}^3-3t_{n+\frac{1}{4}}\right) & 5(t_{n+\frac{1}{4}}^4-6t_{n+\frac{1}{4}}^2+3) & \sum_{j=1}^{6}\frac{\beta^j t_{n+1/4}^{j-1}}{(j-1)!} & \sum_{j=1}^{7}\frac{\beta^j t_{n+1/4}^{j-1}}{(j-1)!} & \sum_{j=1}^{8}\frac{\beta^j t_{n+1/4}^{j-1}}{(j-1)!} & \sum_{j=1}^{9}\frac{\beta^j t_{n+1/4}^{j-1}}{(j-1)!}\\
0 & 1 & 2t_{n+\frac{3}{8}} & 3\left(t_{n+\frac{3}{8}}^2-1\right) & 4\left(t_{n+\frac{3}{8}}^3-3t_{n+\frac{3}{8}}\right) & 5(t_{n+\frac{3}{8}}^4-6t_{n+\frac{3}{8}}^2+3) & \sum_{j=1}^{6}\frac{\beta^j t_{n+3/8}^{j-1}}{(j-1)!} & \sum_{j=1}^{7}\frac{\beta^j t_{n+3/8}^{j-1}}{(j-1)!} & \sum_{j=1}^{8}\frac{\beta^j t_{n+3/8}^{j-1}}{(j-1)!} & \sum_{j=1}^{9}\frac{\beta^j t_{n+3/8}^{j-1}}{(j-1)!}\\
0 & 1 & 2t_{n+\frac{1}{2}} & 3\left(t_{n+\frac{1}{2}}^2-1\right) & 4\left(t_{n+\frac{1}{2}}^3-3t_{n+\frac{1}{2}}\right) & 5(t_{n+\frac{1}{2}}^4-6t_{n+\frac{1}{2}}^2+3) & \sum_{j=1}^{6}\frac{\beta^j t_{n+1/2}^{j-1}}{(j-1)!} & \sum_{j=1}^{7}\frac{\beta^j t_{n+1/2}^{j-1}}{(j-1)!} & \sum_{j=1}^{8}\frac{\beta^j t_{n+1/2}^{j-1}}{(j-1)!} & \sum_{j=1}^{9}\frac{\beta^j t_{n+1/2}^{j-1}}{(j-1)!}\\
0 & 1 & 2t_{n+\frac{5}{8}} & 3\left(t_{n+\frac{5}{8}}^2-1\right) & 4\left(t_{n+\frac{5}{8}}^3-3t_{n+\frac{5}{8}}\right) & 5(t_{n+\frac{5}{8}}^4-6t_{n+\frac{5}{8}}^2+3) & \sum_{j=1}^{6}\frac{\beta^j t_{n+5/8}^{j-1}}{(j-1)!} & \sum_{j=1}^{7}\frac{\beta^j t_{n+5/8}^{j-1}}{(j-1)!} & \sum_{j=1}^{8}\frac{\beta^j t_{n+5/8}^{j-1}}{(j-1)!} & \sum_{j=1}^{9}\frac{\beta^j t_{n+5/8}^{j-1}}{(j-1)!}\\
0 & 1 & 2t_{n+\frac{3}{4}} & 3\left(t_{n+\frac{3}{4}}^2-1\right) & 4\left(t_{n+\frac{3}{4}}^3-3t_{n+\frac{3}{4}}\right) & 5(t_{n+\frac{3}{4}}^4-6t_{n+\frac{3}{4}}^2+3) & \sum_{j=1}^{6}\frac{\beta^j t_{n+3/4}^{j-1}}{(j-1)!} & \sum_{j=1}^{7}\frac{\beta^j t_{n+3/4}^{j-1}}{(j-1)!} & \sum_{j=1}^{8}\frac{\beta^j t_{n+3/4}^{j-1}}{(j-1)!} & \sum_{j=1}^{9}\frac{\beta^j t_{n+3/4}^{j-1}}{(j-1)!}\\
0 & 1 & 2t_{n+\frac{7}{8}} & 3\left(t_{n+\frac{7}{8}}^2-1\right) & 4\left(t_{n+\frac{7}{8}}^3-3t_{n+\frac{7}{8}}\right) & 5(t_{n+\frac{7}{8}}^4-6t_{n+\frac{7}{8}}^2+3) & \sum_{j=1}^{6}\frac{\beta^j t_{n+7/8}^{j-1}}{(j-1)!} & \sum_{j=1}^{7}\frac{\beta^j t_{n+7/8}^{j-1}}{(j-1)!} & \sum_{j=1}^{8}\frac{\beta^j t_{n+7/8}^{j-1}}{(j-1)!} & \sum_{j=1}^{9}\frac{\beta^j t_{n+7/8}^{j-1}}{(j-1)!}\\
0 & 1 & 2t_{n+1} & 3(t_{n+1}^2-1) & 4(t_{n+1}^3-3t_{n+1}) & 5(t_{n+1}^4-6t_{n+1}^2+3) & \sum_{j=1}^{6}\frac{\beta^j t_{n+1}^{j-1}}{(j-1)!} & \sum_{j=1}^{7}\frac{\beta^j t_{n+1}^{j-1}}{(j-1)!} & \sum_{j=1}^{8}\frac{\beta^j t_{n+1}^{j-1}}{(j-1)!} & \sum_{j=1}^{9}\frac{\beta^j t_{n+1}^{j-1}}{(j-1)!}
\end{bmatrix}. \quad (1.12)$$

Solving equation (1.11) in maple soft, using the matrix inversion method, the value of the unknown column vector A is obtained. The value of the vector A is then substituted in equation (1.9) to give a continuous implicit scheme. Thus, applying the transformation $x=\frac{(t-t_n)}{h}$, and algebraic manipulation for all values of $\beta \in \mathbb{R}$ we have a continuous implicit hybrid LMM of the form in equation (1.2) given as

$$y(x)=\alpha_0(x)y_n+h\left[\sum_{j=0}^{1}\beta_j(x)f_{n+j}\right], \quad (1.13)$$

where $j=0,\frac{1}{8},\frac{1}{4},\frac{3}{8},\frac{1}{2},\frac{5}{8},\frac{3}{4},\frac{7}{8}$ and 1, $f_{n+j}=f\big(t_n+jh,y(t_n+jh)\big)$, while $\alpha_0(x)$ *and* $\beta_j(x)$ represent continuous coefficients which are obtained as follow

$$\left.\begin{aligned}
&\alpha_0=1\\
&\beta_0=\frac{xh}{28350}(1310720x^8-6635520x^7+14376960x^6-17418240x^5+12930624x^4-6055560x^3+1771860x^2-308205x+28350)\\
&\beta_{\frac{1}{8}}=-\frac{32x^2h}{14175}(163840x^7-806400x^6+1681920x^5-1932000x^4+1326528x^3-549675x^2+129870x-14175)\\
&\beta_{\frac{1}{4}}=\frac{8x^2h}{14175}(2293760x^7-10967040x^6+22026240x^5-24057600x^4+15411312x^3-5781195x^2+1173690x-99225)\\
&\beta_{\frac{3}{8}}=-\frac{32x^2h}{14175}(1146880x^7-5322240x^6+10298880x^5-10735200x^4+6483456x^3-2259495x^2+420630x-33075)\\
&\beta_{\frac{1}{2}}=\frac{2x^2h}{2835}(4587520x^7-20643840x^6+38522880x^5-38492160x^4+22161888x^3-7343280x^2+1305990x-99225)\\
&\beta_{\frac{5}{8}}=-\frac{32x^2h}{14175}(1146880x^7-4999680x^6+9008640x^5-8672160x^4+4810176x^3-1540665x^2+266490x-19845)\\
&\beta_{\frac{3}{4}}=\frac{8x^2h}{14175}(2293760x^7-9676800x^6+16865280x^5-15724800x^4+8476272x^3-2650725x^2+450030x-33075)\\
&\beta_{\frac{7}{8}}=-\frac{32x^2h}{14175}(163840x^7-668160x^6+1128960x^5-1024800x^4+540288x^3-166005x^2+27810x-2025)\\
&\beta_1=\frac{x^2h}{28350}(1310720x^7-5160960x^6+8478720x^5-7526400x^4+3898944x^3-1181880x^2+196020x-14175)
\end{aligned}\right\} \quad (1.14)$$

When equation (1.13) is evaluated at $t=\frac{1}{8},\frac{1}{4},\frac{3}{8},\frac{1}{2},\frac{5}{8},\frac{3}{4},\frac{7}{8}$, 1 and implemented in block form, it yields a discrete hybrid block method of the type

$$A^{(0)}\boldsymbol{Y}_m=E\boldsymbol{y}_n+hD\boldsymbol{f}(\boldsymbol{y}_n)+hB\boldsymbol{F}(\boldsymbol{Y}_m), \quad (1.15)$$

Where

$$\boldsymbol{Y}_m = \left[y_{n+\frac{1}{8}}, y_{n+\frac{1}{4}}, y_{n+\frac{3}{8}}, y_{n+\frac{1}{2}}, y_{n+\frac{5}{8}}, y_{n+\frac{3}{4}}, y_{n+\frac{7}{8}}, y_{n+1}\right]^T,$$

$$\boldsymbol{y}_n = \left[y_{n-\frac{7}{8}}, y_{n-\frac{3}{4}}, y_{n-\frac{5}{8}}, y_{n-\frac{1}{2}}, y_{n-\frac{3}{8}}, y_{n-\frac{1}{4}}, y_{n-\frac{1}{8}}, y_n\right]^T,$$

$$\boldsymbol{F}(\boldsymbol{Y}_m) = \left[f_{n+\frac{1}{8}}, f_{n+\frac{1}{4}}, f_{n+\frac{3}{8}}, f_{n+\frac{1}{2}}, f_{n+\frac{5}{8}}, f_{n+\frac{3}{4}}, f_{n+\frac{7}{8}}, f_{n+1}\right]^T,$$

$$\boldsymbol{f}(\boldsymbol{y}_n) = \left[f_{n-\frac{7}{8}}, f_{n-\frac{3}{4}}, f_{n-\frac{5}{8}}, f_{n-\frac{1}{2}}, f_{n-\frac{3}{8}}, f_{n-\frac{1}{4}}, f_{n-\frac{1}{8}}, f_n\right]^T,$$

$$A^{(0)} = \begin{bmatrix} 1 & 0 & 0 & 0 & 0 & 0 & 0 & 0 \\ 0 & 1 & 0 & 0 & 0 & 0 & 0 & 0 \\ 0 & 0 & 1 & 0 & 0 & 0 & 0 & 0 \\ 0 & 0 & 0 & 1 & 0 & 0 & 0 & 0 \\ 0 & 0 & 0 & 0 & 1 & 0 & 0 & 0 \\ 0 & 0 & 0 & 0 & 0 & 1 & 0 & 0 \\ 0 & 0 & 0 & 0 & 0 & 0 & 1 & 0 \\ 0 & 0 & 0 & 0 & 0 & 0 & 0 & 1 \end{bmatrix},$$

$$E = \begin{bmatrix} 0 & 0 & 0 & 0 & 0 & 0 & 0 & 1 \\ 0 & 0 & 0 & 0 & 0 & 0 & 0 & 1 \\ 0 & 0 & 0 & 0 & 0 & 0 & 0 & 1 \\ 0 & 0 & 0 & 0 & 0 & 0 & 0 & 1 \\ 0 & 0 & 0 & 0 & 0 & 0 & 0 & 1 \\ 0 & 0 & 0 & 0 & 0 & 0 & 0 & 1 \\ 0 & 0 & 0 & 0 & 0 & 0 & 0 & 1 \\ 0 & 0 & 0 & 0 & 0 & 0 & 0 & 1 \end{bmatrix},$$

$$D = \begin{bmatrix} 0 & 0 & 0 & 0 & 0 & 0 & 0 & \frac{1070017}{29030400} \\ 0 & 0 & 0 & 0 & 0 & 0 & 0 & \frac{32377}{907200} \\ 0 & 0 & 0 & 0 & 0 & 0 & 0 & \frac{12881}{358400} \\ 0 & 0 & 0 & 0 & 0 & 0 & 0 & \frac{4063}{113400} \\ 0 & 0 & 0 & 0 & 0 & 0 & 0 & \frac{41705}{1161216} \\ 0 & 0 & 0 & 0 & 0 & 0 & 0 & \frac{401}{11200} \\ 0 & 0 & 0 & 0 & 0 & 0 & 0 & \frac{149527}{4147200} \\ 0 & 0 & 0 & 0 & 0 & 0 & 0 & \frac{989}{28350} \end{bmatrix},$$

$$B=\begin{bmatrix}
\frac{2233547}{14515200} & -\frac{2302297}{14515200} & \frac{2797679}{14515200} & -\frac{31457}{181440} & \frac{1573169}{14515200} & -\frac{645607}{14515200} & \frac{156437}{14515200} & -\frac{33953}{29030400}\\
\frac{22823}{113400} & -\frac{21247}{453600} & \frac{15011}{113400} & -\frac{2903}{22680} & \frac{9341}{113400} & -\frac{15577}{453600} & \frac{953}{113400} & -\frac{119}{129600}\\
\frac{35451}{179200} & \frac{1719}{179200} & \frac{39967}{179200} & -\frac{351}{2240} & \frac{17217}{179200} & -\frac{7031}{179200} & \frac{243}{25600} & -\frac{369}{358400}\\
\frac{2822}{14175} & \frac{61}{28350} & \frac{4094}{14175} & -\frac{227}{2835} & \frac{1154}{14175} & -\frac{989}{28350} & \frac{122}{14175} & -\frac{107}{113400}\\
\frac{115075}{580608} & \frac{3775}{580608} & \frac{159175}{580608} & -\frac{125}{36288} & \frac{85465}{580608} & -\frac{24575}{580608} & \frac{5725}{580608} & -\frac{175}{165888}\\
\frac{279}{1400} & \frac{9}{5600} & \frac{403}{1400} & -\frac{9}{280} & \frac{333}{1400} & \frac{79}{5600} & \frac{9}{1400} & -\frac{9}{11200}\\
\frac{408317}{2073600} & \frac{24353}{2073600} & \frac{542969}{2073600} & \frac{343}{25920} & \frac{368039}{2073600} & \frac{261023}{2073600} & \frac{111587}{2073600} & -\frac{8183}{4147200}\\
\frac{2944}{14175} & -\frac{464}{14175} & \frac{5248}{14175} & -\frac{454}{2835} & \frac{5248}{14175} & -\frac{464}{14175} & \frac{2944}{14175} & \frac{989}{28350}
\end{bmatrix}.$$

4. Analysis of the Method

4.1 . Zero Stability of the Method

Definition 4.1: [3] if the roots r_n, $n = 1, 2, \ldots, k$ of the characteristics polynomial P(r) given by $P(r) = \left|(rA^{(0)} - E)\right|$ satisfies $|r_n| \le 1$ and every root satisfying $|r_n| \le 1$ has a multiplicity not greater than the order of the differential equation, then the Block Integrator (1.15) is said to be zero-stable, Furthermore, as $h \to 0, P(r) = r^{\alpha-\mu}(r-1)^{\mu}$ where μ is the order of the differential equation, α is the order of the matrices $A^{(0)}$and E (see also [7]).

Thus, for our block integrator, we have

$$P(r)=\left| r\begin{pmatrix}1&0&0&0&0&0&0&0\\0&1&0&0&0&0&0&0\\0&0&1&0&0&0&0&0\\0&0&0&1&0&0&0&0\\0&0&0&0&1&0&0&0\\0&0&0&0&0&1&0&0\\0&0&0&0&0&0&1&0\\0&0&0&0&0&0&0&1\end{pmatrix} - \begin{pmatrix}0&0&0&0&0&0&0&1\\0&0&0&0&0&0&0&1\\0&0&0&0&0&0&0&1\\0&0&0&0&0&0&0&1\\0&0&0&0&0&0&0&1\\0&0&0&0&0&0&0&1\\0&0&0&0&0&0&0&1\\0&0&0&0&0&0&0&1\end{pmatrix}\right| = 0. \qquad (1.16)$$

$P(r) = (r-1)r^7 = 0, => r_1 = r_2 = \cdots = r_7 = 0, r_8 = 1.$

Hence, our block integrator is zero-stable.

4.2. Order and Error Constant

Using the approach described in [6] and [13]. In equation (1.15), we define the linear difference operator connected with the new hybrid block method as

$$L\{y(t), h\} = A^{(0)}\boldsymbol{Y}_m - E\boldsymbol{y}_n - h[D\boldsymbol{f}(\boldsymbol{y}_n) + B\boldsymbol{F}(\boldsymbol{Y}_m)] \qquad (1.17)$$

We assume $y(t)$ has higher derivatives, as such when the Taylor series is used to expand equation (1.17) and the coefficients of h are compared, the result is

$$L\{y(t),h\} = c_0 y(t) + c_1 h y'(t) + c_2 h^2 y''(t) + c_3 h^3 y'''(t) + \cdots + c_p h^p y^p(t) + \ c_{p+1} h^{(p+1)} y^{(p+1)}(t) + \cdots, \qquad (1.18)$$

where

$$c_p = \frac{1}{p!}\left(\sum_{j=1}^{k} j^p \alpha_j - p \sum_{j=1}^{k} j^{p-1} \beta_j\right), p = 0, 1, 2, 3, \ldots, n. \qquad (1.19)$$

Definition 4.2. According to [6], if $c_0 = c_1 = c_2 = c_3 = \cdots = c_p = 0$, $c_{p+1} \neq 0$, then the linear difference operator and the corresponding continuous LMM are considered to be of the order p. The c_{p+1} is termed the error constant and the local truncation error is defined by

$$T_{n+k} = c_{p+1} h^{(p+1)} y^{(p+1)}(t_n) + O\left(h^{(p+2)}\right) \qquad (1.20)$$

Thus from equation (1.15), we have that

$$L\{y(t),h\} = \begin{bmatrix} 1&0&0&0&0&0&0&0\\ 0&1&0&0&0&0&0&0\\ 0&0&1&0&0&0&0&0\\ 0&0&0&1&0&0&0&0\\ 0&0&0&0&1&0&0&0\\ 0&0&0&0&0&1&0&0\\ 0&0&0&0&0&0&1&0\\ 0&0&0&0&0&0&0&1 \end{bmatrix} \begin{bmatrix} y_{n+\frac{1}{8}}\\ y_{n+\frac{1}{4}}\\ y_{n+\frac{3}{8}}\\ y_{n+\frac{1}{2}}\\ y_{n+\frac{5}{8}}\\ y_{n+\frac{3}{4}}\\ y_{n+\frac{7}{8}}\\ y_{n+1} \end{bmatrix} - \begin{bmatrix} 1\\1\\1\\1\\1\\1\\1\\1 \end{bmatrix} [y_n] - h \begin{bmatrix} \frac{2233547}{14515200} & -\frac{2302297}{14515200} & \frac{2797679}{14515200} & -\frac{31457}{181440} & \frac{1573169}{14515200} & -\frac{645607}{14515200} & \frac{156437}{14515200} & -\frac{33953}{29030400} \\ \frac{22823}{113400} & -\frac{21247}{453600} & \frac{15011}{113400} & -\frac{2903}{22680} & \frac{9341}{113400} & -\frac{15577}{453600} & \frac{953}{113400} & -\frac{119}{129600} \\ \frac{35451}{179200} & \frac{1719}{179200} & \frac{39967}{179200} & -\frac{351}{2240} & \frac{17217}{179200} & -\frac{7031}{179200} & \frac{243}{25600} & -\frac{369}{358400} \\ \frac{2822}{14175} & \frac{61}{28350} & \frac{4094}{14175} & -\frac{227}{2835} & \frac{1154}{14175} & -\frac{989}{28350} & \frac{122}{14175} & -\frac{107}{113400} \\ \frac{115075}{580608} & \frac{3775}{580608} & \frac{159175}{580608} & -\frac{125}{36288} & \frac{85465}{580608} & -\frac{24575}{580608} & \frac{5725}{580608} & -\frac{175}{165888} \\ \frac{279}{1400} & \frac{9}{5600} & \frac{403}{1400} & -\frac{9}{280} & \frac{333}{1400} & \frac{79}{5600} & \frac{9}{1400} & -\frac{9}{11200} \\ \frac{408317}{2073600} & \frac{24353}{2073600} & \frac{542969}{2073600} & \frac{343}{25920} & \frac{368039}{2073600} & \frac{261023}{2073600} & \frac{111587}{2073600} & -\frac{8183}{4147200} \\ \frac{2944}{14175} & -\frac{464}{14175} & \frac{5248}{14175} & -\frac{454}{2835} & \frac{5248}{14175} & -\frac{464}{14175} & \frac{2944}{14175} & \frac{989}{28350} \end{bmatrix} \begin{bmatrix} f_{n+\frac{1}{8}}\\ f_{n+\frac{1}{4}}\\ f_{n+\frac{3}{8}}\\ f_{n+\frac{1}{2}}\\ f_{n+\frac{5}{8}}\\ f_{n+\frac{3}{4}}\\ f_{n+\frac{7}{8}}\\ f_{n+1} \end{bmatrix} = \begin{bmatrix} 0\\0\\0\\0\\0\\0\\0\\0 \end{bmatrix} \qquad (1.21)$$

Expanding equation (1.21) in the Taylor series and evaluating the coefficients using equation (1.19) we have

$$c_0 = c_1 = c_2 = c_3 = c_4 = c_5 = c_6 = c_8 = \ c_9 = 0.$$

Therefore the hybrid block method has an order of nine (9) and an error constant as:

$$c_{10} = [\ 7.3505E - 12, \quad 5.9871E - 12, \quad 6.4964E - 12, \quad 6.1760E - 12, \quad 6.4964E - 12, \quad 5.9871E - 12, \quad 7.3505E - 12]^T$$

Region of Absolute Stability of the Method

Definition 4.2 [14]: A region of absolute stability is one in which $r = \lambda h$ in the complex z plane.

For all initial conditions, it is well-defined as the values for which the numerical solutions of $y' = -\lambda y$ satisfy $y_i \to 0$ as $i \to \infty$.

To establish the region of absolute stability of our block integrator, the boundary locus approach is used. This is accomplished by substituting the test equation

$$y' = -\lambda y,$$

into the block formula in equation (1.15). This gives

$$\boldsymbol{A}^{(0)}\boldsymbol{Y}_m(r) = \boldsymbol{E}\boldsymbol{y}_n(r) - h\lambda\boldsymbol{D}\boldsymbol{y}_n(r) - h\lambda\boldsymbol{B}\boldsymbol{Y}_m(r). \quad (1.22)$$

Given that, $\bar{h} = \lambda h$ and $r = e^{i\theta}$, thus we have

$$\bar{h}(r) = -\left(\frac{\boldsymbol{A}^{(0)}\boldsymbol{Y}_m(r) - \boldsymbol{E}\boldsymbol{y}_n(r)}{\boldsymbol{D}\boldsymbol{y}_n(r) + \boldsymbol{B}\boldsymbol{Y}_m(r)}\right), \quad (1.23)$$

which is the characteristics/stability polynomial. Using equation (1.23), we obtain the stability polynomial for our block method as:

$$\begin{aligned}\bar{h}(r) = &\left(\frac{1}{150994944}r^8 - \frac{1}{150994944}r^7\right)h^8 + \left(-\frac{761}{2642411520}r^8 - \frac{761}{2642411520}r^7\right)h^7 \\ &+ \left(\frac{29531}{3963617280}r^8 - \frac{29531}{3963617280}r^7\right)h^6 + \left(-\frac{89}{655360}r^8 - \frac{89}{655360}r^7\right)h^5 \\ &+ \left(\frac{1069}{589824}r^8 - \frac{1069}{589824}r^7\right)h^4 + \left(-\frac{9}{512}r^8 - \frac{9}{512}r^7\right)h^3 + \left(\frac{91}{768}r^8 - \frac{91}{768}r^7\right)h^2 \\ &+ \left(-\frac{1}{2}r^8 - \frac{1}{2}r^7\right)h + r^8 - r^7.\end{aligned}$$

This gives us the absolute stability region shown in Figure 4.1 below.

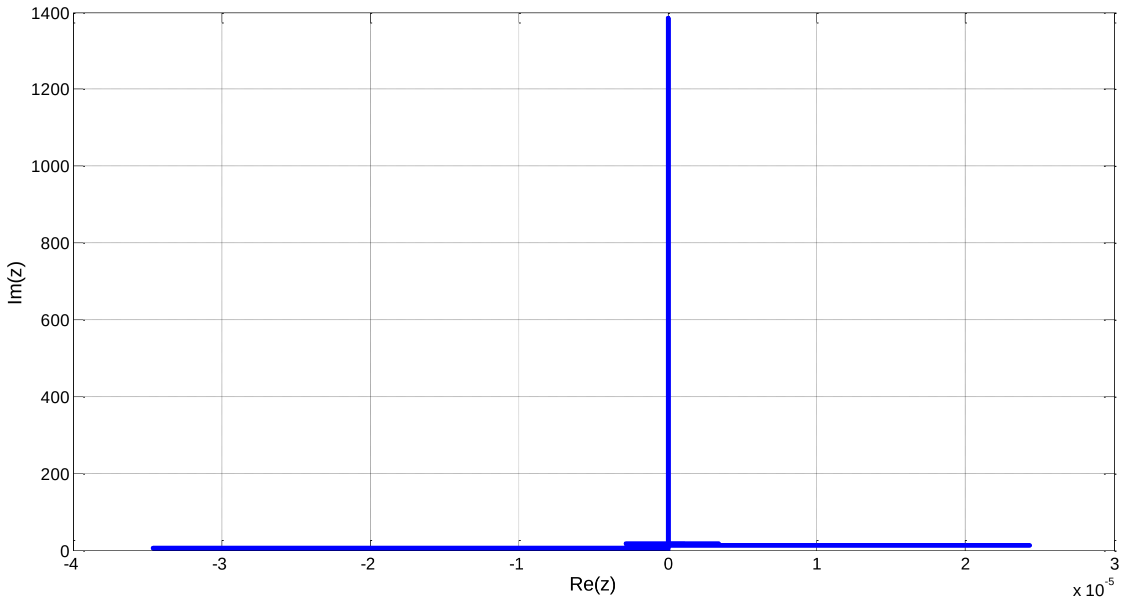

Figure 4.1: Showing the Absolute Stability Region of the Block Method

According to Figure 4.1, the new hybrid block method is effective in handling stiff problems since its RAS (Region of the Absolute Stability) is unbounded [6]. A numerical scheme is considered A-stable if its region of absolute stability R covers the entire complex plane ℂ, which is defined as, $i.e.$ $R = \{Z \in \mathbb{C}/\ Re(Z) < 0\}$ [7]. This confirms that the hybrid block method is an A-stable method.

4.2 Consistency of the Method

If a block method has an order greater than one, it is considered to be consistent [7]. The foregoing analysis shows that our block integrator is consistent.

4.3 Convergence of the Method

An LMM is considered convergent if and only if it satisfies both the requirements of consistency and zero stability [5]. Hence our block integrator is convergent.

5. Numerical Implementations

We compare the results of our method to those obtained by similar methods on some of the most difficult stiff and oscillatory problems in the literature.

The following notations are used in the results tables.

ERROR: The absolute value difference between the exact solution and the computed numerical result is an error. I.e

i. $\boldsymbol{ERROR = |Exact\ solution - Numerical\ result|}$.

ii. $y_{computed}$ = Numerical result **using the new hybrid block method.**

iii. y_{exact} = Exact solution.

Example 5.1: Consider the stiff first-order ODE in [12].

$$y'(t) = \frac{y(1-y)}{2y-1}, \qquad y(0) = \frac{5}{6}, 0 \le t \le 1, \tag{1.24}$$

with the analytical solution $y(t) = \frac{1}{2} + \sqrt{\frac{1}{4} - \frac{5}{35}e^{-t}}$.

Example 5.2: The Prothero-Robinson Oscillatory ODE

We also study the Prothero-Robinson Oscillatory problem solved by [13].

$$y' = L(y - \sin t) + \cos t, \qquad L = -1, \qquad y(0) = 0 \tag{1.25}$$

with the analytical solution $y(t) = \sin t$.

The results obtained at different values of time t, are shown in figures 5.1-5.2, and the absolute error in tables 5.1-5.2.

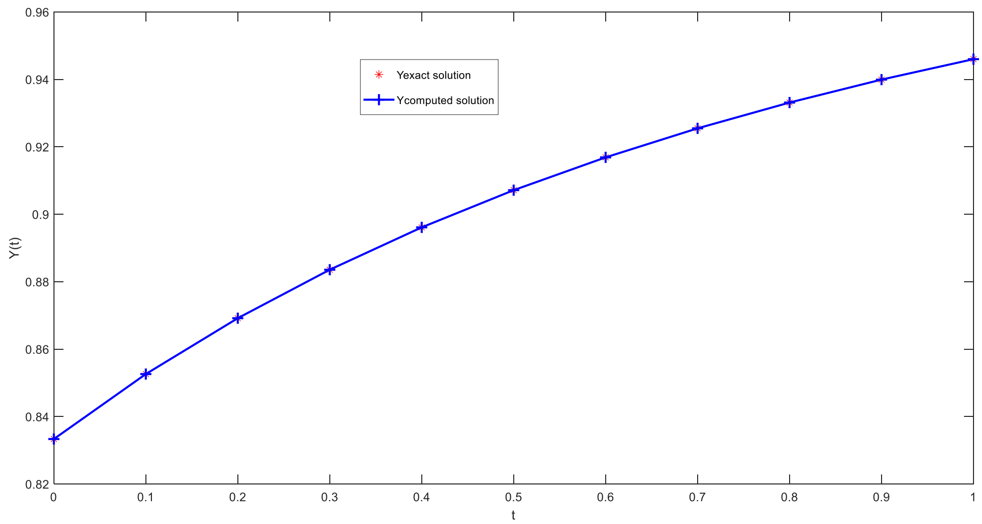

Figure 5.1: Showing the results of Example 5.1 using both analytical and numerical approaches.

h	y_{Exact}	$y_{computed}$	ERROR in New Method	ERROR in [12]
10^{-1}	0.85260195175848715618	0.85260195175848714034	1.584E-17	5.63131E-5
10^{-2}	0.83539987872083210020	0.83539987872083210018	2.0E-20	6.83365E-8
10^{-3}	0.83354149753621050416	0.83354149753621050415	1.0E-20	7.00620E-11
10^{-4}	0.83335416497409883587	0.83335416497409883586	1.0E-20	7.03881E-14
10^{-5}	0.83333541664973972384	0.83333541664973972383	1.0E-20	7.24374E-19

Table 5.1: Results and Absolute Errors of Example 5.1.

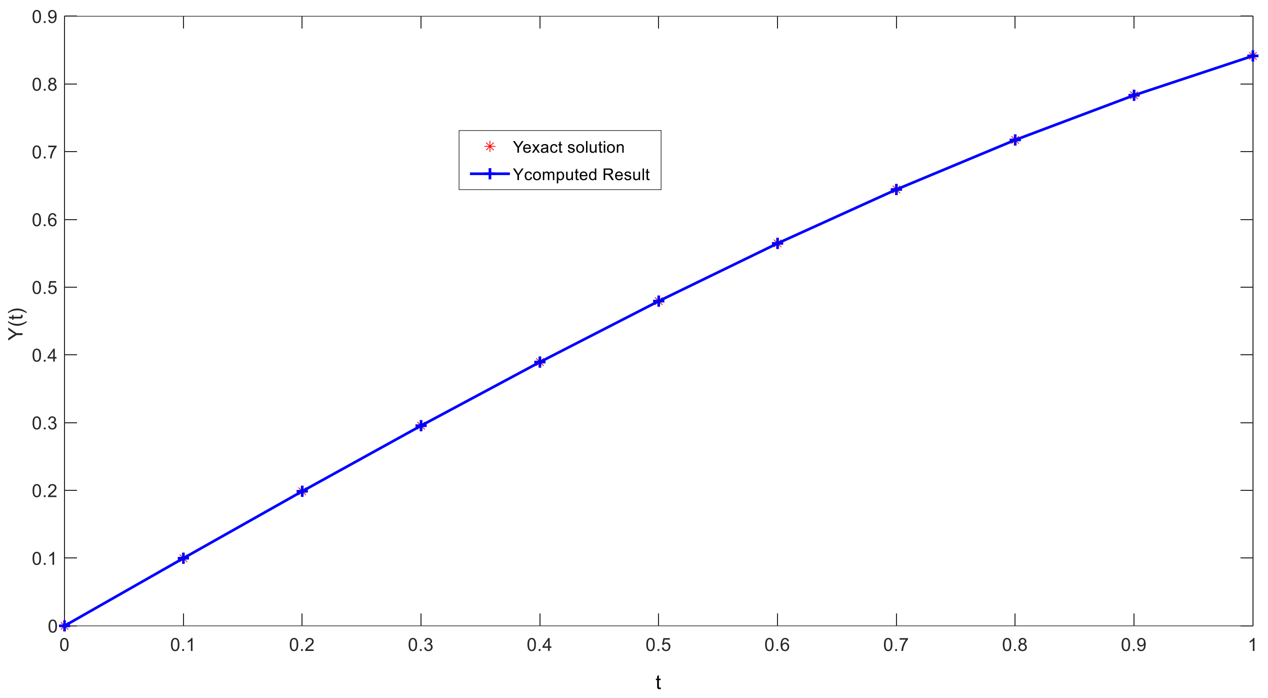

Figure 5.2: Presenting the results of Example 5.2 using both analytical and numerical approaches.

t	y_{Exact}	$y_{computed}$	ERROR in New Method	ERROR in [13]
0.1	0.099833416646828152307	0.099833416646828152301	6.0E-21	1.822016E-14
0.2	0.19866933079506121546	0.19866933079506121544	2.0E-20	2.271482E-14
0.3	0.29552020666133957511	0.29552020666133957508	3.0E-20	4.241108E-14
0.4	0.38941834230865049167	0.38941834230865049164	3.0E-20	1.364169E-14
0.5	0.47942553860420300027	0.47942553860420300024	3.0E-20	6.502551E-14
0.6	0.56464247339503535720	0.56464247339503535714	6.0E-20	9.103963E-14
0.7	0.64421768723769105367	0.64421768723769105357	1.0E-20	1.951339E-14
0.8	0.71735609089952276163	0.71735609089952276154	9.0E-20	7.155093E-14
0.9	0.78332690962748338846	0.78332690962748338836	1.0E-20	5.921081E-14
1.0	0.84147098480789650665	0.84147098480789650656	9.0E-20	8.457038E-14

Table 5.2: Results and Absolute Errors of Example 5.2.

5.1. Discussion of the Results

In this article, we investigated the effectiveness of a new hybrid block method by testing it on two numerical problems: one involving stiff ODEs and the other involving oscillatory ODEs. The stiff problem was previously solved using a seven-step block LMM by [12], while the oscillatory problem was previously solved using a similar derivation of the order seven block method by [13]. Tables 5.1 and 5.2 display the comparative results of problem 5.1 in equation (1.24) and problem 5.2 in equation (1.25), respectively. The new hybrid block method was evaluated against the exact solutions of the two numerical problems, and the results are shown in Figures 5.1-5.2. Our findings demonstrate that the recently developed hybrid block integrator is highly computationally efficient and offers superior performance in precision and stability compared to current methods.

6. Conclusion

This paper presents a novel hybrid block integrator that uses a continuous collocation and interpolation approach to solve stiff and oscillatory first-order ODEs. The hybrid LMM used in this study employs a unique basis function that combines Hermite polynomials and exponential functions, which differs from the approaches used by other researchers. Additionally, the derived LMM is distinct from previous methods. The hybrid block method is both convergent and consistent, with zero stability and an A-stable region of absolute stability. As such, it is well-suited for solving both stiff and oscillatory ODEs.

In terms of accuracy, the novel hybrid block method has outperformed previous methods of similar derivations. The use of combined basis functions in the generation of LMMs is worthy of universal acceptance. The technique indicates that continuous LMMs can be derived from any combination of polynomials and exponential functions utilizing an interpolation and collocation approach.

Author Contributions

All authors contributed equally to this work. They all read and approved the final version of the manuscript.

Conflicts of Interest

The authors declare no conflict of interest.

References

[1] Aboiyar, T., Luga, T., & Iyorter B.V. (2015). Derivation of Continuous Linear Multistep Methods Using Hermite Polynomials as Basis Functions. American Journal of Applied Mathematics and Statistics, 3(6):220-225, doi:10.12691/ajams-3-6-2.

[2] Adesanya, A.O., Sunday, J. & Momoh, A.A. (2014). A New Numerical Integrator for the Solution of General Second Order Ordinary Differential Equations. International Journal of Pure and Applied Mathematics, 97(4):431-445.

[3] Butcher, J. C. (2003). Numerical Methods for Ordinary Differential Equation West Sussex: John Wiley & Sons.

[4] Campbell S.L. and Heberman R. (2011). Introduction to Differential Equations with Dynamical Systems. New Jersey: Princeton University Press. Chap. 1, pp. 1-2.

[5] Dahlquist, G. G. (1956). Convergence and stability in the numerical integration of ordinary differential equations. Math. Scand. 4:33-50.

[6] Fatunla SO. (1988). Numerical methods for initial value problems in ordinary differential Equations. New York: Academic Press Inc;

[7] Fotta A. U., Bello A. and Shelleng Y.I. (2015). Hybrid Block Method for the Solution of First Order Initial Value Problems of Ordinary Differential Equations. IOSR Journal of Mathematics, 2(6):60-66.

[8] Lambert, J. D. (1973). Computational Methods in Ordinary Differential Equations. New York: John Wiley and Sons.

[9] Momoh, A. A., Adesanya, A. O., Fasasi, K. M., and Tahir, A. (2014). A New Numerical Integrator for the Solution of Stiff First Order Ordinary Differential Equations. Engineering Mathematics Letters 5: http://scik.org.

[10] Odekunle, M. R., Adesanya A. O. and Sunday, J. (2012). 4-Point block method for direct integration of first-order ordinary differential equations, International Journal of Engineering Research and Applications, 2:1182-1187.

[11] Okunuga, S.A. & Ehigie, J. (2009). A New Derivation of Continuous Collocation Multistep Methods Using Power Series as Basis Function. Journal of Modern Mathematics and Statistics, 3(2):43-50.

[12] Solomon, G and Hailu, M. (2020). A Seven-Step Block Multistep Method for the Solution of First Order Stiff Differential Equations. Momona Ethiopian Journal of Science 12(1):72-82.

[13] Sunday, J., Odekunle, M.R., James A.A. & Adesanya, A.O. (2014). Numerical Solution of Stiff and Oscillatory Differential Equations Using a Block Integrator. British Journal of Mathematics & Computer Science. 4(17): 2471-2481.

[14] Yan YL. (2011). Numerical methods for differential equations. Kowloon: City University of Hong Kong.

Ikonion Journal of Mathematics (2023) 5(2) 24-52

Ikonion Journal of Mathematics
https://dergipark.org.tr/tr/pub/ikjm
Research Article
Open Access
https://doi.org/10.54286/ikjm.1304566

ISSN: 2687-6531

A New Soft Set Operation: Complementary Soft Binary Piecewise Star (*) Operation

Aslıhan Sezgin * [1], **Ahmet Mücahit Demirci** [2]

Keywords:
Soft set,
Soft set operations,
Conditional Complements.

Abstract — Soft set theory, introduced by Molodtsov, is a crucial mathematical tool for dealing with uncertainty and it has many applications both as theoretically and in applications. Since the beginning, different types of soft set operations have been defined and used in different forms. In this article, we define a new type of soft set operation called the complementary soft binary piecewise star operation and examine its fundamental algebraic properties. Furthermore, by examining the distribution of complementary soft binary piecewise star operations over other type of soft set operations, we aim to identify the relationship between this new soft set operation and others to contribute to the soft set literature. Since proposing a new soft set operation and deriving its algebraic properties and implementations provide several new perspectives for dealing with problems related to parametric data, with the inspiration by this new soft set operation, researchers may be able to propose new cryptographic or decision methods based on soft sets and they may systematically explore soft set algebraic structures associated with new soft set operations.

Subject Classification (2020): 03E75, 20N02.

1. Introduction

Problems in many fields, such as economics, environmental sciences, health sciences, and engineering, have certain uncertainties that prevent them from being successfully solved using classical methods. There are three well-known basic theories that can be considered as mathematical tools for dealing with uncertainty as probability theory, fuzzy set theory, and interval mathematics. However, since each of these theories has its own drawbacks, Molodtsov [21] introduced soft set theory as a mathematical tool to overcome these uncertainties. Since then, this theory has ben applied to many fields including information systems, decision making [6-9,23,24], optimization theory, game theory, operations research, measurement theory, algebraic structures [25] and so on. Soft sets and fuzzy soft sets, one of the first theories in which parameterization tools are used to manage the decision process of uncertainty problems as accurately as possible were discussed in detail by Dalkılıç [10] and these sets were reevaluated and the concept of pure (fuzzy) soft sets was proposed with its properties and examples. First contributions as regards soft set operations were made by Maji et. al [20] and Pei and Miao [26]. After then, several soft set operations (restricted and extended soft set operations)

* aslihan.sezgin@amasya.edu.tr (Corresponding Author)
[1] Amasya University, Department of Mathematics and Science Education, Faculty of Education, 05100, Amasya, Turkey;
[2] Amasya University, Department of Mathematics, Graduate School of Natural and Applied Sciences, 05100, Amasya, Turkey.
Article History: Received: 28.05.2023 — Accepted: 05.09.2023— Published: 12.10.2023

were introduced and examined by Ali et. al [2]. Basic properties of soft set operations were discussed and the interconnections of soft set operations with each other were illustrated by Sezgin and Atagün [29]. They also defined the notion of restricted symmetric difference of soft sets and investigated its properties. A new soft set operation called extended difference of soft sets was defined by Sezgin et.al [37] and extended symmetric difference of soft sets was defined and its properties were investigated by Stojanovic [42]. When the studies are examined, we see that the operations in soft set theory proceed under two main headings, as restricted soft set operations and extended soft set operations. For more about the studies regarding the operation of soft sets, we refer to: [3,4,11-19,22,27-44]

Two conditional complements of sets, i.e. the inclusive complement and the exclusive complement, were proposed as new concepts in set theory, and the relationships between them were studied by Çağman [5]. Inspired by this work, some new complements and then several new additions and to soft set theory as new restricted and extended soft set operations were defined by Aybek [4]. Akbulut [1], Demirci [11], Sarıalioğlu [28] defined a new type of extended operation by changing the form of extended soft set operations using the complement at the first and second row of the piecewise function of extended soft set operations and studied the basic properties of them in detail. Moreover, a new type of soft difference operations was defined in Eren and Çalışıcı [12] and by being inspired this study Yavuz [44] defined some new soft set operations, which ise called soft binary piecewise operations and their basic properties were studied in detail. Also, Sezgin and Sarıalioğlu [36], Sezgin and Atagün [30], Sezgin and Aybek [31], Sezgin et. al [32,33], Sezgin and Çağman [34] continued their work on soft set operations by defining a new type of soft binary piecewise operation. They changed the form of soft binary piecewise operation by using the complement at the first row of the soft binary piecewise operations.

The purpose of this work is to contribute to the soft set theory literature by describing a new soft set operation called the “complementary soft binary piecewise star operation". For this aim, the definition of the operation and its examples are given, and algebraic properties such as closure, associativity, unity, inverse, and abelian properties of this new operation are examined in detail. In particular, we aim to contribute to the soft set literature by obtaining the distributions of complementary soft binary piecewise star operations over other types of soft set operations. The concept of soft set operations is a core concept similar to basic number operations in classical algebra and basic set operations in classical set theory. Proposing new soft set operations and obtaining algebraic properties and their implementations offers new perspectives for solving problems involving parametric data as regards decision-making methods and new cryptographic methods. Also, studying the algebraic structure of soft sets from the perspective of new operations provides deep insight into the algebraic structure of soft sets. This document is organized as follows: Section 2 reminds the basic definitions regarding soft sets. Section 3 provides definitions and examples of the new soft set operation. This is followed by a full analysis of the algebraic properties of this new soft set operation, including closure, associativity, unity, inverse, and abelian properties. To enhance the knowledge of soft sets, Section 4 presents the distribution of complementary soft binary piecewise star operation over extended soft set operations, complementary extended soft set operations, soft binary piecewise operations, complementary soft binary piecewise operations and restricted soft set operation. The conclusion section considers the significance of the research findings and their possible impact on the subject.

2. Preliminaries

In this section, some basic concepts related to soft set theory are compiled and given.

Definition 2.1. Let U be the universal set, E be the parameter set, P(U) be the power set of U and $A \subseteq E$. A pair (F, A) is called a soft set over U where F is a set-valued function such that $F: A \rightarrow P(U)$ [21].

Here, note that Çağman and Enginoğlu [6] redefined the definition of Molodstov's soft sets; however in this paper, we use the Molodtsov's soft set definition by staying faithful to the original definition. Throughout this paper, the set of all the soft sets over U (no matter what the parameter set is) is designated by $S_E(U)$. Let A be a fixed subset of E and $S_A(U)$ be the collection of all soft sets over U with the fixed parameters set A. Clearly, $S_A(U)$ is a subset of $S_E(U)$ and, in fact, all the soft sets are the elements of $S_E(U)$.

Definition 2.2. $(D, \aleph)$ is called a relative null soft set (with respect to the parameter set $\aleph$), denoted by $\emptyset_\aleph$, if $D(t) = \emptyset$ for all $t \in \aleph$ and $(D, \aleph)$ is called a relative whole soft set (with respect to the parameter set $\aleph$), denoted by $U_\aleph$ if $D(t) = U$ for all $t \in \aleph$. The relative whole soft set U_E with respect to the universe set of parameters E is called the absolute soft set over U [2].

Definition 2.3. For two soft sets $(D, \aleph)$ and (J, R), we say that $(D, \aleph)$ is a soft subset of (J, R) and it is denoted by $(D, \aleph) \tilde{\subseteq} (J, R)$, if $\aleph \subseteq R$ and $D(t) \subseteq J(t)$, $\forall t \in \aleph$. Two soft sets $(D, \aleph)$ and (J, R) are said to be soft equal if $(D, \aleph)$ is a soft subset of (J, R) and (J, R) is a soft subset of $(D, \aleph)$ [26].

Definition 2.4. The relative complement of a soft set $(D, \aleph)$, denoted by $(D, \aleph)^r$, is defined by $(D, \aleph)^r = (D^r, \aleph)$, where $D^r: \aleph \rightarrow P(U)$ is a mapping given by $(D, \aleph)^r = U \setminus D(t)$ for all $t \in \aleph$ [2]. From now on, $U \setminus D(t) = [D(t)]'$ will be designated by $D'(s)$ for the sake of designation.

Two conditional complements of sets as new concepts of set theory, that is, inclusive complement and exclusive complement were defined by Çağman [5]. For the ease of illustration, we show these complements as + and θ, respectively. These complements are binary operations and are defined as follows: Let Q and R be two subsets of U. R-inclusive complement of Q is defined by, Q+R= Q'∪R and R-Exlusive complement of Q is defined by $Q\theta$ R = Q'∩R'. Here, U refers to a universe, Q' is the complement of Q over U. For more information, we refer to [35].

The relations between these two complements were examined in detail by Sezgin et.al [35] and they also introduced such new three complements as binary operations of sets as follows: Let Q and R be two subsets of U. Then, Q*R=Q'∪R', $Q\gamma$R= Q'∩R, Q**λ**R=Q∪R'. These set operations were also conveyed to soft sets by Aybek [4] and restricted and extended soft set operations were defined and their properties were examined.

As a summary for soft set operations, we can categorize all types of soft set operations as follows: Let "∇" be used to represent the set operations (i.e., here ∇ can be ∩, ∪,\, Δ, +,θ, *, λ,γ), then restricted soft set operations, extended soft set operations, complementary extended soft set operations, soft binary piecewise operations, complementary soft binary piecewise operations are defined in soft set theory as follows:

Definition 2.5. Let $(D, \aleph)$ and (J, R) be soft sets over U. The restricted ∇ operation of $(D, \aleph)$ and (J, R) is the soft set (Y,S), denoted by $(D, \aleph)\nabla_R(J, R) = (Y, S)$, where $S = \aleph \cap R \neq \emptyset$ and $\forall t \in S$, $Y(t) = D(s) \nabla J(t)$ [2,29].

Definition 2.6. Let $(D,\aleph)$ and (J,R) be soft sets over U. The extended ∇ operation of $(D,\aleph)$ and (J,R) is the soft set (Y,S) denoted by, $(D,\aleph)\nabla_{\varepsilon}(J,R)=(Y,S)$, where $S=\aleph\cup R$ and $\forall t\in S$,

$$Y(s)=\begin{cases} D(t), & t\in\aleph\backslash R,\\ J(t), & t\in R\backslash\aleph,\\ D(t)\nabla J(t), & t\in\aleph\cap R.\end{cases}$$

[2,4,20,37,42]

Definition 2.7. Let $(D,\aleph)$ and (J,R) be soft sets over U. The complementary extended ∇ operation of $(D,\aleph)$ and (J,R) is the soft set (Y,S) denoted by, $(D,\aleph)\overset{*}{\nabla_{\varepsilon}}(J,R)=(Y,S)$, where $S=\aleph\cup R$ and $\forall t\in S$,

$$Y(s)=\begin{cases} D'(t), & t\in\aleph\backslash R\\ J'(t), & t\in R\backslash\aleph,\\ D(t)\nabla J(t), & t\in\aleph\cap R.\end{cases}$$

[1,28].

Definition 2.8. Let $(D,\aleph)$ and (J,R) be soft sets over U. The soft binary piecewise ∇ operation of $(D,\aleph)$ and (J,R) is the soft set $(Y,\aleph)$, denoted by $(D,\aleph)\tilde{\nabla}(J,R)=(Y,\aleph)$, where $\forall s\in\aleph$,

$$Y(s)=\begin{cases} D(s), & s\in\aleph\backslash R\\ D(s)\nabla J(s), & s\in\aleph\cap R\end{cases}$$

[12,44].

Definition 2.9. Let $(D,\aleph)$ and (J,R) be soft sets over U. The complementary soft binary piecewise ∇ operation of $(D,\aleph)$ and (J,R) is the soft set $(Y,\aleph)$ denoted by, $(D,\aleph)\underset{\nabla}{\overset{*}{\sim}}(J,R)=(Y,\aleph)$, where $\forall s\in\aleph$;

$$Y(s)=\begin{cases} D'(s), & s\in\aleph\backslash R\\ D(s)\nabla J(s), & s\in\aleph\cap R\end{cases}$$

[30-34,36].

3. Complementary Soft Binary Piecewise Star (∗) Operation And Its Properties

Definition 3.1. Let $(D,\aleph)$ and (J,R) be soft sets over U. The complementary soft binary piecewise star $(*)$ operation of $(D,\aleph)$ and (J,R) is the soft set $(Y,\aleph)$ denoted by, $(D,\aleph)\underset{*}{\overset{*}{\sim}}(J,R)=(Y,\aleph)$, where $\forall s\in\aleph$,

$$Y(s)=\begin{cases} D'(s), & s\in\aleph\backslash R\\ D'(s)\cup J'(s), & s\in\aleph\cap R\end{cases}$$

Example 3.2. Let E={e_1,e_2,e_3,e_4,e_5} be the parameter set ℵ={e_1, e_3,e_5} and R={e_1, e_2, e_4} be the subsets of E and U={h_1,h_2,h_3,h_4,h_5} be the initial universe set. Assume that (D,ℵ) and (J,R) are the soft sets over U defined as follows: (D,ℵ)={(e_1, {h_1,h_3}), (e_3,{h_2,h_4}), (e_5,{h_2,h_4, h_5})}, (J,R)={(e_1,{h_1,h_4}), (e_2,{h_2,h_3}),(e_4,{ h_4, h_5})}. Let (D, ℵ) $\underset{*}{\overset{*}{\sim}}$ (J,R)=(Y,ℵ). Then,

$$Y(s)=\begin{cases} D'(s), & s\in ℵ\setminus R \\ D'(s) \cup J'(s), & s\in ℵ\cap R \end{cases}$$

Since ℵ={e_1, e_3,e_5} and ℵ\R={e_3, e_5}, so Y(e_3) = D'(e_3)={ h_1,h_3,h_5}, Y(e_5) = D'(e_5)={ h_1,h_3}. And since ℵ∩R={e_1} soY(e_1)=D'(e_1)∪J'(e_1)={h_2,h_4, h_5}∪{h_2,h_3,h_5}={h_2,h_3, h_4, h_5}. Thus, (D, ℵ) $\underset{*}{\overset{*}{\sim}}$ (J,R)={(e_1,{ h_2,h_3, h_4, h_5),} (e_3,{h_1, h_3,h_5}), (e_5, {h_1, h_3})}.

Algebraic Properties of the Operation

1) The set $S_E(U)$ is closed under the operation $\underset{*}{\overset{*}{\sim}}$. That is, when (D,ℵ) and (J,R) are two soft sets over U, then so is (D, ℵ) $\underset{*}{\overset{*}{\sim}}$ (J,R). Hence, the set $S_E(U)$ is closed under the operation $\underset{*}{\overset{*}{\sim}}$.

2) [(D, ℵ) $\underset{*}{\overset{*}{\sim}}$ (J,ℵ)] $\underset{*}{\overset{*}{\sim}}$ (Y, ℵ) ≠ (D, ℵ) $\underset{*}{\overset{*}{\sim}}$ [(J,ℵ) $\underset{*}{\overset{*}{\sim}}$ (Y, ℵ)]

Proof: Let (D, ℵ) $\underset{*}{\overset{*}{\sim}}$ (J,ℵ)=(T,ℵ), where ∀s∈ℵ;

$$T(s)=\begin{cases} D'(s), & s\in ℵ\setminus ℵ=\emptyset \\ D'(s) \cup J'(s), & s\in ℵ\cap ℵ=ℵ \end{cases}$$

Let (T,ℵ) $\underset{*}{\overset{*}{\sim}}$ (Y, ℵ) =(M,ℵ), where ∀s∈ℵ;

$$M(s)=\begin{cases} T'(s), & s\in ℵ\setminus ℵ=\emptyset \\ T'(s) \cup Y'(s), & s\in ℵ\cap ℵ=ℵ \end{cases}$$

Thus,

$$M(s)=\begin{cases} T'(s), & s\in ℵ\setminus ℵ=\emptyset \\ [D(s) \cap J(s)] \cup Y'(s), & s\in ℵ\cap ℵ=ℵ \end{cases}$$

Let (J,ℵ) $\underset{*}{\overset{*}{\sim}}$ (Y,ℵ)=(L,ℵ), where ∀s∈ℵ;

$$L(s)=\begin{cases} J'(s), & s\in\aleph\setminus\aleph=\emptyset \\ J'(s)\cup Y'(s), & s\in\aleph\cap\aleph=\aleph \end{cases}$$

Let $(D,\aleph)\underset{*}{\overset{*}{\sim}}(L,\aleph)=(N,\aleph)$, where $\forall s\in\aleph$;

$$N(s)=\begin{cases} D'(s), & s\in\aleph\setminus\aleph=\emptyset \\ D'(s)\cup L'(s), & s\in\aleph\cap\aleph=\aleph \end{cases}$$

Thus,

$$N(s)=\begin{cases} D'(s), & s\in\aleph\setminus\aleph=\emptyset \\ D'(s)\cup [J(s)\cap Y(s)], & s\in\aleph\cap\aleph=\aleph \end{cases}$$

It is seen that $(M,\aleph)\neq(N,\aleph)$.

That is, for the soft sets whose parameter set are the same, the operation $\underset{*}{\overset{*}{\sim}}$ does not have associativity property.

Moreover, we have the following:

3) $[(D,\aleph)\underset{*}{\overset{*}{\sim}}(J,R)]\underset{*}{\overset{*}{\sim}}(Y,S)\neq(D,\aleph)\underset{*}{\overset{*}{\sim}}[(J,R)\underset{*}{\overset{*}{\sim}}(Y,S)]$

Proof: Let $(D,\aleph)\underset{*}{\overset{*}{\sim}}(J,R)=(T,\aleph)$, where $\forall s\in\aleph$;

$$T(s)=\begin{cases} D'(s), & s\in\aleph\setminus R \quad 7 \\ D'(s)\cup J'(s), & s\in\aleph\cap R \end{cases}$$

Let $(T,\aleph)\underset{*}{\overset{*}{\sim}}(Y,S)=(M,\aleph)$, where $\forall s\in\aleph$;

$$M(s)=\begin{cases} T'(s), & s\in\aleph\setminus S \\ T'(s)\cup Y'(s), & s\in\aleph\cap S \end{cases}$$

Thus,

$$M(s)=\begin{cases} D(s), & s\in(\aleph\setminus R)\setminus S=\aleph\cap R'\cap S' \\ D(s)\cap J(s), & s\in(\aleph\cap R)\setminus S=\aleph\cap R\cap S' \\ D(s)\cup Y'(s), & s\in(\aleph\setminus R)\cap S=\aleph\cap R'\cap S \\ [D(s)\cap J(s)]\cup Y'(s), & s\in(\aleph\cap R)\cap S=\aleph\cap R\cap S \end{cases}$$

Let $(J,R) \underset{*}{\overset{*}{\sim}} (Y,S)=(K,R)$, where $\forall s\in R$;

$$K(s)=\begin{cases} J'(s), & s\in R\backslash S \\ J'(s) \cup Y'(s), & s\in R\cap S \end{cases}$$

Let $(D,\aleph) \underset{*}{\overset{*}{\sim}} (K,R)=(S,\aleph)$, wher $\forall s\in\aleph$;

$$S(s)=\begin{cases} D'(s), & s\in\aleph\backslash R \\ D'(s) \cup K'(s), & s\in\aleph\cap R \end{cases}$$

Thus,

$$S(s)=\begin{cases} D'(s), & s\in\aleph\backslash R \\ D'(s) \cup J(s), & s\in\aleph\cap(R\backslash S)=\aleph\cap R\cap S' \\ D'(s) \cup [J(s) \cap Y(s)], & s\in\aleph\cap(R\cap S)=\aleph\cap R\cap S \end{cases}$$

Here let's handle $s\in\aleph\backslash R$ in the second equation of the first line. Since $\aleph\backslash R=\aleph\cap R'$, if $s\in R'$, then $s\in S\backslash R$ or $s\in(R\cup S)'$. Hence, if $s\in\aleph\backslash R$, then $s\in\aleph\cap R'\cap S'$ or $s\in\aleph\cap R'\cap S$. Thus, it is seen that $(M,\aleph)\neq(S,\aleph)$, that is, for the soft sets whose parameter set are not the same, the operation $\underset{*}{\overset{*}{\sim}}$ does not have associativity property on the set $S_E(U)$.

4) $(D,\aleph) \underset{*}{\overset{*}{\sim}} (J,R)\neq(J,R) \underset{*}{\overset{*}{\sim}} (D,\aleph)$.

Proof: Let $(D,\aleph) \underset{*}{\overset{*}{\sim}} (J,R)=(Y,\aleph)$. Then, $\forall s\in\aleph$;

$$Y(s)=\begin{cases} D'(s), & s\in\aleph\backslash R \\ D'(s) \cup J'(s), & s\in\aleph\cap R \end{cases}$$

Let $(J,R) \underset{*}{\overset{*}{\sim}} (D,\aleph)=(T,R)$. Then, $\forall s\in R$;

$$T(s)=\begin{cases} J'(s), & s\in R\backslash\aleph \\ J'(s) \cup D'(s), & s\in R\cap\aleph \end{cases}$$

Here, while the parameter set of the soft set of the left hand side is $\aleph$; the parameter set of the soft set of the right hand side is R. Thus, by the definition of soft equality

$$(D,\aleph)\overset{*}{\underset{*}{\sim}}(J,R)\neq(J,R)\overset{*}{\underset{*}{\sim}}(D,\aleph).$$

Hence, the operation $\overset{*}{\underset{*}{\sim}}$ does not have commutative property in the set $S_E(U)$, where the parameter sets of the soft sets are different. However it is easy to see that

$$(D,\aleph)\overset{*}{\underset{*}{\sim}}(J,\aleph)=(J,\aleph)\overset{*}{\underset{*}{\sim}}(D,\aleph).$$

That is to say, the operation $\overset{*}{\underset{*}{\sim}}$ does have commutative property where the parameter sets of the soft sets are the same.

5) $(D,\aleph)\overset{*}{\underset{*}{\sim}}(D,\aleph)=(D,\aleph)^r$.

Proof: Let $(D,\aleph)\overset{*}{\underset{*}{\sim}}(D,\aleph)=(Y,\aleph)$. Then, $\forall s\in\aleph$;

$$Y(s)=\begin{cases} D'(s), & s\in\aleph\setminus\aleph=\emptyset \\ D'(s)\cup D'(s), & s\in\aleph\cap\aleph=\aleph \end{cases}$$

Here, $\forall s\in\aleph$, $Y(s)=D'(s)\cup D'(s)=D'(s)$, hence $(Y,\aleph)=(D,\aleph)^r$. That is, the operation $\overset{*}{\underset{*}{\sim}}$ does not have idempotency property on the set $S_E(U)$.

6) $(D,\aleph)\overset{*}{\underset{*}{\sim}}\emptyset_\aleph=\emptyset_\aleph\overset{*}{\underset{*}{\sim}}(D,\aleph)=U_\aleph$.

Proof: Let $\emptyset_\aleph=(S,\aleph)$. Hence, $\forall s\in\aleph$; $S(s)=\emptyset$. Let $(D,\aleph)\overset{*}{\underset{*}{\sim}}(S,\aleph)=(Y,\aleph)$. Then, $\forall s\in\aleph$,

$$Y(s)=\begin{cases} D'(s), & s\in\aleph\setminus\aleph=\emptyset \\ D'(s)\cup S'(s), & s\in\aleph\cap\aleph=\aleph \end{cases}$$

Thus, $\forall s\in\aleph$, $Y(s)=D'(s)\cup S'(s)=D'(s)\cup U=U$. Hence $(Y,\aleph)=U_\aleph$.

7) $(D,\aleph)\overset{*}{\underset{*}{\sim}}\emptyset_E=\emptyset_E\overset{*}{\underset{*}{\sim}}(D,\aleph)=U_\aleph$.

Proof: Let $\emptyset_E=(S,E)$. Hence $\forall s\in E$; $S(s)=\emptyset$. Let $(D,\aleph)\overset{*}{\underset{*}{\sim}}(S,E)=(Y,\aleph)$. Thus, $\forall s\in\aleph$,

$$Y(s)=\begin{cases} D'(s), & s\in\aleph-E=\emptyset \\ D'(s)\cup S'(s), & s\in\aleph\cap E=\aleph \end{cases}$$

Hence, $\forall s\in\aleph$, $Y(s)= D'(s)\cup S'(s)= D'(s)\cup U= U$, so $(Y,\aleph)= U_{\aleph}$.

8) $(D,\aleph)\overset{*}{\underset{*}{\sim}} U_{\aleph}=U_{\aleph}\overset{*}{\underset{*}{\sim}}(D,\aleph)=(D,\aleph)^r$.

Proof: Let $U_{\aleph}=(T,\aleph)$. Hence, $\forall s\in\aleph$, $T(s)=U$. Let $(D,\aleph)\overset{*}{\underset{*}{\sim}}(T,\aleph)=(Y,\aleph)$. Hence, $\forall s\in\aleph$;

$$Y(s)=\begin{cases} D'(s), & s\in\aleph\setminus\aleph=\emptyset \\ D'(s)\cup T'(s), & s\in\aleph\cap\aleph=\aleph \end{cases}$$

Hence, $\forall s\in\aleph$, $Y(s)= D'(s)\cup T'(s)= D'(s)\cup\emptyset= D'(s)$, so $(Y,\aleph)= (D,\aleph)^r$.

9) $(D,P)\overset{*}{\underset{*}{\sim}} U_E=U_E\overset{*}{\underset{*}{\sim}}(D,\aleph)=(D,\aleph)^r$.

Proof: Let $U_E=(T,E)$. Hence, $\forall s\in E$, $T(s)=U$. Let $(D,\aleph)\overset{*}{\underset{*}{\sim}}(T,E)=(Y,\aleph)$, then $\forall s\in\aleph$;

$$Y(s)=\begin{cases} D'(s), & s\in\aleph-E=\emptyset \\ D'(s)\cup T'(s), & s\in\aleph\cap E=\aleph \end{cases}$$

Hence, $\forall s\in\aleph$, $Y(s)= D'(s)\cup T'(s)= D'(s)\cup\emptyset = D'(s)$, so $(Y,\aleph)= (D,\aleph)^r$

10) $(D,\aleph)\overset{*}{\underset{*}{\sim}}(D,\aleph)^r=(D,\aleph)^r\overset{*}{\underset{*}{\sim}}(D,\aleph)= U_{\aleph}$.

Proof: Let $(D,\aleph)^r=(Y,\aleph)$, so $\forall s\in\aleph$, $Y(s)=D'(s)$. Let $(D,P)\overset{*}{\underset{*}{\sim}}(Y,\aleph)=(T,\aleph)$, so $\forall s\in\aleph$,

$$T(s)=\begin{cases} D'(s), & s\in\aleph\setminus\aleph=\emptyset \\ D'(s)\cup Y'(s), & s\in\aleph\cap\aleph=\aleph \end{cases}$$

Hence, $\forall s\in\aleph$, $T(s)= D'(s)\cup Y'(s)= D'(s)\cup D(s)= U$, so $(T,\aleph)= U_{\aleph}$.

11) $[(D,\aleph)\overset{*}{\underset{*}{\sim}}(J,R)]^r=(D,\aleph)\,\tilde{\cap}(J,R)$.

Proof: Let $(D,\aleph)\underset{*}{\overset{*}{\sim}}(J,R)=(Y,\aleph)$. Then, $\forall s\in\aleph$,

$$Y(s)=\begin{cases} D'(s), & s\in\aleph\backslash R \\ D'(s)\cup J'(s), & s\in\aleph\cap R \end{cases}$$

Let $(H,\aleph)^r=(T,\aleph)$, so $\forall s\in\aleph$,

$$T(s)=\begin{cases} D(s), & s\in\aleph\backslash R \\ D(s)\cap J(s), & s\in\aleph\cap R \end{cases}$$

Thus, $(T,\aleph)=(D,\aleph)\,\widetilde{\cap}\,(J,R)$.

In classical theory, $\aleph\cup R=\emptyset\Leftrightarrow\aleph=\emptyset$ and $R=\emptyset$. Now, we have the following:

12) $(D,\aleph)\underset{*}{\overset{*}{\sim}}(J,R)=\emptyset_{\aleph}\Leftrightarrow(D,\aleph)=U_{\aleph}$ and $(J,R)=U_{\aleph\cap R}$.

Proof: Let $(D,\aleph)\underset{*}{\overset{*}{\sim}}(J,R)=(T,\aleph)$. Hence, $\forall s\in\aleph$,

$$T(s)=\begin{cases} D'(s), & s\in\aleph\backslash R \\ D'(s)\cup J'(s), & s\in\aleph\cap R \end{cases}$$

Since $(T,\aleph)=\emptyset_{\aleph}$, $\forall s\in\aleph$, $T(s)=\emptyset$. Hence, $\forall s\in\aleph\backslash R$, $D'(s)=\emptyset$, thus $D(s)=U$ and $\forall s\in\aleph\cap R$, $T(s)=D'(s)\cup J'(s)=\emptyset\Leftrightarrow\forall s\in\aleph\cap R$, $D'(s)=\emptyset$ and $J'(s)=\emptyset\Leftrightarrow\forall s\in\aleph$, $D(s)=U$ and for $\forall s\in\aleph\cap R$, $J(s)=U\Leftrightarrow(D,\aleph)=U_{\aleph}$ and $(J,R)=U_{\aleph\cap R}$.

13) $(D,\aleph)\underset{*}{\overset{*}{\sim}}(J,\aleph)=\emptyset_{\aleph}\Leftrightarrow(D,\aleph)=(J,\aleph)=U_{\aleph}$.

Proof: Let $(D,\aleph)\underset{*}{\overset{*}{\sim}}(J,\aleph)=(T,\aleph)$. Hence, $\forall s\in\aleph$,

$$T(s)=\begin{cases} D'(s), & s\in\aleph\backslash\aleph=\emptyset \\ D'(s)\cup J'(s), & s\in\aleph\cap\aleph=\aleph \end{cases}$$

Since $(T,\aleph)=\emptyset_{\aleph}$, $\forall s\in\aleph$, $T(s)=\emptyset$. Hence, $\forall s\in\aleph$, $T(s)=D'(s)\cup J'(s)=\emptyset\Leftrightarrow\forall s\in\aleph$, $D'(s)=\emptyset$ and $J'(s)=\emptyset\Leftrightarrow\forall s\in\aleph$, $D(s)=U$ and $J(s)=U\Leftrightarrow(D,\aleph)=(J,\aleph)=U_{\aleph}$.

In classical theory, for all $\aleph$, $\emptyset\subseteq\aleph$. Now, we have the following:

14) $\emptyset_{\aleph}\,\widetilde{\subseteq}\,(D,\aleph)\underset{*}{\overset{*}{\sim}}(J,R)$ and $\emptyset_{R}\,\widetilde{\subseteq}\,(J,R)\underset{*}{\overset{*}{\sim}}(D,\aleph)$.

In classical theory, for all $\aleph, \aleph \subseteq U$. Now, we have the following:

15) $(D,\aleph)\overset{*}{\underset{*}{\sim}}(J,R)\ \tilde{\subseteq}\ U_{\aleph}$ and $(J,R)\overset{*}{\underset{*}{\sim}}(D,\aleph)\ \tilde{\subseteq}\ U_R$

In classical theory, $\aleph \subseteq \aleph \cup R$. Now, we have the following:

16) $(D,\aleph)^r\ \tilde{\subseteq}\ (D,\aleph)\overset{*}{\underset{*}{\sim}}(J,R)$, however $(J,R)^r$ needs not to be a soft subset of $(D,\aleph)\overset{*}{\underset{*}{\sim}}(J,R)$.

Proof: Let $(D,\aleph)\overset{*}{\underset{*}{\sim}}(J,R)=(Y,\aleph)$. First of all, $\aleph \subseteq \aleph$. Moreover, $\forall s\in\aleph$,

$$Y(s)=\begin{cases} D'(s), & s\in\aleph\backslash R \\ D'(s)\cup J'(s), & s\in\aleph\cap R \end{cases}$$

Since $\forall s\in\aleph\backslash R$, $D'(s)\subseteq D'(s)$ and $\forall s\in\aleph\cap R$, $D'(s)\subseteq D'(s)\cup J'(s)$, hence $\forall s\in\aleph$, $D'(s)\subseteq Y(s)$. Therefore, $(D,\aleph)^r\ \tilde{\subseteq}\ (Y,\aleph)=(D,\aleph)\overset{*}{\underset{*}{\sim}}(J,R)$,

19) $(D,\aleph)^r\ \tilde{\subseteq}\ (D,\aleph)\overset{*}{\underset{*}{\sim}}(J,\aleph)$, moreover $(J,\aleph)^r\ \tilde{\subseteq}\ (D,\aleph)\overset{*}{\underset{*}{\sim}}(J,\aleph)$.

Proof: Let $(D,\aleph)\overset{*}{\underset{*}{\sim}}(J,\aleph)=(Y,\aleph)$. First of all, $\aleph \subseteq \aleph$. Moreover, $\forall s\in\aleph$,

$$Y(s)=\begin{cases} D'(s), & s\in\aleph\backslash\aleph=\emptyset \\ D'(s)\cup J'(s), & s\in\aleph\cap\aleph=\aleph \end{cases}$$

Since $\forall s\in\aleph, Y(s)=D'(s)\subseteq D'(s)\cup J'(s)$, hence $(D,\aleph)^r\ \tilde{\subseteq}\ (Y,\aleph)=(D,\aleph)\overset{*}{\underset{*}{\sim}}(J,\aleph)$.

4. Distribution Rules

In this section, distributions of complementary soft binary piecewise star $(*)$ operation over other soft set operations such as extended soft set operations, complementary extended soft set operations, restricted soft set operations, soft binary piecewise operations and complementary soft binary piecewise operation are examined in detail and many interesting results are obtained.

Proposition 4.1. Let $(D,\aleph)$, (J,R) and (Y,S) be soft sets over U. Then, for the distributions of complementary soft binary piecewise star $(*)$ operation over extended soft set operations, we have the followings:

i) $(D,\aleph)\overset{*}{\underset{*}{\sim}}[(J,R)\cap_{\varepsilon}(Y,S)]=[(D,\aleph)\overset{*}{\underset{*}{\sim}}(J,R)]\cup_{\varepsilon}[(D,\aleph)\overset{*}{\underset{*}{\sim}}(Y,S)]$.

Proof: Let's first handle the left hand side of the equality and let $(J,R)\cap_{\varepsilon}(Y,S)=(M,R\cup S)$, so $\forall s\in R\cup S$,

$$M(s)=\begin{cases} J(s), & s\in R\setminus S \\ Y(s), & s\in S\setminus R \\ J(s)\cap Y(s), & s\in R\cap S \end{cases}$$

Let $(D,\aleph)\overset{*}{\underset{*}{\sim}}(M,R\cup S)=(N,\aleph)$, $\forall s\in\aleph$,

$$N(s)=\begin{cases} D'(s), & s\in\aleph\setminus(R\cup S) \\ D'(s)\cup M'(s), & s\in\aleph\cap(R\cup S) \end{cases}$$

Hence

$$N(s)=\begin{cases} D'(s), & s\in\aleph\setminus(R\cup S)=\aleph\cap R'\cap S' \\ D'(s)\cup J'(s), & s\in\aleph\cap(R\setminus S)=\aleph\cap R\cap S' \\ D'(s)\cup Y'(s), & s\in\aleph\cap(S\setminus R)=\aleph\cap R'\cap S \\ D'(s)\cup[(J'(s)\cup Y'(s)], & s\in\aleph\cap R\cap S=\aleph\cap R\cap S \end{cases}$$

Now let's handle the right hand side of the equality, that is, $[(D,\aleph)\overset{*}{\underset{*}{\sim}}(J,R)]\cup_{\varepsilon}[(D,\aleph)\overset{*}{\underset{*}{\sim}}(Y,S)]$. Assume that $(D,\aleph)\overset{*}{\underset{*}{\sim}}(J,R)=(V,\aleph)$, then for $\forall s\in\aleph$,

$$V(s)=\begin{cases} D'(s), & s\in\aleph\setminus R \\ D'(s)\cup J'(s), & s\in\aleph\cap R \end{cases}$$

Now let $(D,\aleph)\overset{*}{\underset{*}{\sim}}(Y,S)=(W,\aleph)$. Then, $\forall s\in\aleph$,

$$W(s)=\begin{cases} D'(s), & s\in\aleph\setminus S \\ D'(s)\cup Y'(s), & s\in\aleph\cap S \end{cases}$$

Assume that $(V,\aleph)\cup_{\varepsilon}(W,\aleph)=(T,\aleph)$, then $\forall s\in\aleph$,

$$T(s)=\begin{cases} V(s), & s\in\aleph\setminus\aleph=\emptyset \\ W(s), & s\in\aleph\setminus\aleph=\emptyset \\ V(s)\cup W(s), & s\in\aleph\cap\aleph=\aleph \end{cases}$$

$$T(s)=\begin{cases} D'(s)\cup D'(s), & s\in(\aleph\setminus R)\cap(\aleph\setminus S) \\ D'(s)\cup[D'(s)\cup Y'(s)], & s\in(\aleph\setminus R)\cap(\aleph\cap S) \\ [D'(s)\cup J'(s)]\cup D'(s), & s\in(\aleph\cap R)\cap(\aleph\setminus S) \\ [D'(s)\cup J'(s)]\cup[D'(s)\cup Y'(s)], & s\in(\aleph\cap R)\cap(\aleph\cap S) \end{cases}$$

Thus,

$$T(s)=\begin{cases} D'(s), & s\in ℵ\cap R'\cap S' \\ D'(s)\cup Y'(s), & s\in ℵ\cap R'\cap S \\ D'(s)\cup J'(s), & s\in ℵ\cap R\cap S' \\ [D'(s)\cup J'(s)]\ \cup\ [D'(s)\cup Y'(s)], & s\in ℵ\cap R\cap S \end{cases}$$

It is seen that (N,ℵ)= (T,ℵ).

ii) $(D,ℵ)\underset{*}{\overset{*}{\sim}}[(J,R)\ \cup_\varepsilon (Y,S)] = [(D,ℵ)\underset{*}{\overset{*}{\sim}}(J,R)]\ \cup_\varepsilon\ [(D,ℵ)\underset{*}{\overset{*}{\sim}}(Y,S)]$, where $ℵ\cap R\cap S=\emptyset$.

iii) $(D,ℵ)\underset{*}{\overset{*}{\sim}}[(J,R)\,\lambda_\varepsilon(Y,S)] = [(D,ℵ)\underset{*}{\overset{*}{\sim}}(J,R)]\ \tilde{\cap}\ [(Y,S)\underset{\lambda}{\overset{*}{\sim}}(D,ℵ)]$, where $ℵ\cap R'\cap S=\emptyset$.

iv) $(D,ℵ)\underset{*}{\overset{*}{\sim}}[(J,R)\backslash_\varepsilon(Y,S)] = [(D,ℵ)\underset{*}{\overset{*}{\sim}}(J,R)]\ \tilde{\cup}\ [(Y,S)\underset{\lambda}{\overset{*}{\sim}}(D,ℵ)]$ where $ℵ\cap R'\cap S=\emptyset$.

v) $[(D,ℵ)\cup_\varepsilon(J,R)]\underset{*}{\overset{*}{\sim}}(Y,S)= [(D,ℵ)\underset{*}{\overset{*}{\sim}}(Y,S)]\ \cap_\varepsilon\ [(J,R)\underset{*}{\overset{*}{\sim}}(Y,S)]$

Proof: Let's first handle the left hand side of the equality and let $(D,ℵ)\cap_\varepsilon(J,R)=(M,ℵ\cup R)$, so $\forall s\in ℵ\cup R$,

$$M(s)=\begin{cases} D(s), & s\in ℵ\backslash R \\ J(s), & s\in R\backslash ℵ \\ D(s)\cup J(s), & s\in ℵ\cap R \end{cases}$$

Let $(M,ℵ\cup R)\underset{*}{\overset{*}{\sim}}(Y,S)=(N,ℵ\cup R)$, so $\forall s\in ℵ\cup R$,

$$N(s)=\begin{cases} M'(s), & s\in(ℵ\cup R)\backslash S \\ M'(s)\cup Y'(s), & s\in(ℵ\cup R)\cap S \end{cases}$$

Thus,

$$N(s)=\begin{cases} D'(s), & s\in(ℵ\backslash R)\backslash S=ℵ\cap R'\cap S' \\ J'(s), & s\in(R\backslash ℵ)\backslash S=ℵ'\cap R\cap S' \\ D'(s)\cap J'(s), & s\in(ℵ\cap R)\backslash S=ℵ\cap R\cap S' \\ D'(s)\cup Y'(s), & s\in(ℵ\backslash R)\cap S=ℵ\cap R'\cap S \\ J'(s)\cup Y'(s), & s\in(R\backslash ℵ)\cap S=ℵ'\cap R\cap S \\ [D'(s)\cap J'(s)]\ \cup Y'(s), & s\in(ℵ\cap R)\cap S=ℵ\cap R\cap S \end{cases}$$

Now let's handle the right hand side of the equality: $[(D,ℵ)\underset{*}{\overset{*}{\sim}}(Y,S)]\ \cap_\varepsilon\ [(J,R)\underset{*}{\overset{*}{\sim}}(Y,S)]$. Let $(D,ℵ)\underset{*}{\overset{*}{\sim}}(Y,S)=(V,ℵ)$, so $\forall s\in ℵ$,

$$V(s)=\begin{cases} D'(s), & s\in\aleph\backslash S \\ D'(s)\cup Y'(s), & s\in\aleph\cap S \end{cases}$$

Let $(J,R)\overset{*}{\underset{*}{\sim}}(Y,S)=(W,R)$, so $\forall s\in R$,

$$W(s)=\begin{cases} J'(s), & s\in R\backslash S \\ J'(s)\cup Y'(s), & s\in R\cap S \end{cases}$$

Assume that $(V,\aleph)\cap_{\varepsilon}(W,R)=(T,\aleph\cup R)$, so $\forall s\in\aleph\cup R$,

$$T(s)=\begin{cases} V(s), & s\in\aleph\backslash R \\ W(s), & s\in R\backslash\aleph \\ V(s)\cap W(s), & s\in\aleph\cap R \end{cases}$$

Thus,

$$T(s)=\begin{cases} D'(s), & s\in(\aleph\backslash S)\backslash R=\aleph\cap R'\cap S' \\ D'(s)\cup Y'(s), & s\in(\aleph\cap S)\backslash R=\aleph\cap R'\cap S \\ J'(s), & s\in(R\backslash S)\backslash\aleph=\aleph'\cap R\cap S' \\ J'(s)\cup Y'(s), & s\in(R\cap S)\backslash\aleph=\aleph'\cap R\cap S \\ D'(s)\cap J'(s), & s\in(\aleph\backslash S)\cap(R\backslash S)=\aleph\cap R\cap S' \\ D'(s)\cap[J'(s)\cup Y'(s)], & s\in(\aleph\backslash S)\cap(R\cap S)=\emptyset \\ [D'(s)\cup Y'(s)]\cap J'(s), & s\in(\aleph\cap S)\cap(R\backslash S)=\emptyset \\ [D'(s)\cup Y'(s)]\cap[J'(s)\cup Y'(s)], & s\in(\aleph\cap S)\cap(R\cap S)=\aleph\cap R\cap S \end{cases}$$

It is seen that $(N,\aleph\cup R)=(T,\aleph\cup R)$.

vi) $[(D,\aleph)\cap_{\varepsilon}(J,R)]\overset{*}{\underset{*}{\sim}}(Y,S)=[(D,\aleph)\overset{*}{\underset{*}{\sim}}(Y,S)]\cup_{\varepsilon}[(J,R)\overset{*}{\underset{*}{\sim}}(Y,S)]$

vii) $[(D,\aleph)\lambda_{\varepsilon}(J,R)]\overset{*}{\underset{*}{\sim}}(Y,S)=[(D,\aleph)\overset{*}{\underset{*}{\sim}}(Y,S)]\cap_{\varepsilon}[(J,R)\overset{*}{\underset{\lambda}{\sim}}(Y,S)]$, where $\aleph\cap R\cap S'=\aleph'\cap R\cap S=\emptyset$.

viii) $[(D,\aleph)\backslash_{\varepsilon}(J,R)]\overset{*}{\underset{*}{\sim}}(Y,S)=[(D,\aleph)\overset{*}{\underset{*}{\sim}}(Y,S)]\cup_{\varepsilon}[(J,R)\overset{*}{\underset{\lambda}{\sim}}(Y,S)]$, where $\aleph\cap R\cap S'=\aleph'\cap R\cap S=\emptyset$.

Proposition 4.2. Let $(D,\aleph)$, (J,R) and (Y,S) be soft sets over U. Then, for the distributions of complementary soft binary piecewise star ($*$) operation over complementary extended soft set operations, we have the followings:

i) $(D,\aleph)\overset{*}{\underset{*}{\sim}}[(J,R)\overset{*}{\theta}_{\varepsilon}(Y,S)]=[(D,\aleph)\overset{*}{\underset{+}{\sim}}(J,R)]\cup_{\varepsilon}[(D,\aleph)\overset{*}{\underset{+}{\sim}}(Y,S)]$, where $\aleph\cap R\cap S=\emptyset$

Proof: Let's first handle the left hand side of the equality. Assume $(J,R)\overset{*}{\theta_\varepsilon}(Y,S)=(M,R\cup S)$, so $\forall s\in R\cup S$,

$$M(s)=\begin{cases} J'(s), & s\in R\setminus S \\ Y'(s), & s\in S\setminus R \\ J'(s)\cap Y'(s), & s\in R\cap S \end{cases}$$

Let $(D,\aleph)\underset{*}{\overset{*}{\sim}}(M,R\cup S)=(N,\aleph)$, then $\forall s\in\aleph$,

$$N(s)=\begin{cases} D'(s), & s\in\aleph\setminus(R\cup S) \\ D'(s)\cup M'(s), & s\in\aleph\cap(R\cup S) \end{cases}$$

Hence,

$$N(s)=\begin{cases} D'(s), & s\in\aleph\setminus(R\cup S)=\aleph\cap R'\cap S' \\ D'(s)\cup J(s), & s\in\aleph\cap(R\setminus S)=\aleph\cap R\cap S' \\ D'(s)\cup Y(s), & s\in\aleph\cap(S\setminus R)=\aleph\cap R'\cap S \\ D'(s)\cup[J(s)\cup Y(s)], & s\in\aleph\cap R\cap S=\aleph\cap R\cap S \end{cases}$$

Now let's handle the right hand side of the equality: $[(D,\aleph)\underset{+}{\overset{*}{\sim}}(J,R)]\cup_\varepsilon[(D,\aleph)\underset{+}{\overset{*}{\sim}}(Y,S)]$. Let $(D,\aleph)\underset{+}{\overset{*}{\sim}}(J,R)=(V,\aleph)$, so $\forall s\in\aleph$,

$$V(s)=\begin{cases} D'(s), & s\in\aleph\setminus R \\ D'(s)\cup J(s), & s\in\aleph\cap R \end{cases}$$

Let $(D,\aleph)\underset{+}{\overset{*}{\sim}}(Y,S)=(W,\aleph)$, hence $\forall s\in\aleph$,

$$W(s)=\begin{cases} D'(s), & s\in\aleph\setminus S \\ D'(s)\cup Y(s),, & s\in\aleph\cap S \end{cases}$$

Assume that $(V,\aleph)\cup_\varepsilon(W,\aleph)=(T,\aleph)$, hence $\forall s\in\aleph$,

$$T(s)=\begin{cases} V(s), & s\in\aleph\setminus\aleph=\emptyset \\ W(s), & s\in\aleph\setminus\aleph=\emptyset \\ V(s)\cup W(s), & s\in\aleph\cap\aleph=\aleph \end{cases}$$

Hence,

$$T(s)=\begin{cases} D'(s)\cup D'(s), & s\in(\aleph\setminus R)\cap(\aleph\setminus S) \\ D'(s)\cup[D'(s)\cup Y(s)], & s\in(\aleph\setminus R)\cap(\aleph\cap R) \\ [D'(s)\cup J(s)]\cup D'(s), & s\in(\aleph\cap R)\cap(\aleph\setminus S) \\ [D'(s)\cup J(s)]\cup[D'(s)\cup Y(s)], & s\in(\aleph\cap R)\cap(\aleph\cap S) \end{cases}$$

Thus,

$$T(s)=\begin{cases} D'(s), & s\in\aleph\cap R'\cap S' \\ D'(s)\cup Y(s), & s\in\aleph\cap R'\cap S \\ D'(s)\cup J(s), & s\in\aleph\cap R\cap S' \\ [D'(s)\cup J(s)]\ \cup\ [D'(s)\cup Y(s)], & s\in\aleph\cap R\cap S \end{cases}$$

It is seen that $(N,\aleph)=(T,\aleph)$.

ii) $(D,\aleph)\overset{*}{\underset{*}{\sim}}[(J,R)\overset{*}{*}_{\varepsilon}(Y,S)]=[(D,\aleph)\overset{*}{\underset{+}{\sim}}(J,R)]\ \cup_{\varepsilon}\ [(D,\aleph)\overset{*}{\underset{+}{\sim}}(Y,S)]$ where $\aleph\cap R\cap S=\emptyset$.

iii) $(D,\aleph)\overset{*}{\underset{\theta}{\sim}}[(J,R)\overset{*}{+}_{\varepsilon}(Y,S)]=[(D,\aleph)\overset{*}{\underset{+}{\sim}}(J,R)]\ \tilde{\cap}\ [(Y,S)\overset{*}{\underset{*}{\sim}}(D,\aleph)]$ where $\aleph\cap R'\cap S=\emptyset$.

iv) $(D,\aleph)\overset{*}{\underset{*}{\sim}}[(J,R)\overset{*}{\gamma}_{\varepsilon}(Y,S)]=[(D,\aleph)\overset{*}{\underset{+}{\sim}}(J,R)]\ \tilde{\cup}[(Y,S)\overset{*}{\underset{*}{\sim}}(D,\aleph)]$ where $\aleph\cap R'\cap S=\emptyset$.

v) $[(D,\aleph)\overset{*}{*}_{\varepsilon}(J,R)]\overset{*}{\underset{*}{\sim}}(Y,S)=[(D,\aleph)\tilde{\lambda}(Y,S)]\ \cap_{\varepsilon}\ [(J,R)\tilde{\lambda}(Y,S)]$.

Proof: Let's first handle the left hand side of the equality. Assume $(D,\aleph)\overset{*}{*}_{\varepsilon}(J,R)=(M,\aleph\cup R)$ and $\forall s\in\aleph\cup R$,

$$M(s)=\begin{cases} D'(s), & s\in\aleph\setminus R \\ J'(s), & s\in R\setminus\aleph \\ D'(s)\cup J'(s), & s\in\aleph\cap R \end{cases}$$

Let $(M,\aleph\cup R)\overset{*}{\underset{*}{\sim}}(Y,S)=(N,\aleph\cup R)$ and $\forall s\in\aleph\cup R$,

$$N(s)=\begin{cases} M'(s), & s\in(\aleph\cup R)\setminus S \\ M'(s)\cup Y'(s), & s\in(\aleph\cup R)\cap S \end{cases}$$

Thus,

$$N(s)=\begin{cases} D(s), & s\in(\aleph\setminus R)\setminus S=\aleph\cap R'\cap S' \\ J(s), & s\in(R\setminus\aleph)\setminus S=\aleph'\cap R\cap S' \\ D(s)\cap J(s), & s\in(\aleph\cap R)\setminus S=\aleph\cap R\cap S' \\ D(s)\cup Y'(s), & s\in(\aleph\setminus R)\cap S=\aleph\cap R'\cap S \\ J(s)\cup Y'(s), & s\in(R\setminus\aleph)\cap S=\aleph'\cap R\cap S \\ [D(s)\cap J(s)]\ \cup Y'(s), & s\in(\aleph\cap R)\cap S=\aleph\cap R\cap S \end{cases}$$

Now let's handle the right hand side of the equality: $[(D,\aleph)\tilde{\lambda}(Y,S)] \cap_{\varepsilon} [(J,R)\tilde{\lambda}(Y,S)]$. Let $(D,\aleph)\tilde{\lambda}(Y,S)=(V,\aleph)$ and $\forall s\in\aleph$

$$V(s)=\begin{cases} D(s), & s\in\aleph\setminus S \\ D(s)\cup Y'(s), & s\in\aleph\cap S \end{cases}$$

Let $(J,R)\tilde{\lambda}(Y,S)=(W,R)$ and $\forall s\in R$,

$$W(s)=\begin{cases} J(s), & s\in R\setminus S \\ J(s)\cup Y'(s), & s\in R\cap S \end{cases}$$

Assume that $(V,\aleph)\cap_{\varepsilon}(W,R)=(T,\aleph\cup R)$ and $\forall s\in\aleph\cup R$,

$$T(s)=\begin{cases} V(s), & s\in\aleph\setminus R \\ W(s), & s\in R\setminus\aleph \\ V(s)\cap W(s), & s\in\aleph\cap R \end{cases}$$

Hence,

$$T(s)=\begin{cases} D(s), & s\in(\aleph\setminus S)\setminus R=\aleph\cap R'\cap S' \\ D(s)\cup Y'(s) & s\in(\aleph\cap S)\setminus R=\aleph\cap R'\cap S \\ J(s), & s\in(R\setminus S)\setminus\aleph=\aleph'\cap R\cap S' \\ J(s)\cup Y'(s), & s\in(R\cap S)\setminus\aleph=\aleph'\cap R\cap S \\ D(s)\cap J(s), & s\in(\aleph\setminus S)\cap(R\setminus S)=\aleph\cap R\cap S' \\ D(s)\cap[J(s)\cup Y'(s)], & s\in(\aleph\setminus S)\cap(R\cap S)=\emptyset \\ [D(s)\cup Y'(s)]\cap J(s), & s\in(\aleph\cap S)\cap(R\setminus S)=\emptyset \\ [D(s)\cup Y'(s)]\cap[J(s)\cup Y'(s)], & s\in(\aleph\cap S)\cap(R\cap S)=\aleph\cap R\cap S \end{cases}$$

It is seen that $(N,\aleph\cup R)=(T,\aleph\cup R)$.

vi) $[(D,\aleph)\overset{*}{\theta_{\varepsilon}}(J,R)]\ \underset{*}{\overset{*}{\sim}}\ (Y,S)=[(D,\aleph)\tilde{\lambda}(Y,S)] \cup_{\varepsilon} [(J,R)\tilde{\lambda}(Y,S)]$

vii) $[(D,\aleph)\overset{*}{\gamma_{\varepsilon}}(J,R)]\ \underset{*}{\overset{*}{\sim}}\ (Y,S)=[(D,\aleph)\tilde{\lambda}(Y,S)]\cup_{\varepsilon}[(J,R)\ \underset{*}{\sim}\ (Y,S)]$ where $\aleph\cap R\cap S'=\aleph'\cap R\cap S=\emptyset$.

viii) $[(D,\aleph)\overset{*}{+_{\varepsilon}}(J,R)]\ \underset{*}{\overset{*}{\sim}}\ (Y,S)=[(D,\aleph)\tilde{\lambda}(Y,S)]\cap_{\varepsilon}[(J,R)\tilde{\lambda}(Y,S)]$, where $\aleph\cap R\cap S'=\aleph\cap R\cap S=\emptyset$.

Proposition 4.3. Let $(D,\aleph)$, (J,R) and (Y,S) be soft sets over U. Then, for the distributions of complementary soft binary piecewise star $(*)$ operation over soft binary piecewise operations, we have the followings:

i) $(D,\aleph)\underset{*}{\overset{*}{\sim}}[(J,R)\ \tilde{\cup}\ (Y,S)] = [(D,\aleph)\underset{*}{\overset{*}{\sim}}(J,R)]\ \tilde{\cap}\ [(Y,S)\underset{*}{\overset{*}{\sim}}(D,\aleph)]$.

Proof: Let's first handle the left hand side of the equality and let $(J,R)\tilde{\cup}(Y,S)=(M,R)$, so $\forall s\in R\cup S$,

$$M(s)=\begin{cases} J(s), & s\in R\setminus S \\ J(s)\cup Y(s), & s\in R\cap S \end{cases}$$

$(D,\aleph)\underset{*}{\overset{*}{\sim}}(M,R)=(N,\aleph)$, where $\forall s\in\aleph$;

$$N(s)=\begin{cases} D'(s), & s\in\aleph\setminus R \\ D'(s)\cup M'(s), & s\in\aleph\cap R \end{cases}$$

Thus,

$$N(s)=\begin{cases} D'(s), & s\in\aleph\setminus R \\ D'(s)\cup J'(s), & s\in\aleph\cap(R\setminus S)=\aleph\cap R\cap S' \\ D'(s)\cup[J'(s)\cap Y'(s)], & s\in\aleph\cap R\cap S=\aleph\cap R\cap S \end{cases}$$

Now let's handle the right hand side of the equality: $[(D,\aleph)\underset{*}{\overset{*}{\sim}}(J,R)]\ \tilde{\cap}\ [(Y,S)\underset{*}{\overset{*}{\sim}}(D,\aleph)]$. Assume that $(D,\aleph)\underset{*}{\overset{*}{\sim}}(J,R)=(V,\aleph)$, then for $\forall s\in\aleph$,

$$V(s)=\begin{cases} D'(s), & s\in\aleph\setminus R \\ D'(s)\cup J'(s), & s\in\aleph\cap R \end{cases}$$

Now let $(Y,S)\underset{*}{\overset{*}{\sim}}(D,\aleph)=(W,S)$. Then, $\forall s\in S$,

$$W(s)=\begin{cases} Y'(s), & s\in S\setminus\aleph \\ Y'(s)\cup D'(s), & s\in S\cap\aleph \end{cases}$$

Assume that $(V,\aleph)\ \tilde{\cap}(W,S)=(T,\aleph)$, then $\forall s\in\aleph$,

$$T(s)=\begin{cases} V(s), & s\in\aleph\setminus S \\ V(s)\cap W(s), & s\in\aleph\cap S \end{cases}$$

Thus,

$$T(s)=\begin{cases} D'(s), & s\in(\aleph\setminus R)\setminus S=\aleph\cap R'\cap S' \\ D'(s)\cup J'(s) & s\in(\aleph\cap R)\setminus S=\aleph\cap R'\cap S \\ D'(s)\cap Y'(s), & s\in(\aleph\setminus R)\cap(S\setminus\aleph)=\emptyset \\ D'(s)\cap[Y'(s)\cup D'(s)], & s\in(\aleph\setminus R)\cap(S\cap\aleph)=\aleph\cap R'\cap S \\ [D'(s)\cup J'(s)]\cap Y'(s) & s\in(\aleph\cap R)\cap(S\setminus\aleph)=\emptyset \\ [D'(s)\cup J'(s)]\cap[Y'(s)\cup D'(s)], & s\in(\aleph\cap R)\cap(S\cap\aleph)=\aleph\cap R\cap S \end{cases}$$

Thus,

$$T(s)=\begin{cases} D'(s), & s\in(\aleph\backslash R)\backslash S=\aleph\cap R'\cap S' \\ D'(s)\cup J'(s) & s\in(\aleph\cap R)\backslash S=\aleph\cap R\cap S' \\ D'(s)\cap Y'(s), & s\in(\aleph\backslash R)\cap(S\backslash\aleph)=\emptyset \\ D'(s) & s\in(P\backslash R)\cap(S\cap\aleph)=\aleph\cap R'\cap S \\ [D'(s)\cup J'(s)]\cap Y'(s) & s\in(\aleph\cap R)\cap(S\backslash\aleph)=\emptyset \\ [D'(s)\cup J'(s)]\cap[Y'(s)\cup D'(s)], & s\in(\aleph\cap R)\cap(S\cap\aleph)=\aleph\cap R\cap S \end{cases}$$

Since $\aleph\backslash R=\aleph\cap R'$, if $s\in R'$, then $s\in S\backslash R$ or $s\in(R\cup S)'$. Hence, if $s\in\aleph\backslash R$, $s\in\aleph\cap R'\cap S'$ or $s\in\aleph\cap R'\cap S$. Thus, it is seen that $(N,\aleph)=(T,\aleph)$.

ii) $(D,\aleph)\underset{*}{\overset{*}{\sim}}[(J,R)\ \tilde{\cap}\ (Y,S)]=[(D,\aleph)\underset{*}{\overset{*}{\sim}}(J,R)]\ \tilde{\cap}\ [(Y,S)\underset{*}{\overset{*}{\sim}}(D,\aleph)]$ where $\aleph\cap R\cap S=\emptyset$

iii**)** $(D,\aleph)\underset{*}{\overset{*}{\sim}}[(J,R)\ \tilde{\lambda}\ (Y,S)]=[(D,\aleph)\underset{*}{\overset{*}{\sim}}(J,R)]\ \tilde{\cap}\ [(Y,S)\underset{\lambda}{\overset{*}{\sim}}(D,\aleph)]$.

iv) $(D,\aleph)\underset{*}{\overset{*}{\sim}}[(J,R)\ \tilde{\backslash}\ (Y,S)]=[(D,\aleph)\underset{*}{\overset{*}{\sim}}(J,R)]\ \tilde{\cap}\ [(Y,S)\underset{\lambda}{\overset{*}{\sim}}(D,\aleph)]$.

v) $[(D,\aleph)\ \tilde{\cap}\ (J,R)]\underset{*}{\overset{*}{\sim}}(Y,S)=[(D,\aleph)\underset{*}{\overset{*}{\sim}}(Y,S)]\ \tilde{\cup}\ [(J,R)\underset{*}{\overset{*}{\sim}}(Y,S)]$

Proof: Let's first handle the left hand side of the equality. Suppose $(D,\aleph)\ \tilde{\cap}\ (J,R)=(M,\aleph)$, so $\forall s\in\aleph$ için,

$$M(s)=\begin{cases} D(s), & s\in\aleph\backslash R \\ D(s)\cap J(s), & s\in\aleph\cap R \end{cases}$$

Let $(M,\aleph)\underset{*}{\overset{*}{\sim}}(Y,S)=(N,\aleph)$, so $\forall s\in\aleph$,

$$N(s)=\begin{cases} M'(s), & s\in\aleph\backslash S \\ M'(s)\cup Y'(s), & s\in\aleph\cap S \end{cases}$$

Thus,

$$N(s)=\begin{cases} D'(s), & s\in(\aleph\backslash R)\backslash S=\aleph\cap R'\cap S' \\ D'(s)\cup J'(s), & s\in(\aleph\cap R)\backslash S=\aleph\cap R\cap S' \\ D'(s)\cup Y'(s), & s\in(\aleph\backslash R)\cap S=\aleph\cap R'\cap S \\ [D'(s)\cup J'(s)]\cup Y'(s), & s\in(\aleph\cap R)\cap S=\aleph\cap R\cap S \end{cases}$$

Now let's handle the right hand side of the equality: $[(D,\aleph)\overset{*}{\underset{*}{\sim}}(Y,S)]\ \tilde{\cup}\ [(J,R)\overset{*}{\underset{*}{\sim}}(Y,S)]$. Let $(D,\aleph)\overset{*}{\underset{*}{\sim}}(Y,S)=(V,\aleph)$, so $\forall s\in\aleph$,

$$V(s)=\begin{cases} D'(s), & s\in\aleph\setminus S \\ D'(s)\cup Y'(s), & s\in\aleph\cap S \end{cases}$$

Let $(J,R)\overset{*}{\underset{*}{\sim}}(Y,S)=(W,R)$, so $\forall s\in R$,

$$W(s)=\begin{cases} J'(s), & s\in R\setminus S \\ J'(s)\cup Y'(s), & s\in R\cap S \end{cases}$$

Assume that $(V,\aleph)\tilde{\cup}(W,R)=(T,\aleph)$, so $\forall s\in\aleph$,

$$T(s)=\begin{cases} V(s), & s\in\aleph\setminus R \\ V(s)\cup W(s), & s\in\aleph\cap R \end{cases}$$

Hence,

$$T(s)=\begin{cases} D'(s), & s\in(\aleph\setminus S)\setminus R=\aleph\cap R'\cap S' \\ D'(s)\cup Y'(s), & s\in(\aleph\cap S)\setminus R=\aleph\cap R'\cap S \\ D'(s)\cup J'(s), & s\in(\aleph\setminus S)\cap(R\setminus S)=\aleph\cap R\cap S' \\ D'(s)\cup[J'(s)\cup Y'(s)], & s\in(\aleph\setminus S)\cap(R\cap S)=\emptyset \\ [D'(s)\cup Y'(s)]\cup J'(s), & s\in(\aleph\cap S)\cap(R\setminus S)=\emptyset \\ [D'(s)\cup Y'(s)]\cup[J'(s)\cup Y'(s)], & s\in(\aleph\cap S)\cap(R\cap S)=\aleph\cap R\cap S \end{cases}$$

It is seen that $(N,\aleph)=(T,\aleph)$.

vi) $[(D,\aleph)\ \tilde{\cup}\ (J,R)]\overset{*}{\underset{*}{\sim}}(Y,S)=[(D,\aleph)\overset{*}{\underset{*}{\sim}}(Y,S)]\ \tilde{\cap}\ [(J,R)\overset{*}{\underset{*}{\sim}}(Y,S)]$

vii) $[(D,\aleph)\ \widetilde{\setminus}(J,R)]\overset{*}{\underset{*}{\sim}}(Y,S)=[(D,\aleph)\overset{*}{\underset{*}{\sim}}(Y,S)]\ \tilde{\cup}\ [(J,R)\ \tilde{\lambda}\ (Y,S)]$.

viii) $[(D,\aleph)\ \widetilde{\lambda}(J,R)]\overset{*}{\underset{*}{\sim}}(Y,S)=[(D,\aleph)\overset{*}{\underset{*}{\sim}}(Y,S)]\ \tilde{\cap}\ [(J,R)\ \tilde{\lambda}\ (Y,S)]$.

Proposition 4.4. Let $(D,\aleph)$, (J,R) and (Y,S) be soft sets over U. Then, for the distributions of complementary soft binary piecewise star ($*$) operation over complementary soft binary piecewise operations we have the followings:

i) $(D,\aleph)\overset{*}{\underset{*}{\sim}}[(J,R)\overset{*}{\underset{*}{\sim}}(Y,S)]=[(D,\aleph)\overset{*}{\underset{+}{\sim}}(J,R)]\ \tilde{\cap}\ [(D,\aleph)\overset{*}{\underset{+}{\sim}}(Y,S)]$ where $\aleph\cap R\cap S'=\emptyset$

Proof: Let's first handle the left hand side of the equality, suppose $(J,R)\underset{*}{\overset{*}{\sim}}(Y,S)=(M,R)$, so $\forall s\in R$,

$$M(s)=\begin{cases} J'(s), & s\in R\setminus S \\ J'(s)\cup Y'(s), & s\in R\cap S \end{cases}$$

Let $(D,\aleph)\underset{*}{\overset{*}{\sim}}(M,R)=(N,\aleph)$, so $\forall s\in\aleph$,

$$N(s)=\begin{cases} D'(s), & s\in\aleph\setminus R \\ D'(s)\cup M'(s), & s\in(\aleph\cap R \end{cases}$$

Thus,

$$N(s)=\begin{cases} D'(s), & s\in\aleph\setminus R \\ D'(s)\cup J(s), & s\in\aleph\cap(R\setminus S)=\aleph\cap R\cap S' \\ D'(s)\cup\ [(J(s)\cap H(s)], & s\in\aleph\cap R\cap S=\aleph\cap R\cap S \end{cases}$$

Now let's handle the right hand side of the equality: $(D,\aleph)\underset{+}{\overset{*}{\sim}}(J,R)]\ \tilde{\cap}\ [(D,\aleph)\underset{+}{\overset{*}{\sim}}(Y,S)]$. Let $(D,\aleph)\underset{+}{\overset{*}{\sim}}(J,R)=(V,\aleph)$, so $\forall s\in\aleph$,

$$V(s)=\begin{cases} D'(s), & s\in\aleph\setminus R \\ D'(s)\cup J(s), & s\in\aleph\cap R \end{cases}$$

Let $(D,\aleph)\underset{+}{\overset{*}{\sim}}(Y,S)=(W,\aleph)$, so $\forall s\in\aleph$,

$$W(s)=\begin{cases} D'(s), & s\in\aleph\setminus S \\ D'(s)\cup Y(s), & s\in\aleph\cap S \end{cases}$$

Assume that $(V,\aleph)\tilde{\cap}(W,\aleph)=(T,\aleph)$, so $\forall s\in\aleph$,

$$T(s)=\begin{cases} V(s), & s\in\aleph\setminus\aleph=\emptyset \\ V(s)\cap W(s), & s\in(\aleph\cap\aleph=\aleph \end{cases}$$

Thus,

$$T(s)=\begin{cases} D'(s) & s\in(\aleph\setminus R)\cap(\aleph\setminus S)=\aleph\cap R'\cap S' \\ D'(s)\cap\ [D'(s)\cup Y(s)], & s\in(\aleph\setminus R)\cap(\aleph\cap S)=\aleph\cap R'\cap S \\ [D'(s)\cup J(s)]\cap D'(s), & s\in(\aleph\cap R)\cap(\aleph\setminus S)=\aleph\cap R\cap S' \\ [D'(s)\cup J(s)]\cap[D'(t)\cup Y(t)], & s\in(\aleph\cap R)\cap(\aleph\cap S)=\aleph\cap R\cap S \end{cases}$$

Thus,

$$T(s)=\begin{cases} D'(s) & s\in(\aleph\backslash R)\cap(\aleph\backslash S)=\aleph\cap R'\cap S' \\ D'(s), & s\in(\aleph\backslash R)\cap(\aleph\cap S)=\aleph\cap R'\cap S \\ D'(s), & s\in(\aleph\cap R)\cap(\aleph\backslash S)=\aleph\cap R\cap S' \\ [D'(s)\cup J(s)]\cap[D'(t)\cup Y(t)], & s\in(\aleph\cap R)\cap(\aleph\cap S)=\aleph\cap R\cap S \end{cases}$$

Since $\aleph\backslash R=\aleph\cap R'$, if $s\in R'$, then $s\in S\backslash R$ or $s\in(R\cup S)'$. Hence, if $s\in\aleph\backslash R$, $s\in\aleph\cap R'\cap S'$ or $s\in\aleph\cap R'\cap S$. Thus, it is seen that $(N,\aleph)=(T,\aleph)$.

ii) $(D,\aleph)\underset{*}{\overset{*}{\sim}}[(J,R)\underset{\theta}{\overset{*}{\sim}}(Y,S)]=[(D,\aleph)\underset{+}{\overset{*}{\sim}}(J,R)]\;\tilde{\cup}\;[(D,\aleph)\underset{+}{\overset{*}{\sim}}(Y,S)]$, where $\aleph\cap R'\cap S=\emptyset$

iii) $(D,\aleph)\underset{*}{\overset{*}{\sim}}[(J,R)\underset{\gamma}{\overset{*}{\sim}}(Y,S)]=[(D,\aleph)\underset{+}{\overset{*}{\sim}}(J,R)]\;\tilde{\cup}\;[(Y,S)\underset{*}{\overset{*}{\sim}}(D,\aleph)]$, where $\aleph\cap R'\cap S=\emptyset$

iv) $(D,\aleph)\underset{*}{\overset{*}{\sim}}[(J,R)\underset{+}{\overset{*}{\sim}}(Y,S)]=[(D,\aleph)\underset{+}{\overset{*}{\sim}}(J,R)]\;\tilde{\cap}\;[(Y,S)\underset{*}{\overset{*}{\sim}}(D,\aleph)]$

v) $(D,\aleph)\underset{*}{\overset{*}{\sim}}[(J,R)\underset{\cap}{\overset{*}{\sim}}(Y,S)]=[(D,\aleph)\underset{*}{\overset{*}{\sim}}(J,R)]\tilde{\cup}[(Y,S)\underset{*}{\overset{*}{\sim}}(D,\aleph)]$, where $\aleph\cap R\cap S'=\emptyset$ and $\aleph\cap R'\cap S=\emptyset$.

vi) $[(D,\aleph)\underset{\theta}{\overset{*}{\sim}}(J,R)]\underset{*}{\overset{*}{\sim}}(Y,S)=[(D,\aleph)\tilde{\lambda}(Y,S)]\;\tilde{\cup}\;[(J,R)\tilde{\lambda}(Y,S)]$

Proof: Let's first handle the left hand side of the equality. Let $(D,\aleph)\underset{\theta}{\overset{*}{\sim}}(J,R)=(M,\aleph)$, so $\forall s\in\aleph$,

$$M(s)=\begin{cases} D'(s), & s\in\aleph\backslash R \\ D'(s)\cap J'(s), & s\in\aleph\cap R \end{cases}$$

Let $(M,\aleph)\underset{*}{\overset{*}{\sim}}(Y,S)=(N,\aleph)$, so $\forall s\in\aleph$,

$$N(s)=\begin{cases} M'(s), & s\in\aleph\backslash S \\ M'(s)\cup Y'(s), & s\in\aleph\cap S \end{cases}$$

Thus,

$$N(s)=\begin{cases} D(s), & s\in(\aleph\backslash R)\backslash S=\aleph\cap R'\cap S' \\ D(s)\cup J(s), & s\in(\aleph\cap R)\backslash S=\aleph\cap R\cap S' \\ D(s)\cup Y'(s), & s\in(\aleph\backslash R)\cap S=\aleph\cap R'\cap S \\ [D(s)\cup J(s)]\cup Y'(s), & s\in\aleph\cap R\cap S=\aleph\cap R\cap S \end{cases}$$

Now let's handle the right hand side of the equality: $[(D,\aleph)\tilde{\lambda}(Y,S)]\ \tilde{\cup}\ [(J,R)\tilde{\lambda}(Y,S)]$. Let $(D,\aleph)\tilde{\lambda}(Y,S)=(V,\aleph)$, so $\forall s\in\aleph$,

$$V(s)=\begin{cases} D(s), & s\in\aleph\setminus S \\ D(s)\cup Y'(s), & s\in\aleph\cap S \end{cases}$$

Let $(J,R)\ \tilde{\lambda}\ (Y,S)=(W,R)$, so $\forall s\in R$,

$$W(s)=\begin{cases} J(s), & s\in R\setminus S \\ J(s)\cup Y'(s), & s\in R\cap S \end{cases}$$

Let $(V,\aleph)\ \tilde{\cup}\ (W,R)=(T,\aleph)$, so $\forall s\in\aleph$,

$$T(s)=\begin{cases} V(s), & s\in\aleph\setminus R \\ V(s)\cup W(s), & s\in\aleph\cap R \end{cases}$$

Thus,

$$T(s)=\begin{cases} D(s), & s\in((P\setminus S)\setminus R=\aleph\cap R'\cap S' \\ D(s)\cup Y'(s), & s\in(\aleph\cap S)\setminus R=\aleph\cap R'\cap S \\ D(s)\cup J(s), & s\in(\aleph\setminus S)\cap(R\setminus S)=\aleph\cap R\cap S' \\ D(s)\cup [J(s)\cup Y'(s)], & s\in(\aleph\setminus S)\cap(R\cap S)=\emptyset \\ [D(s)\cup Y'(s)]\cup J(s), & s\in(\aleph\cap S)\cap(R\setminus S)=\emptyset \\ [D(s)\cup Y'(s)]\cup J([s)\cup Y'(s)], & s\in(\aleph\cap S)\cap(R\cap S)=\aleph\cap R\cap S \end{cases}$$

It is seen that $(N,\aleph)=(T,\aleph)$.

vii) $(D,P)\ \underset{*}{\overset{*}{\sim}}\ (J,R)]\ \underset{*}{\overset{*}{\sim}}\ (Y,S)=\ [(D,\aleph)\tilde{\lambda}\,(Y,S)]\ \tilde{\cap}\ [(J,R)\ \tilde{\lambda}\,(Y,S)]$

viii)$[\ (D,P)\ \underset{\gamma}{\overset{*}{\sim}}\ (J,R)]\ \underset{*}{\overset{*}{\sim}}\ (Y,S)=\ [(D,\aleph)\underset{\lambda}{\tilde{}}\ (Y,S)]\ \tilde{\cup}\ [(J,R)\ \underset{*}{\tilde{}}\ (Y,S)]$, where $\aleph\cap R\cap S'=\emptyset$

ix) $[\ (D,P)\ \underset{+}{\overset{*}{\sim}}\ (J,R)]\ \underset{*}{\overset{*}{\sim}}\ (Y,S)=\ [(D,\aleph)\underset{\lambda}{\tilde{}}\ (Y,S)]\ \tilde{\cap}\ [(J,R)\ \underset{\lambda}{\overset{*}{\sim}}\ (Y,S)]$, where $\aleph\cap R\cap S=\emptyset$

Proposition 4.5. Let $(D,\aleph)$, (J,R) and (Y,S) be soft sets over U. Then, for the distributions of complementary soft binary piecewise star $(*)$ operation over restricted soft set operations, we have the followings:

i)$(D,\aleph)\underset{*}{\overset{*}{\sim}}[(J,R)\ \cap_R(Y,S)]=[(D,\aleph)\underset{*}{\overset{*}{\sim}}\ (J,R)]\cap_R\ [(D,\aleph)\underset{*}{\overset{*}{\sim}}\ (Y,S)]$, where $\aleph\cap R\cap S=\emptyset$.

Proof: Let's first handle the left hand side of the equality, suppose $(J,R)\ \cap_R(Y,S)=(M,R\cap S)$ and so $\forall s\in R\cap S$, $M(s)=J(s)\cap Y(s)$. Let $(D,\aleph)\underset{*}{\overset{*}{\sim}}\ (M,R\cap S)=(N,\aleph)$, so $\forall s\in\aleph$,

$$N(s)=\begin{cases} D'(s), & s\in\aleph\setminus(R\cap S) \\ D'(s)\cup M'(s), & s\in\aleph\cap(R\cap S) \end{cases}$$

Thus,

$$N(s)=\begin{cases} D'(s), & s\in\aleph\setminus(R\cap S) \\ D'(s)\cup[J'(s)\cup Y'(s)], & s\in\aleph\cap(R\cap S) \end{cases}$$

Now let's handle the right hand side of the equality: $[(D,\aleph)\underset{*}{\overset{*}{\sim}}(J,R)]\ \cap_R\ [(D,\aleph)\underset{*}{\overset{*}{\sim}}(Y,S)]$. Let $(D,\aleph)\underset{*}{\overset{*}{\sim}}(J,R)=(V,\aleph)$, so $\forall s\in\aleph$,

$$V(s)=\begin{cases} D'(s), & s\in\aleph\setminus R \\ D'(s)\cup J'(s), & s\in\aleph\cap R \end{cases}$$

Let $(D,\aleph)\underset{*}{\overset{*}{\sim}}(Y,S)=(W,\aleph)$, so $\forall s\in\aleph$,

$$W(s)=\begin{cases} D'(s), & s\in\aleph\setminus S \\ D'(s)\cup Y'(s), & s\in\aleph\cap S \end{cases}$$

Assume that $(V,\aleph)\cap_R(W,\aleph)=(T,\aleph)$, and so $\forall s\in\aleph$, $T(s)=V(s)\cap W(s)$,

$$T(s)=\begin{cases} D'(s)\cap D'(s), & s\in(P\setminus R)\cap(\aleph\setminus S) \\ D'(s)\cap[D'(s)\cup Y'(s)], & s\in(\aleph\setminus R)\cap(\aleph\cap S) \\ [D'(s)\cup J'(s)]\cap D'(s), & s\in(\aleph\cap R)\cap(\aleph\setminus S) \\ [D'(s)\cup J'(s)]\cap[D'(s)\cup Y'(s)], & s\in(\aleph\cap R)\cap(\aleph\cap S) \end{cases}$$

Hence,

$$T(s)=\begin{cases} D'(s), & s\in\aleph\cap R'\cap S' \\ D'(s), & s\in\aleph\cap R'\cap S \\ D'(s), & s\in\aleph\cap R\cap S' \\ [D'(s)\cap J'(s)]\cup[D'(s)\cap Y'(s)], & s\in\aleph\cap R\cap S \end{cases}$$

Considering the parameter set of the first equation of the first row, that is, $\aleph\setminus(R\cap S)$; since $\aleph\setminus(R\cap S)=\aleph\cap(R\cap S)'$, an element in $(R\cap S)'$ may be in $R\setminus S$, in $S\setminus R$ or $(R\cup S)$. Then, $\aleph\setminus(R\cap S)$ is equivalent to the following 3 states: $\aleph\cap(R\cap S')$, $\aleph\cap(R'\cap S)$ and $\aleph\cap(R'\cap S')$. Hence, $(N,\aleph)=(T,\aleph)$.

ii) $(D,\aleph)\underset{*}{\overset{*}{\sim}}[(J,R)\ \cup_R(Y,S)]\ =\ [(D,\aleph)\underset{*}{\overset{*}{\sim}}(J,R)]\ \cap_R\ [(D,\aleph)\underset{*}{\overset{*}{\sim}}(Y,S)]$.

iii) $(D,\aleph)\underset{*}{\overset{*}{\sim}}[(J,R) *_R (Y,S)] = [(D,\aleph)\underset{+}{\overset{*}{\sim}}(J,R)] \cap_R [(D,\aleph)\underset{+}{\overset{*}{\sim}}(Y,S)]$.

iv) $(D,\aleph)\underset{*}{\overset{*}{\sim}}[(J,R)\ \theta_R(Y,S)]=[(D,\aleph)\underset{+}{\overset{*}{\sim}}(J,R)]\cap_R[(D,\aleph)\underset{+}{\overset{*}{\sim}}(Y,S)]$, where $\aleph\cap R\cap S=\emptyset$.

v) $(D,\aleph)\underset{*}{\overset{*}{\sim}}[(J,R)\ \backslash_R\ (Y,S)]=[(D,\aleph)\underset{*}{\overset{*}{\sim}}(J,R)] \cap_R [(D,\aleph)\underset{+}{\overset{*}{\sim}}(Y,S)]$.

vi) $(D,\aleph)\underset{*}{\overset{*}{\sim}}[(J,R) +_R(Y,S)] = [(D,\aleph)\underset{+}{\overset{*}{\sim}}(J,R)] \cap_R [(D,\aleph)\underset{*}{\overset{*}{\sim}}(Y,S)]$.

vi) $(D,\aleph)\underset{*}{\overset{*}{\sim}}[(J,R)\ \gamma_R(Y,S)] =[(D,\aleph)\underset{\gamma}{\overset{*}{\sim}}(J,R)]\cup_R [(D,\aleph)\underset{\theta}{\overset{*}{\sim}}(Y,S)]$, where $\aleph\cap R\cap S =\emptyset$.

viii) $[(D,\aleph) \cup_R (J,R)]\underset{*}{\overset{*}{\sim}}(Y,S)= [(D,\aleph)\underset{*}{\overset{*}{\sim}}(Y,S)] \cap_R [(J,R)\underset{*}{\overset{*}{\sim}}(Y,S)]$.

Proof: Let's first handle the left hand side of the equality, suppose $(D,\aleph) \cup_R(J,R)=(M,\aleph\cap R)$ so, $\forall s\in\aleph\cap R$, $M(s)=D(s)\cup J(s)$. Let $(M,\aleph\cap R)\underset{*}{\overset{*}{\sim}}(Y,S) =(N,\aleph\cap R)$, so $\forall s\in\aleph\cap R$,

$$N(s)=\begin{cases} M'(s), & s\in(\aleph\cap R)\backslash S \\ M'(s)\cup Y'(s), & s\in(\aleph\cap R)\cap S \end{cases}$$

Hence,

$$N(s)=\begin{cases} D'(s)\cap J'(s), & s\in(\aleph\cap R)\backslash S= \aleph\cap R\cap S' \\ [D'(s)\cap J'(s)]\cup Y'(s), & s\in(\aleph\cap R)\cap S \end{cases}$$

Now let's handle the right hand side of the equality: $[(D,\aleph)\underset{*}{\overset{*}{\sim}}(Y,S)] \cap_R [(J,R)\underset{*}{\overset{*}{\sim}}(Y,S)]$. Let $(D,\aleph)\underset{*}{\overset{*}{\sim}}(Y,S)=(V,\aleph)$, so $\forall s\in\aleph$,

$$V(s)=\begin{cases} D'(s), & s\in\aleph\backslash S \\ D'(s)\cup Y'(s), & s\in\aleph\cap S \end{cases}$$

Let $(J,R)\underset{*}{\overset{*}{\sim}}(Y,S)=(W,R)$, so $\forall s\in R$,

$$W(s)=\begin{cases} J'(s), & s\in R\backslash S \\ J'(s)\cup Y'(s), & s\in R\cap S \end{cases}$$

Suppose that $(V,\aleph)\cap_R (W,R)=(T,\aleph\cap R)$, so $\forall s\in\aleph\cap R$, $T(s)=V(s)\cap W(s)$. Thus,

$$T(s)=\begin{cases} D'(s)\cap J'(s), & s\in(\aleph\setminus S)\cap(R\setminus S)=\aleph\cap R\cap S' \\ D'(s)\cap[J'(s)\cup Y'(s)], & s\in(\aleph\setminus S)\cap(R\cap S)=\emptyset \\ [D'(s)\cup Y'(s)]\cap J'(s), & s\in(\aleph\cap S)\cap(R\setminus S)=\emptyset \\ [D'(s)\cup Y'(s)]\cap[J'(s)\cup Y'(s)], & s\in(\aleph\cap S)\cap(R\cap S)=\aleph\cap R\cap S \end{cases}$$

It is seen that $(N,\aleph\cap R)=(T,\aleph\cap R)$,

ix) $[(D,\aleph)\cap_R (J,R)]\underset{*}{\overset{*}{\sim}}(Y,S)=[(D,\aleph)\underset{*}{\overset{*}{\sim}}(Y,S)]\cup_R[(J,R)\underset{*}{\overset{*}{\sim}}(Y,S)]$.

x**)** $[(D,\aleph)*_R (J,R)]\underset{*}{\overset{*}{\sim}}(Y,S)=[(D,\aleph)\tilde{\lambda}(Y,S)]\cap_R[(J,R)\tilde{\lambda}(Y,S)]$.

xi) $[(D,\aleph)\theta_R(J,R)]\underset{*}{\overset{*}{\sim}}(Y,S)=[(D,\aleph)\tilde{\setminus}(Y,S)]\cup_R[(J,R)\tilde{\setminus}(Y,S)]$.

5. Conclusion

The concept of soft set operations is an essential concept similar to fundamental operations on numbers and basic operations on sets. Proposing new soft operations and deriving their algebraic properties and implementations provide new perspectives for dealing with problems related to parametric data. The operations in soft set theory have proceed under two main headings up to now, as restricted soft set operations and extended soft set operations. In this paper, we contribute to the soft set literature by defining a new kind of soft set operation. Inspired by these ideas, in this paper we have defined a new soft set operation which we call complementary soft binary piecewise star operation. The basic algebraic properties of the operations have been investigated. Moreoverby examining the distribution rules, we have obtained the relationships between this new soft set operation and other types of soft set operations such as extended soft set operations, complementary extended soft set operations, soft binary piecewise operations, complementary soft binary piecewise operations and restricted soft set operations. This paper can be regarded as a theoretical study for soft sets and some future studies may continue by examining the distribution of other soft set operations over complementary soft binary piecewise star operation. Furthermore, since soft sets are a powerful mathematical tool for detecting insecure objects, researchers may be able to propose new cryptographic or decision methods based on soft sets with the help of this new soft set operation. Also, the study of soft algebraic structures can be handled again in terms of algebraic properties by the operations defined in this article and thus studying the algebraic structure of soft sets from the perspective of this new operation provides deep insight into the algebraic structure of soft sets.

Author Contributions

All authors contributed equally to this work. They all read and approved the final version of the manuscript.

Conflicts of Interest

The authors declare no conflict of interest.

References

[1] Akbulut, E. (2023) New type of extended operations of soft set: Complementary extended lambda and difference operations. MSc. Thesis, Amasya University, The Graduate School of Natural and Applied Sciences Master of Science in Mathematics Department, Amasya.

[2] Ali, M.I., Feng, F., Liu, X., Min, W.K., Shabir, M. (2009) On some new operations in soft set theory. Computers and Mathematics with Applications, 57(9): 1547-1553.

[3] Ali, M.I., Shabir, M., Naz, M., (2011) Algebraic structures of soft sets associated with new operations, Computers and Mathematics with Applications 61 2647–2654.

[4] Aybek, F. (2023) New restricted and extended soft set operations. MSc. thesis, Amasya University, The Graduate School of Natural and Applied Sciences Master of Science in Mathematics Department, Amasya.

[5] Çağman N. (2021) Conditional complements of sets and their application to group theory. Journal of New Results in Science, 10 (3): 67-74.

[6] Çağman N., Enginoğlu, S. (2010) Soft set theory and uni-int decision making, Eurepean Journal of Operational Research, 207: 848-855.

[7] Dalkılıç O. (2021) A novel approach to soft set theory in decision-making under uncertainty, International Journal of Computer Mathematics, 98:10, 1935-1945.

[8] Dalkılıç O. (2021) Determining the (non-)membership degrees in the range (0,1) independently of the decision-makers for bipolar soft sets, Journal of Taibah University for Science, 15:1, 609-618.

[9] Dalkılıç O. (2022) Determining the membership degrees in the range (0, 1) for hypersoft sets independently of the decision-maker, International Journal of Systems Science, 53:8, 1733-1743.

[10] Dalkılıç O. (2022) Approaches that take into account interactions between parameters: pure (fuzzy) soft sets, International Journal of Computer Mathematics, 99:7, 1428 1437.

[11] Demirci A.M. (2023) New type of extended operations of soft set: Complementary extended plus, union and theta operations. MSc. Thesis, Amasya University, The Graduate School of Natural and Applied Sciences Master of Science in Mathematics Department, Amasya.

[12] Eren Ö.F. and Çalışıcı H. (2019) On some operations of soft sets, The Fourth International Conference on Computational Mathematics and Engineering Sciences (CMES-2019), Antalya.

[13] Feng, F., Li, Y.M., Davvaz, B., Ali, M. I., (2010) Soft Sets Combined With Fuzzy Sets and Rough Sets: A Tantative Approach, Soft Computing, 14 899–911.

[14] Fu, L., Notes on soft set operations, (2011) ARPN Journal of systems and softwares, 1, 205-208.

[15] Ge, X., Yang S., (2011) Investigations on some operations of soft sets, World academy of Science, Engineering and Technology, 75 1113-1116.

[16] Husain, S., Shamsham, Km., (2018) A study of properties of soft set and its applications, International Research Journal of Engineering and Technology, 5 (1) 363-372.

[17] Jayanta, S., (2014) On algebraic structure of soft sets, Annals of Fuzzy Mathematics and Informatics, Volume 7 (6) 1013-1020.

[18] Jiang, J., Tang, Y., Chen, Q., Wang, J., Tang, S., (2010) Extending soft sets with description logics, Computers and Mathematics with Applications, 59 2087–2096.

[19] Neog, I.J, Sut, D.K., (2011) A new Approach to the Theory of Soft Set, International Journal of Computer Applications, 32 (2) 1-6.

[20] Maji, P.K, Bismas. R., Roy, A.R. (2003) Soft set theory. Computers and Mathematics with Applications, 45 (1): 555-562.

[21] Molodtsov, D. (1999) Soft set theory-first results. Computers and Mathematics with Applications, 37 (1): 19-31

[22] Onyeozili, L.A., T.A., Gwary, (2014) A study of the fundamentals of soft set theory, Internatıonal Journal Of Scıentıfıc & Technology Research, 3 (4) 132-143.

[23] Özlü, Ş., (2022a) Interval valued q- rung orthopair hesitant fuzzy choquet aggregating operators in multi-criteria decision making problems. Gazi University Journal of Science Part C: Design and Technology, 10 (4). 1006-1025.

[24] Özlü Ş., (2022b) Interval valued bipolar fuzzy prioritized weighted dombi averaging operator based on multi-criteria decision making problems. Gazi University Journal of Science Part C: Design and Technology, 10 (4). 841-857.

[25] Özlü Ş. and Sezgin A., (2021) Soft covered ideals in semigroups. Acta Universitatis Sapientiae Mathematica, 12 (2). 317-346.

[26] Pei, D. and Miao, D. (2005) From Soft Sets to Information Systems. In: Proceedings of Granular Computing. IEEE, 2: 617-621.

[27] Ping, Z., Qiaoyan, W.,(2013) Operations on Soft Sets Revisited, Journal of Applied Mathematics, Volume 2013 Article ID 105752 7 pages.

[28] Sarıalioğlu, M. (2023) New type of extended operations of soft set: Complementary extended gamma, intersection and star operations. MSc. Thesis, Amasya University, The Graduate School of Natural and Applied Sciences Master of Science in Mathematics Department, Amasya.

[29] Sezgin, A. and Atagün, A.O. (2011) On operations of soft sets. Computers and Mathematics with Applications, 61(5):1457-1467.

[30] Sezgin A. and Atagün, A.O., (2023) New soft set operation: Complementary soft binary piecewise plus operation. accepted in Matrix Science Mathematic.

[31] Sezgin A. and Aybek, F. (2023) New soft set operation: Complementary soft binary piecewise gamma operation. Matrix Science Mathematics (7) 1, 27-45.

[32] Sezgin A., Aybek F., Güngör Bilgili N. (2023a) New soft set operation: Complementary soft binary piecewise union operation. Acta Informatica Malaysia 7(1), 38-53.

[33] Sezgin A., Aybek F., Atagün A.O. (2023b) New soft set operation: Complementary soft binary piecewise intersection operation. accepted in Black Sea Journal of Engineering and Science.

[34] Sezgin A. and Çağman N. (2023) New soft set operation: Complementary soft binary piecewise difference operation. accepted in Osmaniye Korkut Ata University Journal of the Institute of Science and Technology.

[35] Sezgin A., Çağman N., Atagün A.O., Aybek F. (2023c) Complemental binary operations of sets and their application to group theory, accepted in Information Management and Computer Science.

[36] Sezgin A. and Sarıalioğlu, M. (2023) New soft set operation: Complementary soft binary piecewise theta operation. accepted in Journal of Kadirli Faculty of Applied Sciences.

[37] Sezgin, A., Shahzad A. and Mehmood, A. (2019) New Operation on Soft Sets: Extended Difference of Soft Sets. Journal of New Theory, (27): 33-42.

[38] Singh, D., Onyeozili, L.A., (2012) Some conceptual misunderstanding of the fundamentals of soft set theory, ARPN Journal of systems and softwares, 2 (9) 251-254.

[39] Singh, D., Onyeozili, L.A., (2012) Some results on Distributive and absorption properties on soft operations, IOSR Journal of mathematics, 4 (2) 18-30.

[40] Singh, D., Onyeozili, L.A., (2012) On some new properties on soft set operations, International Journal of Computer Applications, 59 (4) 39-44.

[41] Singh, D., Onyeozili, L.A., (2012) Notes on soft matrices operations, ARPN Journal of science and technology, 2(9) 861-869.

[42] Stojanovic, N.S. (2021) A new operation on soft sets: extended symmetric difference of soft sets. Military Technical Courier, 69(4): 779-791.

[43] Yang, C.F., (2008) “A note on: “Soft set theory” [Computers & Mathematics with Applications 45 (2003), no. 4-5, 555–562],” Computers & Mathematics with Applications, 56 (7) 1899–1900.

[44] Yavuz E., (2023) Soft binary piecewise operations and their properties, MSc. Thesis, Amasya University, The Graduate School of Natural and Applied Sciences Master of Science in Mathematics Department, Amasya.

Ikonion Journal of Mathematics (2023) 5(2) 53-64

Ikonion Journal of Mathematics

https://dergipark.org.tr/tr/pub/ikjm

Research Article

Open Access

https://doi.org/ 10.54286/ikjm.1303219

ISSN: 2687-6531

On Data Dependency and Solutions of Nonlinear Fredholm Integral Equations with the Three-Step Iteration Method

Lale CONA[1], Kadir ŞENGÜL[2]

Keywords:
Banach Fixed Point Theorem; Nonlinear Fredholm Integral Equations; Three-Step Iteration Method; Data Dependency.

Abstract — In this study, the solution of the second type of homogeneous nonlinear Fredholm integral equations is investigated using a three-step iteration algorithm. In other words, it has been shown that the sequences obtained from this algorithm converge to the solution of the mentioned equations. Also, data dependency is obtained for the second type of homogeneous nonlinear Fredholm integral equations and this result is supported by an example.

Subject Classification (2020): 45B05, 47H10.

1. Introduction

The widely used fixed point theory has its origins in the approximation methods of Liouville, Cauchy, Lipschitz, Peano and Picard towards the end of the 19th century (for more detail see [2],[3],[7],[9],[10]). In 1922, Stephan Banach introduced the Banach fixed point theorem, which proved the existence and uniqueness of the fixed point under various conditions [22]. One of the important results obtained is that the sequence obtained by Picard iteration converges to the fixed point [6]. Since iteration methods have wide application areas, many researches have been done on this subject. This process, which started with Picard, has developed and has survived to the present day. There are two main points to consider when defining the iteration method. The first is that the iteration to be defined is faster than existing iteration methods, and the second is that this iteration method is simple. For detailed information about iteration methods frequently used in the literature, you can refer to the following sources: [1], [10]- [20].

In addition to many iteration methods developed in this process, the strong convergence of these methods, convergence equivalence, convergence speed and whether the fixed points of these transformations are data dependent were investigated for certain transformation classes ([4],[8],[10],[11],[20]- [24]).The knowledge of which method converges faster for two iteration methods whose convergence is equivalent is of great importance in applied mathematics. Another

[1] lalecona@gumushane.edu.tr (Corresponding Author); [2] kadirsengul@outlook.com
[1] Faculty of Engineering and Natural Sciences, Mathematical Engineering, Gumushane University, Gumushane, Turkey
[2] Institute of Graduate Education, Mathematical Engineering, Gumushane University, Gumushane, Turkey.
Article History: Received: 26.05.2023 — Accepted: 15.09.2023 — Published: 11.10.2023

transformation, called the approximation operator, can be used, which is close to the one used when constructing an iteration. Since this approximation operator has a different fixed point, the questions of how close the fixed point of the transformation and the fixed point of the approximation operator are to each other and how to calculate the distance between them bring up the concept of data dependency of fixed points.

One of the most common uses of fixed point theory, especially in applied mathematics, is the theory of integral equations. It is very important to determine the existence and uniqueness of integral equations. Fixed point theory is one of the most important tools used for this purpose. In our study, Fredholm integral equations, which are used in modeling many current problems, are discussed with the new three-step iteration method developed by Karakaya et al [14]. The reason why we use this iteration algorithm is that it has been proven to be faster than many iteration algorithms such as Picard, Mann, Ishikawa, Noor, SP, CR, Sahu-S and Picard-S [3]. Briefly, our study examines the strong convergence of the sequence obtained from the new three-step iteration method to the solution and the dependence of this solution on the data, under operators corresponding to nonlinear Fredholm integral equations.

2. Known Results

Definition 1. Let (X,d) be a metric space and $T : X \to X$ be a mapping. T is called a Lipschitzian mapping, if there is a $\lambda > 0$ number such that

$$d(Tx,Ty) \leq \lambda d(x,y)$$

for all $x,y \in X$ [10].

Definition 2. Let (X,d) be a metric space and $T : X \to X$ be a Lipschitzian mapping. T is called a contraction mapping, if there is at least one $\lambda \in (0,1)$ real number such that

$$d(Tx,Ty) \leq \lambda d(x,y)$$

for all $x,y \in X$. λ is called the contraction ratio [10].

Definition 3. Let X be a normed space and $T : X \to X$ be a Lipschitzian mapping. T is called a contraction mapping, if there is at least one $\lambda \in (0,1)$ real number such that

$$\|Tx - Ty\| \leq \lambda \|x - y\|$$

for all $x,y \in X$ [10].

Geometrically, Definition 2 and Definition 3 can be interpreted as Tx and Ty, which are images of any x and y points, are closer together than x and y [10].

Theorem 1. (Banach Fixed Point Theorem) If (X,d) is a complete metric space and $T : X \to X$ is a contraction mapping,

- T has one and only one fixed point $x \in X$.
- For any $x_0 \in X$, iteration sequence $(T^n x_0)$ (ie iteration sequence (x_n) defined by $x_n = Tx_{n-1}$ for all $n \in \mathbb{N}$) converges to unique fixed point of T [6].

The following three-step iteration algorithm, defined by Karakaya et al. in 2017, has been shown to be faster than many iteration algorithms such as Picard, Mann, Ishikawa, Noor, SP, S, CR and Picard-S [14]:

Definition 4. The iteration method

$$\left.\begin{array}{l} x_0 \in X \\ x_{n+1} = Ty_n \\ y_n = (1-\beta_n)z_n + \beta_n T z_n \\ z_n = Tx_n \end{array}\right\} \tag{1}$$

is called the three-step iteration method, where X is a Banach space, $T : X \to X$ is an operator and $\{\beta_n\}_{n=0}^{\infty} \subset [0,1]$ is a sequence satisfying certain conditions [14].

Definition 5. The integral equations in the form of

$$x(t) = \lambda \int_a^b k\big(t,s,x(s)\big)ds, \tag{2}$$

where $k(t,s,x)$ is the known function defined over the region

$$D = \{(t,s,x) \in \mathbb{R}^3 : a \le t,s \le b, \quad -\infty < x < \infty\}$$

and $x(t)$ an unknown function whose solution is desired, and λ is any numerical parameter, are called the second type of nonlinear Fredholm integral equations. Here, k is called the kernel of the integral equation [2].

Lemma 1. $C([a,b], \|\cdot\|_\infty)$ is the space of all continuous functions in the interval $[a,b]$ defined by

$$d(x,y) = \sup_{t\in[a,b]} \|x(t) - y(t)\|_\infty.$$

Now, let the theorem be expressed which gives the existence and uniqueness conditions of the second type of nonlinear Fredholm integral equations:

Theorem 2. Consider the operator $T : C([a,b], \|\cdot\|_\infty) \to C([a,b], \|\cdot\|_\infty)$ defined by

$$Tx(t) = \lambda \int_a^b k\big(t,s,x(s)\big)ds. \tag{3}$$

$k(t,s,x)$ is continuous over the region

$$D = \{(t,s,x) \in \mathbb{R}^3 : a \le t,s \le b, \quad -\infty < x < \infty\}$$

and if $L > 0$ exists such that

$$|k(t,s,x_1) - k(t,s,x_2)| \le L|x_1 - x_2|$$

for

$$\forall (t,s,x_1),(t,s,x_2) \in D_r = \{(t,s,x) \in \mathbb{R}^3 : a \le t,s \le b, \ \ |x| \le r \ (r > 0)\},$$

there is only one solution $x^*(t)$ of equation (2) in $C([a,b])$ when $|\lambda| < \lambda_0$. Here

$$\lambda_0 = \min\left\{\frac{1}{L(b-a)}, \frac{r}{rL(b-a)+L_0}\right\}$$

and

$$L_0 = \max_{t,s\in[a,b]}\left\{\int_a^b |k(t,s,0)|ds\right\}.$$

The sequence $(x_n(t))$ defined as

$$x_n(t) = \lambda\int_a^b k\big(t,s,x_{n-1}(s)\big)ds \ , \quad n = 1,2,\dots$$

converges smoothly to the function $x^*(t)$ for any initial function $x_0 \in \{C([a,b]),\ \|x\|_\infty \leq r\}$ [2].

Definition 6. Let $A_1, A_2 : Y \to Y$ be operators. If $\|A_1x - A_2x\| \leq \varepsilon$ for each $x \in Y$ and constant $\varepsilon > 0$, then A_2 is called the approximation operator of A_1 [24].

Lemma 2. Let $\{a_n\}_{n=0}^{\infty}$ and $\{b_n\}_{n=0}^{\infty}$ be two non-negative real sequences satisfting the following condition:

$$a_{n+1} \leq (1-\mu_n)a_n + b_n \ ,$$

where $\mu_n \in (0,1)$ for each $n \geq n_0, \sum_{n=0}^{\infty}\mu_n = \infty$ and $\frac{b_n}{\mu_n} \to 0$ as $n \to \infty$. Then $\lim_{n\to\infty}a_n = 0$ [25].

Lemma 3. Let $\{a_n\}_{n=0}^{\infty}$ be a non-negative real sequence and there exists $n_0 \in \mathbb{N}$ such that for each $n \geq n_0$ satisfting the following condition:

$$a_{n+1} \leq (1-\mu_n)a_n + \mu_n\gamma_n \ ,$$

where $\mu_n \in (0,1)$ such that $\sum_{n=0}^{\infty}\mu_n = \infty$ and $\gamma_n \geq 0$. Then the following inequality holds:

$$0 \leq \limsup_{n\to\infty} a_n \leq \limsup_{n\to\infty}\gamma_n$$

[24].

3. Main Results

Theorem 3. Let $T : C([a,b],\|\cdot\|_\infty) \to C([a,b],\|\cdot\|_\infty)$ be an operator and $\{\beta_n\}_{n=0}^{\infty} \subset [0,1]$ be a sequence satisfying certain conditions. In this case, the integral equation given by equation (2) has a unique solution in the form of $x^* \in C[a,b]$ and the sequence $\{x_n\}_{n=0}^{\infty}$ obtained from the iteration algorithm given by equation (1) converges to this solution.

Proof Consider the sequence $\{x_n\}_{n=0}^{\infty}$ obtained from the iteration algorithm given by equation (1) constructed with the operator $T : C([a,b],\|\cdot\|_\infty) \to C([a,b],\|\cdot\|_\infty)$. It will be shown that for $n \to \infty$ is $x_n \to x^*$. Using equation (1), equation (2) and conditions of Theorem 2, we are obtained the following inequality:

$$|x_{n+1}(t) - x^*(t)| = |Ty_n(t) - Tx^*(t)|$$

$$= \left|\lambda \int_a^b k(t,s,y_n(s))ds - \lambda \int_a^b k(t,s,x^*(s))ds\right|$$
$$= |\lambda| \left|\int_a^b k(t,s,y_n(s)) - k(t,s,x^*(s))ds\right|$$
$$\leq |\lambda| \int_a^b \left|k(t,s,y_n(s)) - k(t,s,x^*(s))\right|ds$$
$$\leq |\lambda| L \int_a^b |y_n(s) - x^*(s)|ds$$
$$\leq |\lambda| L(b-a)\|y_n - x^*\|_\infty$$
$$\leq \lambda_0 L(b-a)\|y_n - x^*\|_\infty \,. \tag{4}$$

Similarly, by making the necessary calculations, the following inequalities are obtained:

$$\|y_n - x^*\|_\infty = \|(1-\beta_n)z_n + \beta_n T z_n - Tx^*\|_\infty$$
$$= \|z_n - x^* + \beta_n(Tz_n - z_n)\|_\infty$$
$$\leq \|z_n - x^*\|_\infty \,, \tag{5}$$

$$|z_n - x^*| = |Tx_n - Tx^*|$$
$$= \left|\lambda \int_a^b k(t,s,x_n(s))ds - \lambda \int_a^b k(t,s,x^*(s))ds\right|$$
$$= |\lambda| \left|\int_a^b k(t,s,x_n(s)) - k(t,s,x^*(s))ds\right|$$
$$\leq |\lambda| \int_a^b \left|k(t,s,x_n(s)) - k(t,s,x^*(s))\right|ds$$
$$\leq |\lambda| L \int_a^b |x_n(s) - x^*(s)|ds$$
$$\leq |\lambda| L(b-a)\|x_n - x^*\|_\infty$$
$$\leq \lambda_0 L(b-a)\|x_n - x^*\|_\infty \,. \tag{6}$$

Then, taking the supremum of both sides of inequality (6),

$$\|z_n - x^*\|_\infty \leq \lambda_0 L(b-a)\|x_n - x^*\|_\infty \tag{7}$$

is obtained. If inequality (7) and inequality (5) are written in inequality (4),

$$\|x_{n+1}(t) - x^*(t)\|_\infty \leq \lambda_0^2 L^2 (b-a)^2 \|x_n - x^*\|_\infty$$

And by applying induction to the last inequality, the following inequality is obtained:

$$\|x_{n+1}(t) - x^*(t)\|_\infty \leq \alpha^2 \|x_n - x^*\|_\infty$$
$$\leq \alpha^4 \|x_{n-1} - x^*\|_\infty$$
$$\leq \alpha^6 \|x_{n-2} - x^*\|_\infty$$
$$\vdots$$
$$\leq \alpha^{2(n+1)} \|x_0 - x^*\|_\infty$$

then

$$\|x_{n+1}(t) - x^*(t)\|_\infty \leq \alpha^{2(n+1)} \|x_0 - x^*\|_\infty \,,$$

is found. Thus, since $0 < \alpha < 1$,

$$\lim_{n\to\infty} \|x_{n+1}(t) - x^*(t)\|_\infty = 0 \,.$$

So, the proof is completed.

Now, let us examine the data dependency of the solution of the integral equation given by equation (2) using the iteration algorithm given in equation (1). On the other hand, for data dependency, consider the integral equation

$$u(t) = \lambda_1 \int_a^b h(t,s,u(s))ds\,, \tag{8}$$

where $h(t,s,u)$ is a continuous function given over the region

$$D = \{(t,s,u) \in \mathbb{R}^3 : a \le t,s \le b\,, \quad -\infty < u < \infty\}\,,$$

and λ_1 is a parameter. If equation (8) is written with the operator $S : C([a,b],\|\cdot\|_\infty) \to C([a,b],\|\cdot\|_\infty)$,

$$S(u(t)) = \lambda_1 \int_a^b h(t,s,u(s))ds \tag{9}$$

is obtained. If the iteration algorithm given in equation (1) is reconstructed with operators $T(3)$ and $S(9)$, respectively,

$$\left.\begin{aligned} x_{n+1}(t) &= \lambda \int_a^b k(t,s,y_n(s))ds \\ y_n(t) &= (1-\beta_n)z_n(t) + \beta_n\left[\lambda \int_a^b k(t,s,z_n(s))ds\right] \\ z_n(t) &= \lambda \int_a^b k(t,s,x_n(s))ds \end{aligned}\right\} \tag{10}$$

and

$$\left.\begin{aligned} u_{n+1}(t) &= \lambda_1 \int_a^b h(t,s,v_n(s))ds \\ v_n(t) &= (1-\beta_n)w_n(t) + \beta_n\left[\lambda_1 \int_a^b h(t,s,w_n(s))ds\right] \\ w_n(t) &= \lambda_1 \int_a^b h(t,s,u_n(s))ds \end{aligned}\right\} \tag{11}$$

iteration algorithms can be written.

Theorem 4. Let the sequence $\{\beta_n\}_{n=0}^{\infty} \subset [0,1]$ satisfy the condition $\beta_n \ge \frac{1}{2}$ for each $n \in \mathbb{N}$. Consider the sequence $\{x_n\}_{n=0}^{\infty}$ obtained from equation (10) and the sequence $\{u_n\}_{n=0}^{\infty}$ obtained from equation (11). Let the solutions of equation (2) and equation (8) be x^* and u^*, respectively, with the conditions of Theorem 2. Let the constant ε exists such that $\|k(t,s,p(s)) - h(t,s,p(s))\|_\infty \le \varepsilon$ for each $a \le t,s \le b$ and $-\infty < p < \infty$. $k(t,s,p)$ and $h(t,s,p)$ are continuous functions given over the region

$$A = \{(t,s,p) \in \mathbb{R}^3 : a \le t,s \le b,\ -\infty < p < \infty\}.$$

λ and λ_1 are parameters.

If $x_n \to x^*$ and $u_n \to u^*$ as $n \to \infty$, then the inequality

$$\|x^* - u^*\| \le \frac{3\varepsilon\lambda_{\max}(b-a)}{1-\lambda_{\max}(b-a)L}$$

is valid, with $\lambda_{\max} = \max\{|\lambda|, |\lambda_1|\}$.

Proof With the hypotheses of the theorem, the following inequality is obtained:

$$\|x_{n+1} - u_{n+1}\|_\infty = \left\|\lambda \int_a^b k(t,s,y_n(s))ds - \lambda_1 \int_a^b h(t,s,v_n(s))ds\right\|_\infty$$

$$\leq \left\| \lambda_{\max} \int_a^b \begin{pmatrix} k(t,s,y_n(s)) - k(t,s,v_n(s)) \\ +k(t,s,v_n(s)) - h(t,s,v_n(s)) \end{pmatrix} ds \right\|_\infty$$

$$\leq \lambda_{\max} \begin{pmatrix} L \int_a^b \|y_n(s) - v_n(s)\|_\infty ds \\ + \int_a^b \|k(t,s,v_n(s)) - h(t,s,v_n(s))\|_\infty ds \end{pmatrix}$$

$$\leq \lambda_{\max}(b-a)(L\|y_n - v_n\|_\infty + \varepsilon)$$

$$\leq \lambda_{\max}(b-a)L\|y_n - v_n\|_\infty + \lambda_{\max}(b-a)\varepsilon. \tag{12}$$

Similarly,

$$\|y_n - v_n\|_\infty \leq (1-\beta_n)\|z_n - w_n\|_\infty + \beta_n \left\| \lambda \int_a^b k(t,s,z_n)ds - \lambda_1 \int_a^b h(t,s,w_n)ds \right\|_\infty$$

$$\leq (1-\beta_n)\|z_n - w_n\|_\infty + \beta_n \left\| \lambda_{\max} \int_a^b k(t,s,z_n) - h(t,s,w_n)ds \right\|_\infty$$

$$\leq (1-\beta_n)\|z_n - w_n\|_\infty + \beta_n \lambda_{\max} \int_a^b \|k(t,s,z_n) - h(t,s,w_n)\|_\infty ds$$

$$\leq (1-\beta_n)\|z_n - w_n\|_\infty + \beta_n \lambda_{\max} \int_a^b \left\| \begin{matrix} k(t,s,z_n) - k(t,s,w_n) \\ +k(t,s,w_n) - h(t,s,w_n) \end{matrix} \right\|_\infty ds$$

$$\leq (1-\beta_n)\|z_n - w_n\|_\infty + \beta_n \lambda_{\max} \left(L \int_a^b \|z_n - w_n\|_\infty ds + \int_a^b \varepsilon ds \right)$$

$$\leq (1-\beta_n)\|z_n - w_n\|_\infty + \beta_n \lambda_{\max}(b-a)(L\|z_n - w_n\|_\infty + \varepsilon)$$

$$\leq [1 - \beta_n + \beta_n \lambda_{\max}(b-a)L]\|z_n - w_n\|_\infty + \beta_n \lambda_{\max}(b-a)\varepsilon \tag{13}$$

and

$$\|z_n - w_n\|_\infty = \left\| \lambda \int_a^b k(t,s,x_n)ds - \lambda_1 \int_a^b h(t,s,u_n)ds \right\|_\infty$$

$$\leq \lambda_{\max} \left\| \int_a^b k(t,s,x_n) - h(t,s,u_n)ds \right\|_\infty$$

$$\leq \lambda_{\max} \int_a^b \left\| \begin{matrix} k(t,s,x_n) - k(t,s,u_n) \\ +k(t,s,u_n) - h(t,s,u_n) \end{matrix} \right\|_\infty ds$$

$$\leq \lambda_{\max} \left(L \int_a^b \|x_n - u_n\|_\infty ds + \int_a^b \varepsilon ds \right)$$

$$\leq \lambda_{\max}(b-a)(L\|x_n - u_n\|_\infty + \varepsilon)$$

$$\leq \lambda_{\max}(b-a)L\|x_n - u_n\|_\infty + \lambda_{\max}(b-a)\varepsilon$$

$$\leq \|x_n - u_n\|_\infty + \lambda_{\max}(b-a)\varepsilon \tag{14}$$

are found. If inequality (14) is written in inequality (13),

$$\|y_n - v_n\|_\infty \leq [1 - \beta_n + \beta_n \lambda_{\max}(b-a)L]\|z_n - w_n\|_\infty + \beta_n \lambda_{\max}(b-a)\varepsilon$$

$$\leq [1 - \beta_n + \beta_n \lambda_{\max}(b-a)L][\|x_n - u_n\|_\infty + \lambda_{\max}(b-a)\varepsilon] + \beta_n \lambda_{\max}(b-a)\varepsilon$$

$$\leq [1 - \beta_n + \beta_n \lambda_{\max}(b-a)L]\|x_n - u_n\|_\infty + [\lambda_{\max}(b-a)\varepsilon] + \beta_n \lambda_{\max}(b-a)\varepsilon$$

$$\leq [1 - \beta_n + \beta_n \lambda_{\max}(b-a)L]\|x_n - u_n\|_\infty + \varepsilon \lambda_{\max}(b-a)(1+\beta_n)$$

is obtained. If the last inequality is written in inequality (12),

$$\|x_{n+1} - u_{n+1}\|_\infty \leq \|y_n - v_n\|_\infty + \lambda_{\max}(b-a)\varepsilon$$

$$\leq [1 - \beta_n + \beta_n \lambda_{\max}(b-a)L]\|x_n - u_n\|_\infty + \varepsilon \lambda_{\max}(b-a)(1+\beta_n) + \lambda_{\max}(b-a)\varepsilon$$

$$\leq [1-\beta_n+\beta_n\lambda_{\max}(b-a)L]\|x_n-u_n\|_\infty+\varepsilon\lambda_{\max}(b-a)(2+\beta_n)$$
$$\leq \{1-\beta_n(1-\lambda_{\max}(b-a)L)\}\|x_n-u_n\|_\infty+\varepsilon\lambda_{\max}(b-a)(2+\beta_n)$$
$$\leq \{1-\beta_n(1-\lambda_{\max}(b-a)L)\}\|x_n-u_n\|_\infty+\beta_n(1-\lambda_{\max}(b-a)L)\frac{3\varepsilon\lambda_{\max}(b-a)}{1-\lambda_{\max}(b-a)L} \quad (15)$$

is found. If is chosen a_n , μ_n , γ_n as follows in inequality (15), satisfies the conditions of Lemma 3.

$$a_n=\|x_n-u_n\|_\infty,$$
$$\mu_n=\beta_n(1-\lambda_{\max}(b-a)L)\in(0,1),$$
$$\gamma_n=\frac{3\varepsilon\lambda_{\max}(b-a)}{1-\lambda_{\max}(b-a)L}\geq 0.$$

$\beta_n\geq\frac{1}{2}$ requires $\sum_{n=0}^{\infty}\beta_n=\infty$ for each $n\in\mathbb{N}$. Then,

$$0\leq\limsup_{n\to\infty}\|x_n-u_n\|_\infty\leq\limsup_{n\to\infty}\gamma_n=\limsup_{n\to\infty}\frac{3\varepsilon\lambda_{\max}(b-a)}{1-\lambda_{\max}(b-a)L}$$

is obtained. Since $x_n\to x^*$ and $u_n\to u^*$as $n\to\infty$,

$$\|x^*-u^*\|_\infty\leq\frac{3\varepsilon\lambda_{\max}(b-a)}{1-\lambda_{\max}(b-a)L} \quad (16)$$

is found.

Example 1.

$$x(t)=\frac{17}{64}\int_0^1\frac{1}{1+x^2(s)}ds$$

where $k(t,s,x)=\frac{1}{1+x^2(s)}$ is a continuous function given over the region

$$D=\{(t,s,x):0\leq t,s\leq 1\,,\quad -\infty<x<\infty\}.$$

The partial derivative of $k(t,s,x)$:

$$\frac{\partial k}{\partial x}=-\frac{2x}{(1+x^2)^2}$$

is bounded over the region D.

$$\left|\frac{\partial k}{\partial x}\right|=\left|-\frac{2x}{(1+x^2)^2}\right|\leq 1\,,\quad (t,s,x)\in D$$

In this case, $k(t,s,x)$ satisfies the Lipschitz condition with the coefficient $L=1$.

$$\lambda=\frac{17}{64},\qquad a=0,\qquad b=1,\qquad \alpha=|\lambda|L(b-a)=\frac{17}{64}<1\,.$$

The equation in question has only one continuous solution x^* on [0,1].

Let's define the following algorithm with the operator

$$Tx_n(t)=\frac{17}{64}\int_0^1\frac{1}{1+x_n^2(s)}ds$$

for the solution:

$$x_{n+1}(t) = Ty_n(t) = \frac{17}{64}\int_0^1 \frac{1}{1+y_n^2(s)}ds$$
$$y_n(t) = (1-\beta_n)z_n(t) + \beta_n Tz_n(t) = (1-\beta_n)z_n(t) + \beta_n\left(\frac{17}{64}\int_0^1 \frac{1}{1+z_n^2(s)}ds\right)$$
$$z_n(t) = Tx_n(t) = \frac{17}{64}\int_0^1 \frac{1}{1+x_n^2(s)}ds.$$

On the other hand, let's consider the integral equation

$$u(t) = \frac{65}{256}\int_0^1 \frac{s}{1+u^2(s)}ds\ ,$$

where

$$h(t,s,u) = \frac{s}{1+u^2(s)}$$

is a continuous function given over the region

$$G = \{(t,s,u) : 0 \le t,s \le 1\ ,\quad -\infty < u < \infty\}\ .$$

The partial derivative of $h(t,s,u)$:

$$\frac{\partial h}{\partial u} = -\frac{2su}{(1+u^2)^2}$$

is bounded over the region G.

$$\left|\frac{\partial h}{\partial u}\right| = \left|-\frac{2su}{(1+u^2)^2}\right| \le 1\ ,\ \ (t,s,u) \in G$$

In this case, $h(t,s,u)$ satisfies the Lipschitz condition with the coefficient $L = 1$.

$$\lambda_1 = \frac{65}{256}\ ,\ \ a = 0\ ,\ \ b = 1\ ,\ \ \alpha = |\lambda_1|L(b-a) = \frac{65}{256} < 1\ .$$

The equation in question has only one continuous solution u^*on [0,1].

Let's define the following algorithm with the operator

$$S(u_n(t)) = \frac{65}{256}\int_0^1 \frac{s}{1+u^2(s)}ds$$

for the solution:

$$u_{n+1}(t) = Sv_n(t) = \frac{65}{256}\int_0^1 \frac{s}{1+v^2(s)}ds$$
$$v_n(t) = (1-\beta_n)w_n(t) + \beta_n Sw_n(t) = (1-\beta_n)w_n(t) + \beta_n\left(\frac{65}{256}\int_0^1 \frac{s}{1+w^2(s)}ds\right)$$
$$w_n(t) = Su_n(t) = \frac{65}{256}\int_0^1 \frac{s}{1+u^2(s)}ds.$$

Thus,

$$\lambda_{\max} = \max\{|\lambda|, |\lambda_1|\} = \max\left\{\frac{17}{64}, \frac{65}{256}\right\} = \frac{17}{64}$$

is found. Let the constant ε exists such that

$$\begin{aligned}\left\|k(t,s,p(s))-h(t,s,p(s))\right\|_{\infty} &= \left\|\frac{1}{1+p^2}-\frac{s}{1+p^2}\right\|_{\infty}\\ &\leq \left\|\frac{1}{1+p^2}\right\|_{\infty}\\ &\leq 1=\varepsilon\end{aligned}$$

for each $(t,s,p)\in A$. So, all the conditions of Theorem 4 are satisfied. Therefore, inequation (16) is valid. If the found values are written in the inequation (16),

$$\|x^*-u^*\|_{\infty}\leq\frac{3\varepsilon\lambda_{\max}(b-a)}{1-\lambda_{\max}(b-a)L}=\frac{3.1.\frac{17}{64}.1}{1-\frac{17}{64}.1.1}=\frac{51}{47}\simeq 1.085$$

is obtained. Indeed, $x^*=\frac{1}{4}$ and $u^*=\frac{1}{8}$ are found. So,

$$\|x^*-u^*\|_{\infty}=\left\|\frac{1}{4}-\frac{1}{8}\right\|_{\infty}=\frac{1}{8}=0.125\leq 1.085$$

is found. Thus, the theorem is supported by this example.

4. Conclusion

Many real-life problems are expressed non-linearly. In the modeling of these problems, nonlinear integral equations are mostly used. Fixed point theory is very important for solving these integral equations. The basic idea here is to construct algorithms called iterations by including the equation in an operator class under certain conditions, and to determine the appropriate conditions for the sequence obtained from this iteration to converge to the fixed point of the operator, in other words, to the solution of the equation.In this study, the solution of the second type of homogeneous nonlinear Fredholm integral equations is investigated using a three-step iteration algorithm. In other words, the aim of this study is to show that the sequence obtained from equation (1) iteration method converges strongly to the solution of equation (2). It has been shown that the sequences obtained from this algorithm converge to the solution of the mentioned equations. In addition, data dependence was obtained for the second type of homogeneous nonlinear Fredholm integral equations and this result was supported by an example. Interested researchers can reconstruct the newly described three-step iteration method for more general transformation classes and apply it to many types of integral equations to examine the results of strong convergence and data dependence.

Author Contributions

All authors contributed equally to this work. They all read and approved the final version of the manuscript.

Conflicts of Interest

The authors declare no conflict of interest.

Acknowledgement

We would like to thank the referees who contributed to this article with their comments and suggestions.

References

[1] Agarwal, R. P., O Regan, D., Sahu, D. R. (2007) Iterative construction of fixed points of nearly asymptotically nonexpansive mappings. Journal of Nonlinear and convex Analysis, 8(1): 61-79.

[2] Akbulut, A. (2007) Application of fixed point theorems to Cauchy problem and integral equations. M.Sc. thesis, Gazi University, Ankara, Turkey.

[3] Atalan, Y. (2017) Solutions of some differential and integral equations with fixed point approach. Ph.D. thesis, Yıldız Technical University, İstanbul, Turkey.

[4] Atalan, Y., Gürsoy, F., Khan, A.R. (2021) Convergence of S-iterative method to a solution of Fredholm integral equation and data dependency. Facta Universitiy, 4(36): 685-694.

[5] Atalan, Y. (2019) Examination of the solution of a class of functional-integral equation under iterative approach. Journal of the Institute of Science and Technology, 9(3): 1622-1632.

[6] Banach, S. (1922) Sur les opérations dans les ensembles abstraits et leur application aux équations intégrales. Fundamenta Mathematicae, 3(1): 133-181.

[7] Brouwer, L. E. J. (1911) Über abbildung von mannigfaltigkeiten. Mathematische Annalen, 71(1): 97-115.

[8] Chugh, R., Kumar, V., Kumar, S. (2012) Strong convergence of a new three step iterative scheme in Banach spaces. American Journal of Computational Mathematics, 2(4): 345-357.

[9] Doğan, K. (2016) Some geometrical properties and new fixed point iteration procedures. Ph.D. thesis, Yıldız Technical University, İstanbul, Turkey.

[10] Gürsoy, F. (2014) Investigation of convergences and stabilities of some new fixed point iteration procedures. Ph.D. thesis, Yıldız Technical University, İstanbul, Turkey.

[11] Gürsoy F. (2016) A Picard-S iterative method for approximating fixed point of weak-contraction mappings. Filomat, 30(10): 2829-2845.

[12] Hussain, N., Chugh, R., Kumar, V., Rafiq, A. (2012) On the rate of convergence of Kirk-type iterative schemes. Journal of Applied Mathematics, 2012.

[13] Ishikawa, S. (1974) Fixed points by a new iteration method. Proceedings of the American Mathematical Society, 44(1): 147-150.

[14] Karakaya, V., Atalan, Y., Doğan, K., Bouzara, N. E. H. (2017) Some fixed point results for a new three steps iteration process in Banach spaces. Fixed Point Theory, 18(2): 625-640.

[15] Khan, S. H. (2013) A Picard-Mann hybrid iterative process. Fixed Point Theory and Applications, 2013(69): 1-10.

[16] Kirk, W. A. (1971) On successive approximations for nonexpansive mappings in Banach spaces. Glasgow Mathematical Journal, 12(1): 6-9.

[17] Krasnosel'skii, M. A. (1955) Two comments on the method of successive approximations. Usp. Math. Nauk, 10(1): 123-127.

[18] Mann, W. R. (1953) Mean value methods in iteration. Proceedings of the American Mathematical Society, 4(3): 506-510.

[19] Noor, M. A. (2000) New approximation schemes for general variational inequalities. Journal of Mathematical Analysis and applications, 251(1): 217-229.

[20] Olatinwo, M. O. (2009) Some stability results for two hybrid fixed point iterative algorithms in normed linear space. Matematički Vesnik, 61(4): 247-256.

[21] Phuengrattana, W., Suantai, S. (2011) On the rate of convergence of Mann, Ishikawa, Noor and SP-iterations for continuous functions on an arbitrary interval. Journal of computational and Applied Mathematics, 235(9): 3006-3014.

[22] Picard, E. (1890) Memoire sur la theorie des equations aux derivees partielles et la methode des approximations successives. Journal de Mathématiques Pures et Appliquées, 6: 145-210.

[23] Rhoades, B. E., Şoltuz, Ş. M. (2004) The equivalence between Mann–Ishikawa iterations and multistep iteration. Nonlinear Analysis: Theory, Methods & Applications, 58(1-2): 219-228.
[24] Şoltuz, Ş. M., Grosan, T. (2008) Data dependence for Ishikawa iteration when dealing with contractive-like operators. Fixed Point Theory and Applications, 2008(1): 1-7.
[25] Weng, X. (1991) Fixed point iteration for local strictly pseudo-contractive mapping. Proceedings of the American Mathematical Society, 113(3): 727-731.

Ikonion Journal of Mathematics 5(2) (2023) 65-75

Ikonion Journal of Mathematics

https://dergipark.org.tr/tr/pub/ikjm

Research Article

Open Access

https://doi.org/ 10.54286/ikjm.1256664

ISSN: 2687-6531

Approximate Solutions for A Fractional Shallow Water Flow Model

Hira Tariq[1], **Hadi Rezazadeh**[2], **Mehmet Şenol**[3], **Orkun Taşbozan**[4], **Ali Kurt**[5]

Keywords
Conformable Calculus; Residual Power Series Method, Drinfeld-Sokolov-Wilson Equation, Shallow water waves.

Abstract — This paper presents the solutions of fractional Drinfeld-Sokolov-Wilson (DSW) equations that occur in shallow water flow models using the residual power series method. The fractional derivatives and integrals are considered in the conformable sense. In addition, surface plots of the solutions are given. The solutions and results show that the present method is very efficient and effective due to the lack of a need for complex calculations and that the method also has a wide range of practicability in the resolution of partial differential fractional equations.

Subject Classification (2020): 34KXX, 39AXX.

1. Introduction

The use of fractional differential operators and integral operators in mathematical models has become increasingly popular in recent decades. Fractional calculus has, therefore, found numerous applications in different technical and scientific fields, such as fluid mechanics [1], signal processing [2], thermodynamics [3], biology [4], economics [5], viscoelasticity [6], control [7] and many other physical mechanisms.

In conjunction with these efforts in research, fractional differential equations (FDEs) have also been proposed and implemented in modeling several physical and engineering problems. As a result, an active consulting firm has been involved in discovering reliable and effective methods for resolving FDEs. Since, it is not easy to find the exact solutions of most FDEs, some approximate and numerical schemes must be produced. Some of the numerical methods used to solve FDEs are differential transform method [8] for fractional partial differential equation from finance, Adams-Bashforth method [9] for chaotic differential equations and Fisher's equation, homotopy analysis method [10] for Nizhnik-Novikov-Veselov system, q-homotopy analysis method [11] for seventh-order time-fractional Lax's Korteweg-de Vries and Sawada-Kotera equations, Shehu transform method [12] for Burgers-Fisher, backward Klomogorov and Klein-Gordon

[1]hiratariq47@gmail.com; [2]rezazadehadi1363@gmail.com; [3]msenol@nevsehir.edu.tr; [4]otasbozan@mku.edu.tr; [5]akurt@pau.edu.tr (Corresponding Author)
[1]Department of Mathematics, GC Women University, Sialkot, Pakistan
[2]Faculty of Engineering Technology, Amol University of Special Modern Technologies, Amol, Iran
[3]Department of Mathematics, Faculty of Science and Art, Nevsehir Haci Bektaş Veli University, Nevsehir, Türkiye
[4]Department of Mathematics, Faculty of Science and Art, Hatay Mustafa Kemal University, Hatay, Türkiye
[5]Department of Mathematics, Faculty of Science , Pamukkale University, Denizli, Türkiye
Article History: Received: 26.02.2023 - Accepted: 25.09.2023 - Published: 15.10.2023

equations and some other systems, perturbation-iteration algorithm [13] for fuzzy partial differential equations and Adomian decomposition method [14] for Burger-Huxley's equation.

Besides, as analytical methods, the functional variable method [15] for the Zakharov-Kuznetsov equation, the Benjamin-Bona-Mahony equation and the Korteweg-de Vries equation, Sine-Gordon expansion method [16] for RLW-class equations, modified Khater method and sech-tanh functions expansion method [17] for emerging telecommunication model, $Exp(-\phi(\xi))$-expansion method [18] for nematicons, new extended direct algebraic method [19] for Konno-Ono equation and Kudryashov's method [20] for nonlinear schrödinger equation are worth mentioning.

In this piece of research, the residual power series method [21–23] is used to obtain new approximate solutions for below mentioned time-fractional Drinfeld-Sokolov-Wilson equation that arise in shallow water flow models. We successfully solved differential equations with this method before [26–29]. Also Jaradat et. al.[30] used RPSM for solving DSW equation where the fractional derivatives are in Caputo sense.

Consider the following nonlinear conformable time-fractional DSW equation, as

$$\begin{aligned}&\frac{\partial^\alpha w(x,t)}{\partial t^\alpha}+\mu v(x,t)\frac{\partial v(x,t)}{\partial x}=0,\\&\frac{\partial^\alpha v(x,t)}{\partial t^\alpha}+\eta\frac{\partial^3 v(x,t)}{\partial x^3}+\gamma w(x,t)\frac{\partial v(x,t)}{\partial x}+\xi v(x,t)\frac{\partial w(x,t)}{\partial x}=0,\qquad 0<\alpha<1,\end{aligned}\tag{1.1}$$

subject to the initial conditions

$$\begin{aligned}w(x,0)&=\hbar(x),\\v(x,0)&=\aleph(x).\end{aligned}\tag{1.2}$$

The purpose of this study is to construct a power series solution for Eqs. (1.1) and (1.2) by its power series expansion among its truncated residual function.The major improvement of the RPSM is that by choosing suitable initial conditions, it can be applied directly to the problem without perturbation, linearization or discretization, in other words, without any adjustments. Furthermore, present method is capable of obtaining results without complicated calculations.

The remainder of the study is carried out as follows: In Section 2, we present essential definitions and results for RPSM. Within Section 3, general procedure of the RPSM is summarized In Sections 4, Implementation of RPSM for Drinfeld-Sokolov-Wilson system is presented. In Section 5, numerical results illustrated. Finally, Section 5 is reserved for conclusion.

2. Essential Definitions and Results for RPSM

Suppose that f is an infinitely α-differentiable function, for some $\alpha\in(0,1]$ at a neighborhood of a point $t=t_0$ then f has the following conformable fractional power series expansion [24, 25]:

$$f(t)=\sum_{p=0}^{\infty}\frac{(T_\alpha^{t_0}f)^{(p)}(t-t_0)^{p\alpha}}{\alpha^p p!},\quad t_0<t<t_0+R^{1/\alpha},\ R>0.\tag{2.1}$$

where $(T_\alpha^{t_0}f)^{(p)}$ is the application of the fractional derivative p times. [23, 25] A power series of the form $\sum_{p=0}^{\infty}g_p(x)(t)^{p\alpha}$ for $0\le m-1<\alpha\le m$ is called multiple fractional power series about $t_0=0$, where g_p's are functions of x called the coefficients of the series. [25] Suppose that $u(x,t)$ has the following multiple fractional power series representation at $t_0 = 0$:

$$u(x,t) = \sum_{p=0}^{\infty} g_p(x) t^{p\alpha}, \quad 0 < \alpha \le 1, x \in I, 0 \le t \le R^{1/\alpha}. \tag{2.2}$$

If $u_t^{(p\alpha)}(x,t)$ are continuous on $I \times (0, R^{1/\alpha})$, $k = 0,1,2,\ldots$, then $g_p(x) = \frac{u_t^{(p\alpha)}(x,0)}{\alpha^p p!}$.

3. General Procedure of the RPSM

The main steps of this procedure are described as follows:

Step 1. Suppose that the solution of Eq. (1.1) and Eq. (1.2) is expressed in the form of fractional power series expansion about the initial point $t = 0$, as

$$\begin{aligned} w(x,t) &= \sum_{p=0}^{\infty} h_p(x) \frac{t^{p\alpha}}{\alpha^p p!}, \\ v(x,t) &= \sum_{p=0}^{\infty} z_p(x) \frac{t^{p\alpha}}{\alpha^p p!}, \quad 0 < \alpha \le 1,\ x \in I,\ 0 \le t < R^{\frac{1}{\alpha}}. \end{aligned} \tag{3.1}$$

The RPSM guarantees that the analytical approximate solution for Eq. (1.1) and Eq. (1.2) are in the form of an infinite fractional power series. To obtain the numerical values from these series, let $w_k(x,t)$ and $v_k(x,t)$ denotes the k-th truncated series of $w(x,t)$ and $v(x,t)$, respectively. *i.e.*,

$$\begin{aligned} w_k(x,t) &= \sum_{p=0}^{k} h_p(x) \frac{t^{p\alpha}}{\alpha^p p!}, \\ v_k(x,t) &= \sum_{p=0}^{k} z_p(x) \frac{t^{p\alpha}}{\alpha^p p!}, \quad 0 < \alpha \le 1,\ x \in I,\ 0 \le t < R^{\frac{1}{\alpha}}. \end{aligned} \tag{3.2}$$

Take $k = 0$ and by the initial condition, the 0-th residual power series approximate solution of $w(x,t)$ and $v(x,t)$ can be written in the following form, as

$$\begin{aligned} w_0(x,t) &= h_0(x) = w(x,0) = \hbar(x), \\ v_0(x,t) &= z_0(x) = v(x,0) = \aleph(x). \end{aligned} \tag{3.3}$$

The Eq. (3.2) can be rewritten, as

$$\begin{aligned} w_k(x,t) &= \hbar(x) + \sum_{p=1}^{k} h_p(x) \frac{t^{p\alpha}}{\alpha^p p!}, \\ v_k(x,t) &= \aleph(x) + \sum_{p=1}^{k} z_p(x) \frac{t^{p\alpha}}{\alpha^p p!}, \quad 0 < \alpha \le 1,\ x \in I,\ 0 \le t, \end{aligned} \tag{3.4}$$

where $k = 1,2,3,\ldots$. By viewing the representations of $w_k(x,t)$ and $v_k(x,t)$, the k-th residual power series approximate solutions will be obtained after $h_p(x), z_p(x)$, $p = 1,2,3,\ldots,k$, are available.

Step 2. Define the residual function, for Eq. (1.1) and Eq. (1.2), as

$$\begin{aligned} Res_w(x,t) &= \frac{\partial^\alpha w(x,t)}{\partial t^\alpha} + \mu v(x,t) \frac{\partial v(x,t)}{\partial x}, \\ Res_v(x,t) &= \frac{\partial^\alpha v(x,t)}{\partial t^\alpha} + \eta \frac{\partial^3 v(x,t)}{\partial x^3} + \gamma w(x,t) \frac{\partial v(x,t)}{\partial x} + \xi v(x,t) \frac{\partial w(x,t)}{\partial x} \end{aligned} \tag{3.5}$$

and the k-th residual functions, $k = 1, 2, 3, \ldots$, can be expressed, as

$$\begin{aligned} Res_{w,k}(x,t) &= \frac{\partial^{\alpha} w_k(x,t)}{\partial t^{\alpha}} + \mu v_k(x,t)\frac{\partial v_k(x,t)}{\partial x}, \\ Res_{v,k}(x,t) &= \frac{\partial^{\alpha} v_k(x,t)}{\partial t^{\alpha}} + \eta\frac{\partial^3 v_k(x,t)}{\partial x^3} + \gamma w_k(x,t)\frac{\partial v_k(x,t)}{\partial x} + \xi v_k(x,t)\frac{\partial w_k(x,t)}{\partial x}. \end{aligned} \tag{3.6}$$

From [25], some useful results for $Res_{w,k}(x,t)$ and $Res_{v,k}(x,t)$ which are essential in the residual power series solution for $j = 0, 1, 2, ..., k$ are stated as follows:

$$\begin{aligned} &(i)\ Res_w(x,t) = 0, Res_v(x,t) = 0, \\ &(ii)\ \lim_{k\to\infty} Res_{w,k}(x,t) = Res_w(x,t), \lim_{k\to\infty} Res_{v,k}(x,t) = Res_v(x,t), \quad for\ each\ x \in I\ and\ t \geq 0, \\ &(iii)\ \frac{\partial^{j\alpha}}{\partial t^{j\alpha}} Res_w(x,0) = \frac{\partial^{j\alpha}}{\partial t^{j\alpha}} Res_{w,k}(x,0) = 0, \frac{\partial^{j\alpha}}{\partial t^{j\alpha}} Res_v(x,0) = \frac{\partial^{j\alpha}}{\partial t^{j\alpha}} Res_{v,k}(x,0) = 0. \end{aligned} \tag{3.7}$$

Step 3. Substitute the k-th truncated series of $w(x,t)$ and $v(x,t)$ into Eq. (3.6) and calculate the fractional derivative $\frac{\partial^{(k-1)\alpha}}{\partial t^{(k-1)\alpha}}$ of $Res_{w,k}(x,t)$ and $Res_{v,k}(x,t)$, $k = 1, 2, 3, ...$ at $t = 0$, together with Eq. (3.7), the following algebraic systems are obtained:

$$\begin{aligned} &\frac{\partial^{(k-1)\alpha}}{\partial t^{(k-1)\alpha}} Res_{w,k}(x,0) = 0, \\ &\frac{\partial^{(k-1)\alpha}}{\partial t^{(k-1)\alpha}} Res_{v,k}(x,0) = 0, \quad 0 < \alpha \leq 1,\ k = 1, 2, 3, \ldots. \end{aligned} \tag{3.8}$$

Step 4. After solving the systems (3.8), the values of the coefficients $h_p(x), z_p(x),\ p = 1, 2, 3, ..., k$ are obtained. Thus, the k-th residual power series approximate solutions is derived.

In the next discussion, the 1st, 2nd, 3rd and 4th residual power series approximate solutions are determined in detail by following the above steps.

4. Implementation of RPSM

For $\boldsymbol{k} = \mathbf{1}$, the 1st-residual power series solutions can be written, as

$$\begin{aligned} w_1(x,t) &= \hbar(x) + h_1(x)\frac{t^{\alpha}}{\alpha}, \\ v_1(x,t) &= \aleph(x) + z_1(x)\frac{t^{\alpha}}{\alpha}. \end{aligned} \tag{4.1}$$

The 1st-residual functions can be written, as

$$\begin{aligned} Res_{w,1}(x,t) &= \frac{\partial^{\alpha} w_1(x,t)}{\partial t^{\alpha}} + \mu v_1(x,t)\frac{\partial v_1(x,t)}{\partial x}, \\ Res_{v,1}(x,t) &= \frac{\partial^{\alpha} v_1(x,t)}{\partial t^{\alpha}} + \eta\frac{\partial^3 v_1(x,t)}{\partial x^3} + \gamma w_1(x,t)\frac{\partial v_1(x,t)}{\partial x} + \xi v_1(x,t)\frac{\partial w_1(x,t)}{\partial x}. \end{aligned} \tag{4.2}$$

Substitute the 1st truncated series, $w_1(x,t)$ and $v_1(x,t)$ into the 1st residual functions, $Res_{w,1}(x,t)$ and $Res_{v,1}(x,t)$, respectively. *i.e.*,

$$\begin{aligned} Res_{w,1}(x,t) &= h_1(x) + \mu\Big(\aleph(x) + z_1(x)\frac{t^\alpha}{\alpha}\Big)\Big(\aleph^{(1)}(x) + z_1^{(1)}(x)\frac{t^\alpha}{\alpha}\Big), \\ Res_{v,1}(x,t) &= z_1(x) + \eta\Big(\aleph^{(3)}(x) + z_1^{(3)}(x)\frac{t^\alpha}{\alpha}\Big) + \gamma\Big(\hbar(x) + h_1(x)\frac{t^\alpha}{\alpha}\Big)\Big(\aleph^{(1)}(x) + z_1^{(1)}(x)\frac{t^\alpha}{\alpha}\Big) \\ &+ \xi\Big(\aleph(x) + z_1(x)\frac{t^\alpha}{\alpha}\Big)\Big(\hbar^{(1)}(x) + h_1^{(1)}(x)\frac{t^\alpha}{\alpha}\Big) \end{aligned} \tag{4.3}$$

From Eq. (3.8) and Eq. (4.3), it can be written, as

$$\begin{aligned} h_1(x) &= -\big(\mu\aleph(x)\aleph^{(1)}(x)\big), \\ z_1(x) &= -\big(\xi\aleph(x)\hbar^{(1)}(x) + \gamma\hbar(x)\aleph^{(1)}(x) + \eta\aleph^{(3)}(x)\big). \end{aligned} \tag{4.4}$$

The 1st RPS approximate solutions can be written in the following form, as

$$\begin{aligned} w_1(x,t) &= \hbar(x) - \frac{t^\alpha}{\alpha}\Big(\mu\aleph(x)\aleph^{(1)}(x)\Big), \\ v_1(x,t) &= \aleph(x) - \frac{t^\alpha}{\alpha}\Big(\xi\aleph(x)\hbar^{(1)}(x) + \gamma\hbar(x)\aleph^{(1)}(x) + \eta\aleph^{(3)}(x)\Big). \end{aligned} \tag{4.5}$$

For $\boldsymbol{k} = \mathbf{2}$, the 2nd-residual power series solution can be written, as

$$\begin{aligned} w_1(x,t) &= \hbar(x) + h_1(x)\frac{t^\alpha}{\alpha} + h_2(x)\frac{t^{2\alpha}}{2\alpha^2}, \\ v_1(x,t) &= \aleph(x) + z_1(x)\frac{t^\alpha}{\alpha} + z_2(x)\frac{t^{2\alpha}}{2\alpha^2}. \end{aligned} \tag{4.6}$$

Substitute the 2nd truncated series $u_2(x,t)$ into the 2nd residual function $Res_2(x,t)$, *i.e.*,

$$\begin{aligned} Res_{w,2}(x,t) &= h_1(x) + h_2(x)\frac{t^\alpha}{\alpha} + \mu\Big(\aleph(x) + z_1(x)\frac{t^\alpha}{\alpha} + z_2(x)\frac{t^{2\alpha}}{2\alpha^2}\Big)\Big(\aleph^{(1)}(x) + z_1^{(1)}(x)\frac{t^\alpha}{\alpha} + z_2^{(1)}(x)\frac{t^{2\alpha}}{2\alpha^2}\Big), \\ Res_{v,2}(x,t) &= z_1(x) + z_2(x)\frac{t^\alpha}{\alpha} + \eta\Big(\aleph^{(3)}(x) + z_1^{(3)}(x)\frac{t^\alpha}{\alpha} + z_2^{(3)}(x)\frac{t^{2\alpha}}{2\alpha^2}\Big) + \gamma\Big(\hbar(x) + h_1(x)\frac{t^\alpha}{\alpha} \\ &+ h_2(x)\frac{t^{2\alpha}}{2\alpha^2}\Big)\Big(\aleph^{(1)}(x) + z_1^{(1)}(x)\frac{t^\alpha}{\alpha} + z_2^{(1)}(x)\frac{t^{2\alpha}}{2\alpha^2}\Big) + \xi\Big(\aleph(x) + z_1(x)\frac{t^\alpha}{\alpha} \\ &+ z_2(x)\frac{t^{2\alpha}}{2\alpha^2}\Big)\Big(\hbar^{(1)}(x) + h_1^{(1)}(x)\frac{t^\alpha}{\alpha} + h_2^{(1)}(x)\frac{t^{2\alpha}}{2\alpha^2}\Big) \end{aligned} \tag{4.7}$$

From Eq.(3.8) and Eq.(4.7), it can be written, as

$$\begin{aligned} h_2(x) &= -\Big(\mu z_1(x)\aleph^{(1)}(x) + \mu\aleph(x)z_1^{(1)}(x)\Big), \\ z_2(x) &= -\Big(\xi z_1(x)\hbar^{(1)}(x) + \xi\aleph(x)h_1^{(1)}(x) + \gamma h_1(x)\aleph^{(1)}(x) \\ &+ \gamma\hbar(x)z_1^{(1)}(x) + \eta z_1^{(3)}(x)\Big) \end{aligned} \tag{4.8}$$

The 2nd residual power series approximate solutions can be written in the following form, as

$$\begin{aligned} w_2(x,t) &= \hbar(x) - \frac{t^\alpha}{\alpha}\Big(\mu\aleph(x)\aleph^{(1)}(x)\Big) - \frac{t^{2\alpha}}{2\alpha^2}\Big(\mu z_1(x)\aleph^{(1)}(x) + \mu\aleph(x)z_1^{(1)}(x)\Big),\\ v_2(x,t) &= \aleph(x) - \frac{t^\alpha}{\alpha}\Big(\xi\aleph(x)\hbar^{(1)}(x) + \gamma\hbar(x)\aleph^{(1)}(x) + \eta\aleph^{(3)}(x)\Big) - \frac{t^{2\alpha}}{2\alpha^2}\Big(\xi z_1(x)\hbar^{(1)}(x)\\ &\quad + \xi\aleph(x)h_1^{(1)}(x) + \gamma h_1(x)\aleph^{(1)}(x) + \gamma\hbar(x)z_1^{(1)}(x) + \eta z_1^{(3)}(x)\Big). \end{aligned} \tag{4.9}$$

For $\boldsymbol{k} = \mathbf{3}$, substitute the 3rd truncated series,

$$\begin{aligned} w_3(x,t) &= \hbar(x) + h_1(x)\frac{t^\alpha}{\alpha} + h_2(x)\frac{t^{2\alpha}}{2\alpha^2} + h_3(x)\frac{t^{3\alpha}}{6\alpha^3},\\ v_3(x,t) &= \aleph(x) + z_1(x)\frac{t^\alpha}{\alpha} + z_2(x)\frac{t^{2\alpha}}{2\alpha^2} + z_3(x)\frac{t^{3\alpha}}{6\alpha^3}. \end{aligned} \tag{4.10}$$

of Eq. (1.1) and Eq. (1.2) into the 3rd residual function, $Res_3(x,t)$, of Eq.(3.6), i.e.,

$$\begin{aligned} Res_{w,3}(x,t) &= h_1(x) + h_2(x)\frac{t^\alpha}{\alpha} + h_3(x)\frac{t^{2\alpha}}{2\alpha^2} + \mu\Big(\aleph(x) + z_1(x)\frac{t^\alpha}{\alpha} + z_2(x)\frac{t^{2\alpha}}{2\alpha^2} + z_3(x)\frac{t^{3\alpha}}{6\alpha^3}\Big)\Big(\aleph^{(1)}(x)\\ &\quad + z_1^{(1)}(x)\frac{t^\alpha}{\alpha} + z_2^{(1)}(x)\frac{t^{2\alpha}}{2\alpha^2} + z_3^{(1)}(x)\frac{t^{3\alpha}}{6\alpha^3}\Big),\\ Res_{v,3}(x,t) &= z_1(x) + z_2(x)\frac{t^\alpha}{\alpha} + z_3(x)\frac{t^{2\alpha}}{2\alpha^2} + \eta\Big(\aleph^{(3)}(x) + z_1^{(3)}(x)\frac{t^\alpha}{\alpha} + z_2^{(3)}(x)\frac{t^{2\alpha}}{2\alpha^2} + z_3^{(3)}(x)\frac{t^{3\alpha}}{6\alpha^3}\Big)\\ &\quad + \gamma\Big(\hbar(x) + h_1(x)\frac{t^\alpha}{\alpha} + h_2(x)\frac{t^{2\alpha}}{2\alpha^2} + h_3(x)\frac{t^{3\alpha}}{6\alpha^3}\Big)\Big(\aleph^{(1)}(x) + z_1^{(1)}(x)\frac{t^\alpha}{\alpha}\\ &\quad + z_2^{(1)}(x)\frac{t^{2\alpha}}{2\alpha^2} + z_3^{(1)}(x)\frac{t^{3\alpha}}{6\alpha^3}\Big) + \xi\Big(\aleph(x) + z_1(x)\frac{t^\alpha}{\alpha} + z_2(x)\frac{t^{2\alpha}}{2\alpha^2} + z_3(x)\frac{t^{3\alpha}}{6\alpha^3}\Big)\Big(\hbar^{(1)}(x)\\ &\quad + h_1^{(1)}(x)\frac{t^\alpha}{\alpha} + h_2^{(1)}(x)\frac{t^{2\alpha}}{2\alpha^2} + h_3^{(1)}(x)\frac{t^{3\alpha}}{6\alpha^3}\Big) \end{aligned} \tag{4.11}$$

Now, solving the equation $\frac{\partial^{(k-1)\alpha}}{\partial t^{(k-1)\alpha}} Res_k(x,0) = 0$, for $k = 3$ gives the required value of $g_3(x)$, as

$$\begin{aligned} h_3(x) &= -\Big(\mu z_2(x)\aleph^{(1)}(x) + 2\mu z_1(x)z_1^{(1)}(x) + \mu\aleph(x)z_2^{(1)}(x)\Big),\\ z_3(x) &= -\Big(\xi z_2(x)\hbar^{(1)}(x) + 2\xi z_1(x)h_1^{(1)}(x) + \xi\aleph(x)h_2^{(1)}(x) + \gamma h_2(x)\aleph^{(1)}(x)\\ &\quad + 2\gamma h_1(x)z_1^{(1)}(x) + \gamma\hbar(x)z_2^{(1)}(x) + \eta z_2^{(3)}(x)\Big) \end{aligned} \tag{4.12}$$

Based on the previous results for $g_0(x)$, $g_1(x)$ and $g_2(x)$, the 3rd residual power series approximate solution becomes

$$\begin{aligned} w_3(x,t) &= \hbar(x) - \frac{t^\alpha}{\alpha}\Big(\mu\aleph(x)\aleph^{(1)}(x)\Big) - \frac{t^{2\alpha}}{2\alpha^2}\Big(\mu z_1(x)\aleph^{(1)}(x) + \mu\aleph(x)z_1^{(1)}(x)\Big)\\ &\quad - \frac{t^{3\alpha}}{6\alpha^3}\Big(\mu z_2(x)\aleph^{(1)}(x) + 2\mu z_1(x)z_1^{(1)}(x) + \mu\aleph(x)z_2^{(1)}(x)\Big),\\ v_3(x,t) &= \aleph(x) - \frac{t^\alpha}{\alpha}\Big(\xi\aleph(x)\hbar^{(1)}(x) + \gamma\hbar(x)\aleph^{(1)}(x) + \eta\aleph^{(3)}(x)\Big) - \frac{t^{2\alpha}}{2\alpha^2}\Big(\xi z_1(x)\hbar^{(1)}(x)\\ &\quad + \xi\aleph(x)h_1^{(1)}(x) + \gamma h_1(x)\aleph^{(1)}(x) + \gamma\hbar(x)z_1^{(1)}(x) + \eta z_1^{(3)}(x)\Big)\\ &\quad - \frac{t^{3\alpha}}{6\alpha^3}\Big(\xi z_2(x)\hbar^{(1)}(x) + 2\xi z_1(x)h_1^{(1)}(x) + \xi\aleph(x)h_2^{(1)}(x) + \gamma h_2(x)\aleph^{(1)}(x)\\ &\quad + 2\gamma h_1(x)z_1^{(1)}(x) + \gamma\hbar(x)z_2^{(1)}(x) + \eta z_2^{(3)}(x)\Big). \end{aligned} \tag{4.13}$$

For $\boldsymbol{k} = \mathbf{4}$, substitute the 4th truncated series, $w_4(x,t) = \hbar(x) + h_1(x)\frac{t^\alpha}{\alpha} + h_2(x)\frac{t^{2\alpha}}{2\alpha^2} + h_3(x)\frac{t^{3\alpha}}{6\alpha^3} + h_4(x)\frac{t^{4\alpha}}{24\alpha^4}$, $v_4(x,t) = \aleph(x) + z_1(x)\frac{t^\alpha}{\alpha} + z_2(x)\frac{t^{2\alpha}}{2\alpha^2} + z_3(x)\frac{t^{3\alpha}}{6\alpha^3} + z_4(x)\frac{t^{4\alpha}}{24\alpha^4}$ of Eq. (1.1) and Eq. (1.2) into the 4th residual function,$Res_4(x,t)$, of Eq.(3.6), *i.e.*, $Res_4(x,t)$ is equals to

$$\begin{aligned}
Res_{w,4}(x,t) = {} & h_1(x) + h_2(x)\frac{t^\alpha}{\alpha} + h_3(x)\frac{t^{2\alpha}}{2\alpha^2} + h_4(x)\frac{t^{3\alpha}}{6\alpha^3} + \mu\Big(\aleph(x) + z_1(x)\frac{t^\alpha}{\alpha} + z_2(x)\frac{t^{2\alpha}}{2\alpha^2} \\
& + z_3(x)\frac{t^{3\alpha}}{6\alpha^3} + z_4(x)\frac{t^{4\alpha}}{24\alpha^4}\Big)\Big(\aleph^{(1)}(x) + z_1^{(1)}(x)\frac{t^\alpha}{\alpha} + z_2^{(1)}(x)\frac{t^{2\alpha}}{2\alpha^2} + z_3^{(1)}(x)\frac{t^{3\alpha}}{6\alpha^3} \\
& + z_4^{(1)}(x)\frac{t^{4\alpha}}{24\alpha^4}\Big), \\
Res_{v,4}(x,t) = {} & z_1(x) + z_2(x)\frac{t^\alpha}{\alpha} + z_3(x)\frac{t^{2\alpha}}{2\alpha^2} + z_4(x)\frac{t^{3\alpha}}{6\alpha^3} + \eta\Big(\aleph^{(3)}(x) + z_1^{(3)}(x)\frac{t^\alpha}{\alpha} \\
& + z_2^{(3)}(x)\frac{t^{2\alpha}}{2\alpha^2} + z_3^{(3)}(x)\frac{t^{3\alpha}}{6\alpha^3} + z_4^{(3)}(x)\frac{t^{4\alpha}}{24\alpha^4}\Big) + \gamma\Big(\hbar(x) + h_1(x)\frac{t^\alpha}{\alpha} + h_2(x)\frac{t^{2\alpha}}{2\alpha^2} \\
& + h_3(x)\frac{t^{3\alpha}}{6\alpha^3} + h_4(x)\frac{t^{4\alpha}}{24\alpha^4}\Big)\Big(\aleph^{(1)}(x) + z_1^{(1)}(x)\frac{t^\alpha}{\alpha} + z_2^{(1)}(x)\frac{t^{2\alpha}}{2\alpha^2} + z_3^{(1)}(x)\frac{t^{3\alpha}}{6\alpha^3} \\
& + z_4^{(1)}(x)\frac{t^{4\alpha}}{24\alpha^4}\Big) + \xi\Big(\aleph(x) + z_1(x)\frac{t^\alpha}{\alpha} + z_2(x)\frac{t^{2\alpha}}{2\alpha^2} + z_3(x)\frac{t^{3\alpha}}{6\alpha^3} \\
& + z_4(x)\frac{t^{4\alpha}}{24\alpha^4}\Big)\Big(\hbar^{(1)}(x) + h_1^{(1)}(x)\frac{t^\alpha}{\alpha} + h_2^{(1)}(x)\frac{t^{2\alpha}}{2\alpha^2} + h_3^{(1)}(x)\frac{t^{3\alpha}}{6\alpha^3} + h_4^{(1)}(x)\frac{t^{4\alpha}}{24\alpha^4}\Big)
\end{aligned} \tag{4.14}$$

From Eq. (3.8) and Eq. (4.14), it can be written, as

$$\begin{aligned}
h_4(x) = {} & -\Big(\mu z_3(x)\aleph^{(1)}(x) + 3\mu z_2(x)z_1^{(1)}(x) + 3\mu z_1(x)z_2^{(1)}(x) + \mu\aleph(x)z_3^{(1)}(x)\Big), \\
z_4(x) = {} & -\Big(\xi z_3(x)\hbar^{(1)}(x) + \gamma h_3(x)\aleph^{(1)}(x) + 3\xi z_2(x)h_1^{(1)}(x) + 3\xi z_1(x)h_2^{(1)}(x) + \xi\aleph(x)h_3^{(1)}(x) \\
& + 2\gamma h_2(x)z_1^{(1)}(x) + 3\gamma h_1(x)z_2^{(1)}(x) + \gamma\hbar(x)z_3^{(1)}(x) + \eta z_3^{(3)}(x)\Big)
\end{aligned} \tag{4.15}$$

Based on the previous results for $h_0(x)$, $h_1(x)$, $h_2(x)$ and $h_3(x)$ and $z_0(x)$, $z_1(x)$, $z_2(x)$ and $z_3(x)$, the 4th residual power series approximate solution can be obtained. For the convergence analysis, see [25]

5. Numerical Results

To illustrate the authenticity of the RPSM method to solve the nonlinear conformable time-fractional Drinfeld-Sokolov-Wilson equation, three applications are considered. Consider the following time-fractional Drinfeld-Sokolov-Wilson equation, as

$$\begin{aligned}
& \frac{\partial^\alpha w(x,t)}{\partial t^\alpha} + 3v(x,t)\frac{\partial v(x,t)}{\partial x} = 0, \\
& \frac{\partial^\alpha v(x,t)}{\partial t^\alpha} + 2\frac{\partial^3 v(x,t)}{\partial x^3} + 2w(x,t)\frac{\partial v(x,t)}{\partial x} + v(x,t)\frac{\partial w(x,t)}{\partial x} = 0, \qquad 0 < \alpha < 1,
\end{aligned} \tag{5.1}$$

subject to the initial conditions

$$\begin{aligned}
w(x,0) &= 3sech^2(x), \\
v(x,0) &= 2sech(x).
\end{aligned} \tag{5.2}$$

The exact solution of this problem for $\alpha = 1$ is given in , as

$$w(x,t) = 3sech^2(x-2t),$$
$$v(x,t) = 2sech(x-2t). \tag{5.3}$$

It can be observed that numerical results are agreement with the exact solution with a high accuracy. Also, it is clear that the adding new terms of the residual power series approximations can make the overall error smaller.

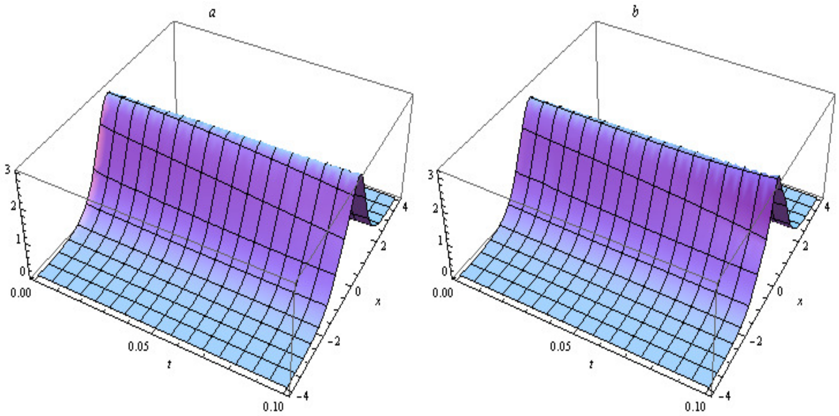

Figure 1. 3D surface plots for the 4th residual power series solution $w_4(x,t)$ with a. $\alpha = 0.8$ and b. $\alpha = 0.9$ for Example 5

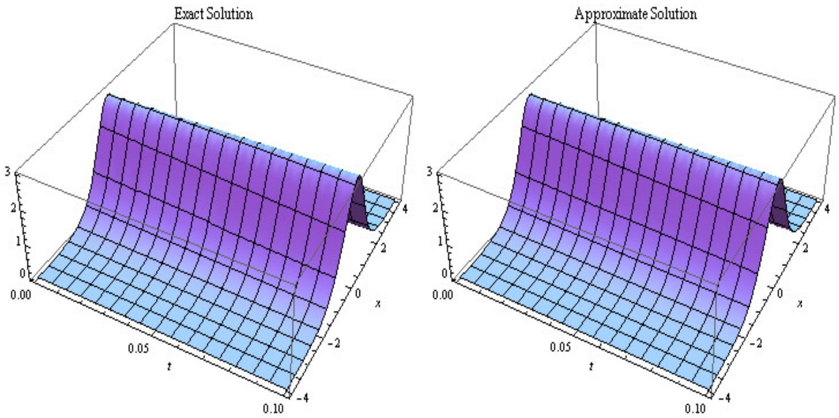

Figure 2. 3D surface plots of exact solution and approximate solution $w_4(x,t)$ at $\alpha = 1$ of Example 5.

6. Conclusion

In this research, we have given an algorithm, namely the Residual Power Series Method (RPSM), for the approximate solution of the fractional Drinfeld - Sokolov - Wilson equation system. The scheme is based on the power series and the solutions are determined in the form of a converging series with simple calculations. The approach offers approximate solutions with a good level of precision. Summing up these results, we can conclude that the residual power series method, in its general form, offers a fair amount of calculations, is an efficient method and simple to apply for nonlinear fractional differential equations in general form.

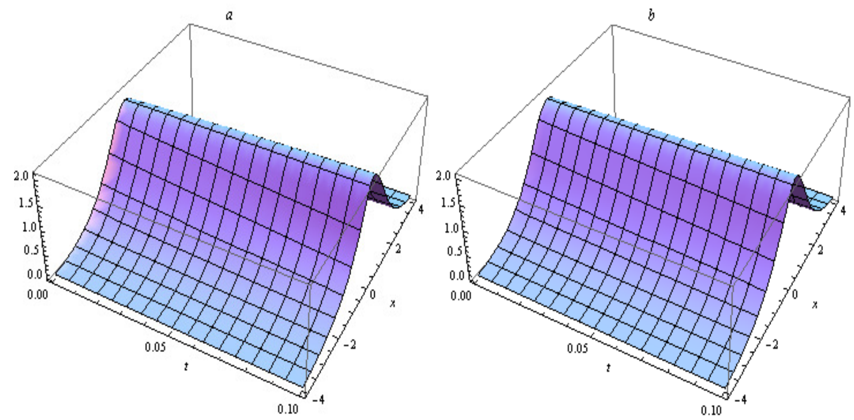

Figure 3. 3D surface plots for the 4th residual power series solution $v_4(x,t)$ with a. $\alpha = 0.8$ and b. $\alpha = 0.9$ for Example 5

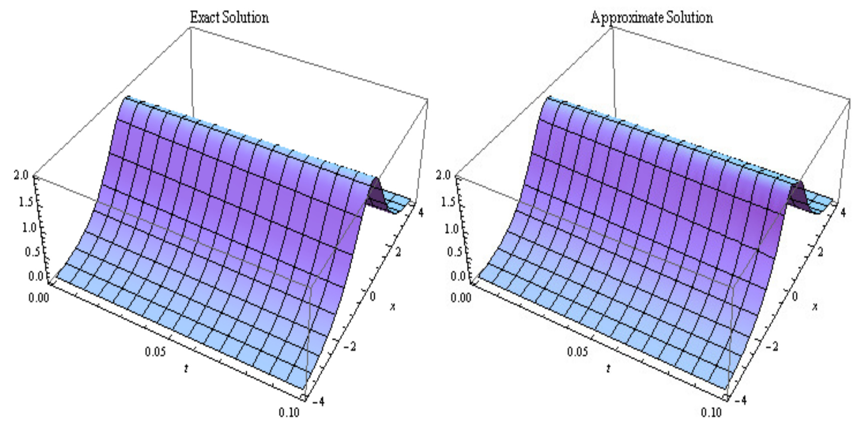

Figure 4. 3D surface plots of exact solution and approximate solution $v_4(x,t)$ at $\alpha = 1$ of Example 5.

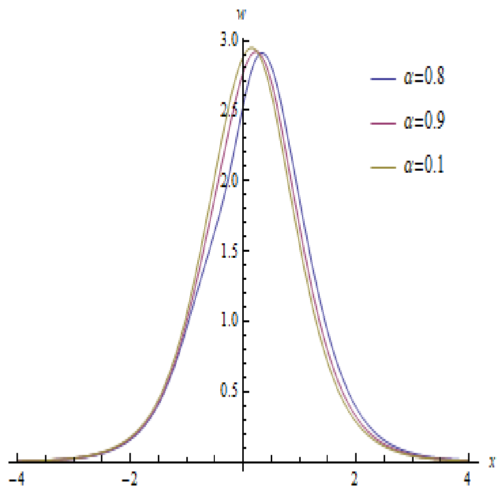

Figure 5. 2D plot of solutions w_3 at $t = 0.1$ for Example 5.

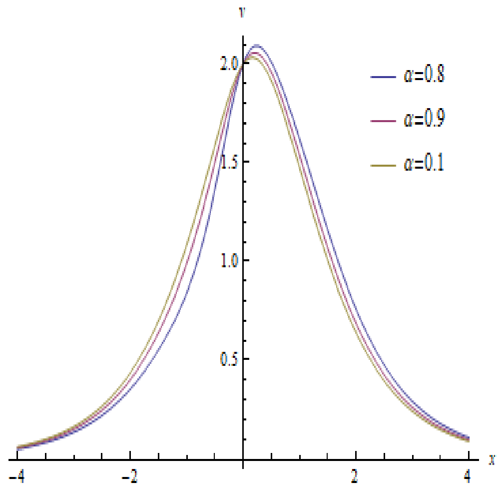

Figure 6. 2D plot of solutions v_2 at $t = 0.1$ for Example 5.

Author Contributions

All authors contributed equally to this work. They all read and approved the final version of the manuscript.

Conflicts of Interest

The authors declare no conflict of interest.

References

[1] Kulish, V. V., Lage, J. L. (2002). Application of fractional calculus to fluid mechanics. J. Fluids Eng., 124(3), 803-806.

[2] Cruz Duarte, J.M., Rosales Garcia, J., Correa Cely, C.R., Garcia Perez, A., Avina Cervantes, J.G. (2018). A closed form expression for the Gaussian-based Caputo-Fabrizio fractional derivative for signal processing applications. Communications in Nonlinear Science and Numerical Simulation, 61, 138-148.

[3] He, J.H., Ji, F.Y. (2019). Two-scale mathematics and fractional calculus for thermodynamics. Thermal Science, 23(4), 2131-2133.

[4] Landman, K. A., Pettet, G. J., Newgreen, D. F. (2003). Mathematical models of cell colonization of uniformly growing domains. Bulletin of mathematical biology, 65(2), 235-262.

[5] Tarasov, V. E. (2019). On history of mathematical economics: Application of fractional calculus. Mathematics, 7(6), 509.

[6] Ionescu, C., Kelly, J.F. (2017). Fractional calculus for respiratory mechanics: Power law impedance, viscoelasticity, and tissue heterogeneity. Chaos, Solitons & Fractals, 102, 433-440.

[7] Tufenkci, S., Senol, B., Alagoz, B. B. (2019, September). Disturbance Rejection Fractional Order PID Controller Design in v-domain by Particle Swarm Optimization. In 2019 International Artificial Intelligence and Data Processing Symposium (IDAP) (pp. 1-6). IEEE.

[8] Yavuz, M., Ozdemir, N., Okur, Y. Y. (2016, July). Generalized differential transform method for fractional partial differential equation from finance. In Proceedings, International Conference on Fractional Dif-

ferentiation and its Applications, Novi Sad, Serbia (pp. 778-785).

[9] Atangana, A., Owolabi, K.M. (2018). New numerical approach for fractional differential equations. Mathematical Modelling of Natural Phenomena, 13(1), 3.

[10] Kurt, A., Tasbozan, O., Baleanu, D. (2017). New solutions for conformable fractional Nizhnik-Novikov-Veselov system via G'/G G'/G expansion method and homotopy analysis methods. Optical and Quantum Electronics, 49, 1-16.

[11] Akinyemi, L. (2019). q-Homotopy analysis method for solving the seventh-order time-fractional Laxâs Korteweg-de Vries and Sawada-Kotera equations. Computational and Applied Mathematics, 38(4), 191.

[12] Akinyemi, L., Iyiola, O. S. (2020). Exact and approximate solutions of time-fractional models arising from physics via Shehu transform. Mathematical Methods in the Applied Sciences, 43(12), 7442-7464.

[13] Senol, M., Atpinar, S., Zararsiz, Z., Salahshour, S., Ahmadian, A. (2019). Approximate solution of time-fractional fuzzy partial differential equations. Computational and Applied Mathematics, 38(1), 1-18.

[14] Hammouch, Z., Mekkaoui, T. (2012). Adomian decomposition method for solving a time-fractional Burger-Huxley's equation. Nonlinear Studies, 19(3).

[15] Rezazadeh, H., Vahidi, J., Zafar, A., Bekir, A. (2019). The Functional Variable Method to Find New Exact Solutions of the Nonlinear Evolution Equations with Dual-Power-Law Nonlinearity. International Journal of Nonlinear Sciences and Numerical Simulation. DOI: https://doi.org/10.1515/ijnsns-2019-0064.

[16] Korkmaz, A., Hepson, O. E., Hosseini, K., Rezazadeh, H., Eslami, M. (2018). Sine-Gordon expansion method for exact solutions to conformable time fractional equations in RLW-class. Journal of King Saud University-Science. 32 (1), 567-574.

[17] Park, C., Khater, M.M., Abdel-Aty, A.H., Attia, R.A., Rezazadeh, H., Zidan, A.M., Mohamed, A.B. (2020). Dynamical analysis of the nonlinear complex fractional emerging telecommunication model with higherâorder dispersive cubic-quintic. Alexandria Engineering Journal, 59(3), 1425-1433.

[18] Raza, N., Afzal, U., Butt, A. R., Rezazadeh, H. (2019). Optical solitons in nematic liquid crystals with Kerr and parabolic law nonlinearities. Optical and Quantum Electronics, 51(4), 107.

[19] Mirhosseini-Alizamini, S. M., Rezazadeh, H., Srinivasa, K., Bekir, A. (2020). New closed form solutions of the new coupled Konno-Oono equation using the new extended direct algebraic method. Pramana, 94, 1-12.

[20] Biswas, A., Rezazadeh, H., Mirzazadeh, M., Eslami, M., Zhou, Q., Moshokoa, S. P., & Belic, M. (2018). Optical solitons having weak non-local nonlinearity by two integration schemes. Optik, 164, 380-384.

[21] Arqub, O. A. (2013). Series solution of fuzzy differential equations under strongly generalized differentiability. Journal of Advanced Research in Applied Mathematics, 5(1), 31-52.

[22] Arqub, O. A., El-Ajou, A., Bataineh, A. S., Hashim, I. (2013, January). A representation of the exact solution of generalized Lane-Emden equations using a new analytical method. In Abstract and Applied Analysis (Vol. 2013). Hindawi.

[23] El-Ajou, A., Arqub, O. A., Zhour, Z. A., Momani, S. (2013). New results on fractional power series: theories and applications. Entropy, 15(12), 5305-5323.

[24] Abdeljawad, T. (2015). On conformable fractional calculus. Journal of computational and Applied Mathematics, 279, 57-66.

[25] Senol, M., Tasbozan, O., Kurt, A. (2019). Numerical solutions of fractional Burgers' type equations with conformable derivative. Chinese Journal of Physics, 58, 75-84.

[26] Tariq, H., Akram, G. (2017). New traveling wave exact and approximate solutions for the nonlinear Cahn-Allen equation: evolution of a nonconserved quantity. Nonlinear Dynamics, 88, 581-594.

[27] Tariq, H., Sadaf, M., Akram, G., Rezazadeh, H., Baili, J., Lv, Y.P., Ahmad, H. (2021). Computational study for the conformable nonlinear Schrödinger equation with cubic-quintic-septic nonlinearities. Results in Physics, 30, 104839.

[28] Tariq, H., Günerhan, H., Rezazadeh, H., Adel, W. (2021). A numerical approach for the nonlinear temporal conformable fractional foam drainage equation. Asian-European Journal of Mathematics, 14(06), 2150089.

[29] Tariq, H., Akram, G. (2017). Residual power series method for solving time-space-fractional Benney-Lin equation arising in falling film problems. Journal of Applied Mathematics and Computing, 55(1), 683-708.

[30] Jaradat, H. M., Al-Shara, S., Khan, Q. J., Alquran, M., Al-Khaled, K. (2016). Analytical solution of time-fractional Drinfeld-Sokolov-Wilson system using residual power series method. IAENG International Journal of Applied Mathematics, 46(1), 64-70.

Ikonion Journal of Mathematics
https://dergipark.org.tr/tr/pub/ikjm
Research Article
Open Access
https://doi.org/10.54286/ikjm.1335660

ISSN: 2687-6531

The Numerical Solutions of the Conformable Time-Fractional Noyes Field Model via a New Hybrid Method

Bedir Kaan ÖNER [1], Halil ANAÇ [2]

Keywords:
Conformable time-fractional Noyes Field model,
q-Sawi homotopy analysis transform method,
Conformable Sawi transform

Abstract — This article employs a novel method, namely the conformable q-Sawi homotopy analysis transform method (Cq-SHATM) to investigate the numerical solutions of the nonlinear conformable time-fractional Noyes-Field model. The proposed method, namely Cq-SHATM, is a hybrid approach that integrates the q-homotopy analysis transform method and the Sawi transform using the concept of conformable derivative. 3D graps of the solutions obtained with this method were drawn. Additionally, 2D graphs of the solutions were obtained in the Maple software program. The computer simulations were conducted in order to validate the efficacy and reliability of the proposed method.

Subject Classification (2020): 65H05,26A33,35R11.

1. Introduction

Beyond the integer order of calculus is the arbitrary order of fractional calculus (FC). When renowned scientists Leibniz and L'Hospital first spoke to one another in roughly 1695, it was discussed. Because fractional calculus may be used to accurately describe a wide variety of nonlinear phenomena, several writers have recently begun to investigate it. Differential equations of the fractional order variety have an impact on both genetic material and non-local material features. Many well-known mathematicians have studied and written on fractional calculus. They created the foundation for fractional calculus through their work. Nowadays, systems that vary over time are frequently studied and nonlinear models created using fractional partial differential equations. Numerous concepts, including chaos theory, have been connected to fractional-order calculus theory. In order to characterize the characteristics of natural systems that don't behave linearly, fractional differential equations are used. We obtain precise answers to fractional differential equations that model nonlinear processes using a variety of analytical and numerical techniques [1–13].

Mohand and Mahgoub [14] introduced a novel integral transform known as the Sawi transform. Problems with population increase and decay were satisfactorily explained using the Sawi transform [15]. In [16], it introduces the "Sawi decomposition method," a novel approach for solving Volterra

[1] onerbedir@outlook.com; [2] halilanac0638@gmail.com (Corresponding Author)
[1] Graduate Education Institute, Gumushane University, Gumushane, Turkey
[2] Torul Vocational School, Gumushane University, Gumushane, Turkey
Article History: Received: 31.07.2023 — Accepted: 24.10.2023 — Published: 20.11.2023

integral equations and its application. The Sawi transformation is employed in the computation of solutions for systems of ordinary differential equations, specifically in the context of determining the concentration of chemical reactants involved in a series chemical reaction [17]. A novel double fuzzy transform, referred to as the double fuzzy Sawi transform, is proposed. This paper presents a formal proof of fundamental properties associated with the single fuzzy Sawi transform and the double fuzzy Sawi transform. The present study employs a technique to derive the precise solution of a non-homogeneous linear fuzzy telegraph equation, incorporating a generalized Hukuhara partial differentiability [18].

The Belousov–Zhabotinsky (B-Z) reaction is a classic example of a chemical oscillating reaction. It was discovered independently by Boris Belousov and Anatol Zhabotinsky in the 1950s. The B-Z reaction is a type of non-equilibrium chemical system that exhibits periodic changes in color, indicating oscillations between different chemical states. One of the remarkable aspects of the B-Z reaction is its ability to exhibit spontaneous oscillations in concentrations of different chemical species. These oscillations are typically observed through changes in color, and the reaction cycles through various states over time. The reaction is autocatalytic, meaning that one of the products of the reaction catalyzes its own formation. This positive feedback loop is essential for the oscillatory behavior observed in the system. The B-Z reaction is relatively complex and involves the interaction of multiple chemical species. It typically includes the oxidation of an organic compound by bromate ions in the presence of various catalysts, such as cerium ions. While the B-Z reaction itself is a fascinating example of chemical kinetics and nonlinear dynamics, its practical applications are limited. However, the principles learned from studying such systems contribute to our understanding of complex dynamic behavior in chemical systems. The Belousov–Zhabotinsky reaction has been of interest in the fields of chemistry and physics, particularly for its ability to illustrate concepts related to chaos and nonlinear dynamics. Researchers have also explored its potential relevance to understanding certain biological processes, as oscillatory behavior is observed in various biological systems. The B-Z reaction is often demonstrated in educational settings to illustrate the dynamic and unpredictable behavior that can arise in chemical systems, challenging the common perception of chemical reactions as static processes.In the current study, we take into consideration the Belousov-Zhabotinsky (B-Z) nonlinear oscillatory system with conformable time-fractional derivative in Caputo sense. The B-Z family of oscillating chemical reactions is intriguing because it can exhibit both spatial traveling concentration waves and temporal oscillations, both of which are accompanied by striking color changes [19]. In a closed system, this reaction can produce up to many thousands of oscillatory cycles, making it possible to study the chemical waves and patterns without having to constantly replace the reactants [20].

For this B-Z, the streamlined conformable time-fractional Noyes-Field model is given as

$$\begin{cases} {}_tT_\mu \rho(x,t) = \vartheta_1 \dfrac{\partial^2 \rho(x,t)}{\partial x^2} + \beta\delta w(x,t) + \rho - \rho^2 - \delta\rho w(x,t), \\ {}_tT_\mu w(x,t) = \vartheta_2 \dfrac{\partial^2 w(x,t)}{\partial x^2} + \gamma w(x,t) - \lambda\rho(x,t) w(x,t). \end{cases} \tag{1}$$

where, ${}_tT_\mu$ is conformable time-fractional oder $\mu \in (0,1]$ in Caputo sense and $0 < t < 1$.

Since the operator in a nonlinear problem with fractional order is described by an integral, these issues are frequently more challenging to solve. The exact and numerical solutions to the fractional problems, however, have been investigated using a variety of computing approaches that have been created. Some of the utilized methods are Adomian decomposition method (ADM) [21-23], variational iteration method (VIM) [24], homotopy analysis method (HAM) [25-28], differential transform method (DTM) [29-30], homotopy perturbation method (HPM) [31-33], residual power series method (RPSM) [34-36], Laplace decomposition method (LDM) [37], q-homotopy analysis method (q-HAM) [38-44], q-homotopy analysis transform method (q-HATM) [45], fractional reduced differential transofrm method (FRDTM) [45], conformable fractional Elzaki decomposition method (CFEDM) [46], conformable q-homotopy analysis transform method (Cq-HATM) [47], conformable Shehu homotopy perturbation method (CSHPM) [47], conformable fractional q-Shehu homotopy analysis transform method (CFq-SHATM) [48], conformable Shehu transform decomposition method (CSTDM) [48]. The main goal of this study is to come up with a new method: the conformable q-Sawi homotopy analysis transform method (Cq-SHATM).

Here is a list of the rest of the study. The basics of conformable fractional calculus and the Sawi transform are explained in the second part. In Section 3, the new conformable fractional numerical methods are presented. Section 4 shows an example of the conformable time-fractional Noyes Field model. In Section 5, the result is given.

2. Preliminaries

Now let's give the definitions to be used in the study.

Definition 2.1. [49-52] Let a function $f: [0,\infty) \to \mathbb{R}$. Then, the conformable fractional derivative of f order μ is described by

$$T_\mu(f)(x) = \lim_{\varepsilon\to 0} \frac{f(x+\varepsilon x^{1-\mu}) - f(x)}{\varepsilon}, \tag{2}$$

for all $x > 0, \mu \in (0,1]$.

Theorem 2.1. [49-50, 52] Let $\mu \in (0,1]$ and f, g be μ −differentiable at a point $x > 0$. Then

$(i)\ T_\mu(af + bg) = aT_\mu(f) + bT_\mu(g)$, for all $a, b \in \mathbb{R}$, (3)

$(ii)\ T_\mu(x^p) = px^{p-1}$, for all $p \in \mathbb{R}$, (4)

$(iii)\ T_\mu(\tau) = 0, for\ all\ constant\ functions, f(t) = \tau,$ (5)

$(iv)\ T_\mu(fg) = fT_\mu(g) + gT_\mu(f),$ (6)

$$(v)\ T_\mu\left(\frac{f}{g}\right) = \frac{gT_\mu(f) - fT_\mu(g)}{g^2}. \tag{7}$$

Definition 2.2. Let $0 < \mu \le 1$, $f: [0,\infty) \to \mathbb{R}$ be real valued function. Then, the conformable fractional Sawi transform (CFST) of order μ of f is defined by

$$ {}_{c}S_{\mu}[f(t)](v) = R_{\mu}(v) = \frac{1}{v^2}\int_0^{\infty} exp\left(\frac{-t^{\mu}}{v\mu}\right) f(t)t^{\mu-1}dt\,, v > 0. \tag{8} $$

Definition 2.3. Let $0 < \mu \leq 1$, $f: [0,\infty) \to \mathbb{R}$ be real valued function. The conformable fractional Sawi transform for the conformable fractional-order derivative of the function $f \in \mathbb{C}_{\eta}(\eta \geq -1)$ is defined by

$$ {}_{c}S_{\mu}\left[T_{\mu}f(t)\right](v) = \frac{1}{v^{\mu}}R_{\mu}(v) - \sum_{k=0}^{\sigma-1}\left(\frac{1}{v}\right)^{\mu-(k-1)} f^{(k)}(0^{+}), \sigma - 1 < \mu \leq \sigma. \tag{9} $$

3. Conformable q-Sawi Homotopy Analysis Transform Method

We will introduce a new method. Consider the conformable time-fractional nonlinear partial differential equation (CTFNPDE) to explain the fundamental idea of Cq-SHATM:

$$ {}_{t}T_{\mu}w(x,t) + Aw(x,t) + Hw(x,t) = f(x,t), n - 1 < \mu \leq n, \tag{10} $$

where A is a linear operator, H is a nonlinear operator, $f(x,t)$ is a source term, and ${}_{t}T_{\mu}$ is a conformable time-fractional derivative of order μ.

Applying the conformable fractional Sawi transform to Eq. (10) and utilizing the initial condition, then we have

$$ \frac{{}_{c}S_{\mu}[w(x,t)]}{v^{\mu}} - \sum_{k=0}^{m-1}\left(\frac{1}{v}\right)^{\mu-(k-1)} w^{(k)}(x,0) = {}_{c}S_{\mu}[f(x,t) - Aw(x,t) - Hw(x,t)]. \tag{11} $$

Rearranging the last equation, then we get

$$ \begin{aligned} {}_{c}S_{\mu}[w(x,t)] - v^{\mu}\sum_{k=0}^{m-1}\left(\frac{1}{v}\right)^{\mu-(k-1)} w^{(k)}(x,0) + v^{\mu}\ {}_{c}S_{\mu}[Aw(x,t) + Hw(x,t)] \\ - v^{\mu}\ {}_{c}S_{\mu}[f(x,t)] = 0. \end{aligned} \tag{12} $$

With the help of HAM, we can describe the nonlinear operator for real function $\varphi(x,t;q)$ as follows:

$$ N[\varphi(x,t;q)] = {}_{c}S_{\mu}[\varphi(x,t;q)] - v^{\mu}\sum_{k=0}^{m-1}\left(\frac{1}{v}\right)^{\mu-(k-1)} \varphi^{(k)}(x,t;q)(0^{+}) + v^{\mu}\ {}_{c}S_{\mu}[A\varphi(x,t;q) $$

$$ +H\varphi(x,t;q)] - v^{\mu}\ {}_{c}M_{\alpha}[f(x,t)], \tag{13} $$

where $q\epsilon\left[0,\frac{1}{n}\right]$.

We construct a homotopy as follows:

$$(1 - nq)\ {}_cS_\alpha[\varphi(x,t;q) - w_0(x,t)] = hqH^*(x,t)H[\varphi(x,t;q)], \tag{14}$$

where, $h \neq 0$ is an auxiliary parameter and ${}_cS_\alpha$ represents conformable fractional Sawi transform. For $q = 0$ and $q = \frac{1}{n}$, the results of Eq. (14) are as follows:

$$\varphi(x,t;0) = w_0(x,t), \varphi\left(x,t;\frac{1}{n}\right) = w(x,t). \tag{15}$$

Thus, by amplifying q from 0 to $\frac{1}{n}$, then the solution $\varphi(x,t;q)$ converges from $w_0(x,t)$ to the solution $w(x,t)$.

Using the Taylor theorem around q and then expanding $\varphi(x,t;q)$, we get

$$\varphi(x,t;q) = w_0(x,t) + \sum_{i=1}^{\infty} w_m(x,t)q^m, \tag{16}$$

where

$$w_m(x,t) = \frac{1}{m!}\frac{\partial^m \varphi(x,t;q)}{\partial q^m}|_{q=0}. \tag{17}$$

Eq. (16) converges at $q = \frac{1}{n}$ for the appropriate $w_0(x,t)$, n and h. Then, we have

$$w(x,t) = w_0(x,t) + \sum_{m=1}^{\infty} w_m(x,t)\left(\frac{1}{n}\right)^m. \tag{18}$$

If we differentiate the zeroth order deformation Eq. (14) m-times with respect to q and we divide by $m!$, respectively, then for $q = 0$, we acquire

$${}_cS_\alpha[w_m(x,t) - k_m w_{m-1}(x,t)] = hH^*(x,t)\mathcal{R}_m(\vec{w}_{m-1}), \tag{19}$$

where the vectors are described by

$$\vec{w}_m = \{w_0(x,t), w_1(x,t), \dots, w_m(x,t)\}. \tag{20}$$

Applying the inverse conformable fractional Sawi transform to Eq. (20), we get

$$w_m(x,t) = k_m w_{m-1}(x,t) + h\left({}_cS_\alpha\right)^{-1}[H^*(x,t)\mathcal{R}_m(\vec{w}_{m-1})], \tag{21}$$

where

$$\mathcal{R}_m(\vec{w}_{m-1}) = {}_cS_\alpha[w_{m-1}(x,t)] - \left(1 - \frac{k_m}{n}\right)\frac{1}{v}w_0(x,t) + v^\mu\ {}_cS_\mu[Aw_{m-1}(x,t)$$

$$+ H_{m-1}(x,t) - f(x,t)], \tag{22}$$

and

$$k_m = \begin{cases} 0, & m \leq 1, \\ n, & m > 1. \end{cases} \tag{23}$$

Here, H_m^* is homotopy polynomial and presented by

$$H_m^* = \frac{1}{m!}\frac{\partial^m \varphi(x,t;q)}{\partial q^m}|_{q=0} \text{ and } \varphi(x,t;q) = \varphi_0 + q\varphi_1 + q^2\varphi_2 + \cdots. \tag{24}$$

Using Eqs. (21) - (22), we get

$$\begin{aligned} w_m(x,t) = (k_m + h)w_{m-1}(x,t) - \left(1 - \frac{k_m}{n}\right) w_0(x,t) \\ + \mathrm{h}\left({}_cS_\alpha\right)^{-1}\left[v^\mu \ {}_cS_\mu[Aw_{m-1}(x,t) + H_{m-1}(x,t) - f(x,t)]\right]. \end{aligned} \tag{25}$$

When Cq-SHATM is utilized, the series solution is given by

$$w(x,t) = \sum_{m=0}^{\infty} w_m(x,t)\left(\frac{1}{n}\right)^m. \tag{26}$$

4. Applications

Example 4.1. [45] Consider the conformable time-fractional Noyes Field model

$$\begin{cases} \dfrac{\partial^\mu \rho(x,t)}{\partial t^\mu} = \dfrac{\partial^2 \rho(x,t)}{\partial x^2} + \rho - \rho^2 - \delta\rho w(x,t), \\ \dfrac{\partial^\mu w(x,t)}{\partial t^\mu} = \dfrac{\partial^2 w(x,t)}{\partial x^2} - \lambda\rho w(x,t), \end{cases} \tag{27}$$

where $\lambda \neq 1$ and δ are positive constants, $x \in [-10,10], t \in [0,1], 0 < \mu \leq 1$, subject to initial conditions

$$\begin{cases} \rho(x,0) = \dfrac{1}{\left(\exp\left(\sqrt{\frac{\lambda}{6}}x\right)+1\right)^2}, \\ w(x,0) = \dfrac{(1-\lambda)\exp\left(\sqrt{\frac{\lambda}{6}}x\right)\left(\exp\left(\sqrt{\frac{\lambda}{6}}x\right)+1\right)}{\delta\left(\exp\left(\sqrt{\frac{\lambda}{6}}x\right)+1\right)^2}. \end{cases} \tag{28}$$

Cq-SHATM solution

Implementing the conformable fractional Sawi transform to Eqs. (27) and using Eqs. (28), then it is obtained as

$$\frac{{}_cS_\mu[\rho(x,t)]}{v} - \frac{\rho(x,0)}{v^2} = {}_cS_\mu\left[\frac{\partial^2 \rho(x,t)}{\partial x^2} + \rho - \rho^2 - \delta\rho w(x,t)\right], \tag{29}$$

$$\frac{{}_cS_\mu[w(x,t)]}{v} - \frac{w(x,0)}{v^2} = {}_cS_\mu\left[\frac{\partial^2 w(x,t)}{\partial x^2} - \lambda\rho w(x,t)\right]. \tag{30}$$

Rearranging Eqs.(29)-(30), then we have

$${}_cS_\mu[\rho(x,t)] = \frac{\rho(x,0)}{v} + v\ {}_cS_\mu\left[\frac{\partial^2\rho(x,t)}{\partial x^2} + \rho - \rho^2 - \delta\rho w(x,t)\right], \tag{31}$$

$${}_cS_\mu[w(x,t)] = \frac{w(x,0)}{v} + v\ {}_cS_\mu\left[\frac{\partial^2 w(x,t)}{\partial x^2} - \lambda\rho(x,t)w(x,t)\right]. \tag{32}$$

We define the nonlinear operators by using Eqs. (31)-(32), as

$$N^1[\varphi(x,t;q)\,] = {}_cS_\mu[\varphi(x,t;q)\,] - \frac{1}{v\left(\exp\left(\sqrt{\frac{\lambda}{6}}x\right)+1\right)^2}$$

$$+v\ {}_cS_\mu\left[\frac{\partial^2\varphi(x,t;q)}{\partial x^2} + \varphi(x,t;q) - \varphi^2(x,t;q) - \delta\varphi(x,t;q)\psi(x,t;q)\right], \tag{33}$$

$$N^2[\psi(x,t;q)\,] = {}_cS_\mu[\psi(x,t;q)\,] - \frac{(1-\lambda)\exp\left(\sqrt{\frac{\lambda}{6}}x\right)\left(\exp\left(\sqrt{\frac{\lambda}{6}}x\right)+1\right)}{\delta v\left(\exp\left(\sqrt{\frac{\lambda}{6}}x\right)+1\right)^2}$$

$$+v\ {}_cS_\mu\left[\frac{\partial^2\psi(x,t;q)}{\partial x^2} - \lambda\varphi(x,t;q)\psi(x,t;q)\right]. \tag{34}$$

By applying the proposed algorithm, the $m-th$ order deformation equations are defined by

$${}_cS_\mu[\rho_m(x,t) - k_m\rho_{m-1}(x,t)] = h\mathcal{R}_{1,m}[\vec{\rho}_{m-1}], \tag{35}$$

$${}_cS_\mu[w_m(x,t) - k_m w_{m-1}(x,t)] = h\mathcal{R}_{2,m}[\vec{w}_{m-1}], \tag{36}$$

where

$$\mathcal{R}_{1,m}[\vec{\rho}_{m-1}] = {}_cS_\mu[\vec{\rho}_{m-1}(x,t)] - \left(1-\frac{k_m}{n}\right)\frac{1}{v\left(\exp\left(\sqrt{\frac{\lambda}{6}}x\right)+1\right)^2}$$

$$-v\ {}_cS_\mu\left[\frac{\partial^2\rho_{m-1}(x,t)}{\partial x^2} + \rho_{m-1}(x,t) - \sum_{r=0}^{m-1}\rho_r(x,t)\rho_{m-1-r}(x,t) - \delta\sum_{r=0}^{m-1}\rho_r(x,t)w_{m-1-r}(x,t)\right], \tag{37}$$

$$\mathcal{R}_{2,m}[\vec{w}_{m-1}] = {}_{c}S_{\mu}[\vec{w}_{m-1}(x,t)] - \left(1-\frac{k_m}{n}\right)\frac{(1-\lambda)\exp\left(\sqrt{\frac{\lambda}{6}}x\right)\left(\exp\left(\sqrt{\frac{\lambda}{6}}x\right)+1\right)}{\delta v\left(\exp\left(\sqrt{\frac{\lambda}{6}}x\right)+1\right)^2}$$

$$-v\ {}_{c}S_{\mu}\left[\frac{\partial^2 w_{m-1}(x,t)}{\partial x^2} - \lambda\sum_{r=0}^{m-1}\rho_r(x,t)w_{m-1-r}(x,t)\right]. \quad (38)$$

On applying inverse conformable Sawi transform to Eqs. (35)-(36), then we have

$$\rho_m(x,t) = k_m\rho_{m-1}(x,t) + h\left({}_{c}S_{\mu}\right)^{-1}\{\mathcal{R}_{1,m}[\vec{p}_{m-1}]\}, \quad (39)$$

$$w_m(x,t) = k_m w_{m-1}(x,t) + h\left({}_{c}S_{\mu}\right)^{-1}\{\mathcal{R}_{2,m}[\vec{w}_{m-1}]\}. \quad (40)$$

By the use of initial conditions, then we obtain

$$\rho_0(x,t) = \frac{1}{\left(\exp\left(\sqrt{\frac{\lambda}{6}}x\right)+1\right)^2}, \quad (41)$$

$$w_0(x,t) = \frac{(1-\lambda)\exp\left(\sqrt{\frac{\lambda}{6}}x\right)\left(\exp\left(\sqrt{\frac{\lambda}{6}}x\right)+2\right)}{\delta\left(\exp\left(\sqrt{\frac{\lambda}{6}}x\right)+1\right)^2}. \quad (42)$$

To find the values of $\rho_1(x,t)$ and $w_1(x,t)$, putting $m = 1$ in Eqs. (39)-(40), then we obtain

$$\rho_1(x,t) = -\frac{2}{3}h\frac{t^{\mu}\exp\left(\frac{x\sqrt{6\lambda}}{6}\right)\left(\left(\left(\left(\frac{3}{2}+\lambda\right)\delta+\frac{3}{2}\lambda-\frac{3}{2}\right)\exp\left(\frac{x\sqrt{6\lambda}}{6}\right)+\left(-\frac{\lambda}{2}+3\right)\delta+3\lambda-3\right)}{\mu\delta\left(\exp\left(\frac{x\sqrt{6\lambda}}{6}\right)+1\right)^4}, \quad (43)$$

$$w_1(x,t) = \frac{5}{3}\frac{t^{\mu}(-1+\lambda)\lambda\exp\left(\frac{x\sqrt{6\lambda}}{6}\right)}{\mu\delta\left(\exp\left(\sqrt{\frac{\lambda}{6}}x\right)+1\right)^3}. \quad (44)$$

In the same way, if we put $m = 2$ in Eqs. (39)-(40), we can obtain the values of $\rho_2(x,t)$ and $w_2(x,t)$

$$w_2(x,t)=\frac{-5h(n+h)t^{\mu}(-1+\lambda)\lambda\exp\left(\frac{x\sqrt{6\lambda}}{6}\right)}{3\mu\delta\left(\exp\left(\sqrt{\frac{\lambda}{6}}x\right)+1\right)^3}+\frac{8}{9\mu^2\delta^2\left(\exp\left(\sqrt{\frac{\lambda}{6}}x\right)+1\right)^6}$$

$$\times\Bigg[h^2t^{2\mu}\lambda(-1+\lambda)\exp\left(\frac{x\sqrt{6\lambda}}{6}\right)\left(\frac{-9}{4}(-1+\lambda)(\delta-1)\exp\left(\frac{x\sqrt{6\lambda}}{6}\right)+\left(\left(\delta+\frac{9}{16}\right)\lambda+\frac{9}{16}\delta\right.\right.$$

$$\left.\left.-\frac{9}{16}\right)\exp\left(\frac{x\sqrt{6\lambda}}{6}\right)+\frac{3}{4}\left(-3+(3+\frac{\delta}{8}\right)\lambda+3\delta)\exp\left(\frac{x\sqrt{6\lambda}}{6}\right)-\frac{25}{32}\lambda\delta)\Bigg]. \tag{46}$$

In this way, the other terms can be found. So, the Cq-SHATM solutions of the Eq. (27) are given by

$$\rho(x,t)=\rho_0(x,t)+\sum_{m=1}^{\infty}\rho_m(x,t)\left(\frac{1}{n}\right)^m, \tag{47}$$

$$w(x,t)=w_0(x,t)+\sum_{m=1}^{\infty}w_m(x,t)\left(\frac{1}{n}\right)^m. \tag{48}$$

If we put $\mu=1, n=1,\ h=-1$ in Eqs. (47)-(48), then the obtained results

$$\sum_{m=1}^{M}\rho_m(x,t)\left(\frac{1}{n}\right)^m, \sum_{m=1}^{M}w_m(x,t)\left(\frac{1}{n}\right)^m$$

converges to the exact solutions

$$\rho(x,t)=\frac{\exp\left(\frac{5\lambda}{3}t\right)}{\left(\exp\left(\sqrt{\frac{\lambda}{6}}x\right)+\exp\left(\frac{5\lambda}{6}t\right)\right)^2}\, w(x,t)=\frac{(1-\lambda)\exp\left(\sqrt{\frac{\lambda}{6}}x\right)\left(\exp\left(\sqrt{\frac{\lambda}{6}}x\right)+2\exp\left(\frac{5\lambda}{6}t\right)\right)}{\delta\left(\exp\left(\sqrt{\frac{\lambda}{6}}x\right)+\exp\left(\frac{5\lambda}{6}t\right)\right)^2}$$

of the Eqs. (27) when $M\to\infty$.

Figure 1 shows the 3D graphs of $\rho(x,t)$ solution for Cq-SHATM, $w(x,t)$solution for Cq-SHATM, exact solutions of $\rho(x,t)$, $w(x,t)$ and absolute errors.

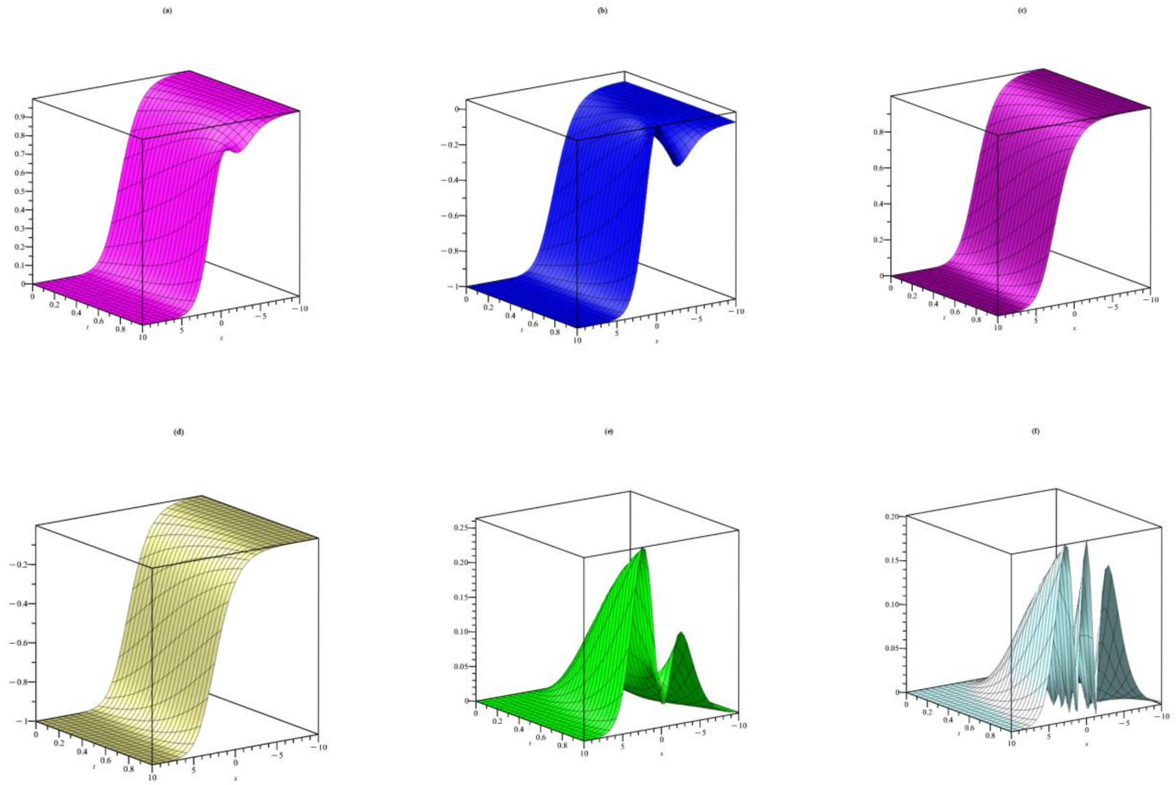

Figure 1. **(a)** Nature of $\rho(x,t)$solution with Cq-SHATM **(b)** Nature of $w(x,t)$solution with Cq-SHATM **(c)** Exact of $\rho(x,t)$ solution **(d)** Exact of $w(x,t)$ solution **(e)** Nature of absolute error=$|\rho_{exact} - \rho_{Cq-SHATM}|$ **(f)** Nature of absolute error=$|w_{exact} - w_{Cq-SHATM}|$ at $h = -1, n = 1, \mu = 1, \lambda = 3, \delta = 2$ for Eqs. (37).

Figure 2 depicts comparison 2D plots of $\rho(x,t)$ solution with Cq-SHATM, $w(x,t)$ solution with Cq-SHATM, and exact solutions for distinct μ values.

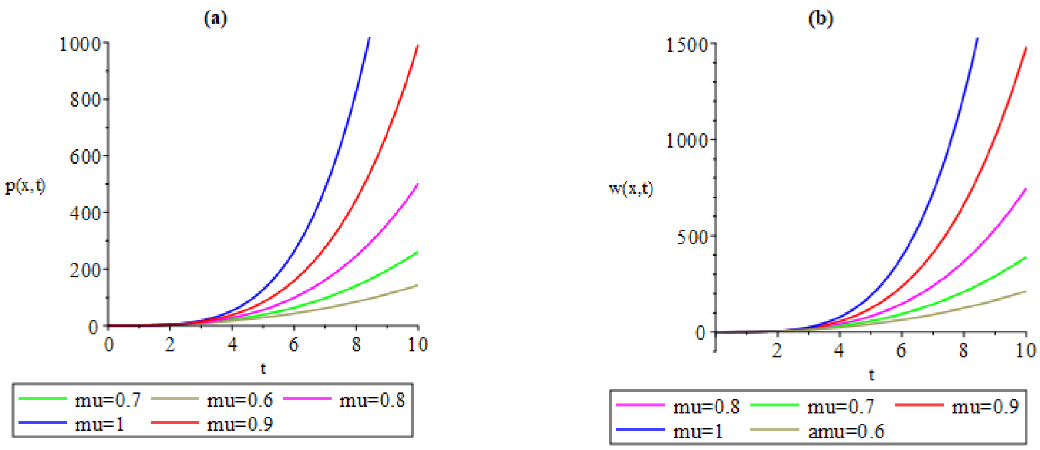

Figure 2. The comparison of the $\rho(x,t)$ solution with Cq-SHATM and exact solution **(b)** The comparison of the $w(x,t)$ solution with Cq-SHATM and exact solution at $h = -1, n = 1, x = 0.5,\ \lambda = 3, \delta = 2$ with different μ for Eqs. (37).

A comparison of the absolute error for $\rho(x,t)$ between Cq-SHATM and FRDTM [45] for Eq. (37) with $\mu = 1, \lambda = 3, \delta = 2, h = -1, n = 1$ is presented in Table 1.

x		t			
		0.001	0.003	0.005	0.007
Cq-SHATM	0.00	0.0001878902	0.0005660070	0.0009472246	0.0013315278
FRDTM		1.0149996100	1.0137464930	1.0124902750	1.0112309720
Cq-SHATM	1.00	0.0000976247	0.0002956422	0.0004973550	0.0007027695
FRDTM		0.8256007700	0.8248666560	0.8241288453	0.8233873339
Cq-SHATM	2.00	0.0000370568	0.0001128071	0.0001907491	0.0002708944
FRDTM		0.4254561817	0.4251463250	0.4248342767	0.4245200242
Cq-SHATM	3.00	0.0000114341	0.0000349498	0.0000593341	0.0000845935
FRDTM		0.1584645226	0.1583613457	0.1582572998	0.1581523788

Table 1. Comparison of absolute error for $\rho(x,t)$ between Cq-SHATM and FRDTM [45] for Eq. (37) with $\mu = 1, \lambda = 3, \delta = 2, h = -1, n = 1$.

Comparing the absolute errors for $w(x,t)$ for Eq. (37) with $\mu = 1, \lambda = 3, \delta = 2, h = -1, n = 1$ for Cq-SHATM and FRDTM [45] is provided in Table 2.

x		t			
		0.001	0.003	0.005	0.07
Cq-SHATM	0.00	3.9×10^{-7}	3.5×10^{-6}	9.7×10^{-6}	1.9×10^{-5}
FRDTM		1.0149996100	1.0137464930	1.0124902750	1.0112309720
Cq-SHATM	1.00	4.6×10^{-7}	4.1×10^{-6}	0.0000115353	0.0000226217
FRDTM		0.8256007696	0.8248666555	0.8241288453	0.8233873341
Cq-SHATM	2.00	2.7×10^{-7}	2.4×10^{-6}	6.8×10^{-6}	0.0000134002
FRDTM		0.4254561817	0.4251463250	0.4248342767	0.4245200246
Cq-SHATM	3.00	1.0×10^{-7}	9.6×10^{-7}	2.7×10^{-6}	5.3×10^{-6}
FRDTM		0.1584645226	0.1583613454	0.1582572998	0.1581523789

Table 2. Comparison of absolute error for $w(x,t)$ between Cq-SHATM and FRDTM [45] for Eq. (37) with $\mu = 1, \lambda = 3, \delta = 2, h = -1, n = 1$.

5. Conclusion (if necessary)

Figure 1 displays the three-dimensional graphs of the Cq-SHATM solutions $\rho(x,t)$ and $w(x,t)$, the exact solutions of $\rho(x,t)$ and $w(x,t)$, as well as the absolute errors for Eq. (27). Figure 2 illustrates a comparison of two-dimensional plots of the solutions $\rho(x,t)$ and $w(x,t)$ obtained using the Cq-SHATM, as well as the corresponding exact solutions for different values of μ. Table 1 presents a comparison of the absolute error for the function $\rho(x,t)$ between the Cq-SHATM and FRDTM methods [45] for Eq. (27), with the parameter values $\mu = 1, \lambda = 3, \delta = 2, h = -1$, and $n = 1$. Table 2 presents a comparison of the absolute errors of $w(x,t)$ for Eq. (27) with the given parameter values $\mu = 1, \lambda = 3, \delta = 2, h = -1$, and $n = 1$, between Cq-SHATM and FRDTM in [45]. The data presented in Tables 1-2 indicates that the Cq-SHATM exhibits a significantly lower error rate in comparison to the FRDTM in [45]. The results presented in Tables 1-2 demonstrate that the techniques proposed in this study yield significantly superior outcomes compared to those achieved through the utilization of FRDTM.

The present study aims to examine the behavior of conformable time-fractional Noyes Field model through the utilization of Cq-SHATM. In addition, the utilization of the MAPLE software has been employed to generate two-dimensional and three-dimensional graphs that illustrate the solutions to Eq. (37) for various values of $\mu = 1$. Observations have been made regarding the variations in the overall structure of the surface graphs produced by the Maple computational software for Eq. (37). Differences in the overall configuration of surface graphs generated by the Maple software for Eq. (37) have been observed. The study findings indicated that the approaches presented in Tables 1-2 produced results that are much better than those obtained through the use of FRDTM, with the independent variable being t and x being held at a constant value. A new hybrid method is proposed. This method is Cq-SHATM, which is a combination of the conformable Sawi transform and the q-homotopy analysis transform method. With this new method, new numerical solutions of the conformable Noyes-Field model have been obtained. It has been observed that this solution provides better results than the FRDTM existing in the literature. The effectiveness and advantages of the recently developed method for tackling nonlinear conformable time-fractional models have been acknowledged. The recent method proposed for the resolution of nonlinear conformable time-fractional models have been determined to possess distinct advantages and demonstrate notable efficacy.

Author Contributions

All authors contributed equally to this work. They all read and approved the final version of the manuscript.

Conflicts of Interest

The authors declare no conflict of interest.

References

[1] Miller, K. S., Ross, B. 1993. An introduction to the fractional calculus and fractional differential equations, Wiley, New York, 376 p.

[2] Podlubny, I. 1999. Fractional differential equations, mathematics in science and engineering, Academic Press, New York, 365 p.

[3] Baleanu, D., Diethelm, K., Scalas, E., Trujillo, J. J. 2012. *Fractional calculus: models and numerical methods,* World Scientific, London, 476 p.

[4] Povstenko, Y. 2015. Linear fractional diffusion-wave equation for scientists and engineers. Birkhäuser, Switzerland, 460 p.

[5] Ala, V. 2022. New exact solutions of space-time fractional Schrödinger-Hirota equation. Bulletin of the Karaganda university Mathematics series, 107(3), 17-24.

[6] Ala, V. 2023. Exact Solutions of Nonlinear Time Fractional Schrödinger Equation with Beta- Derivative. Fundamentals of Contemporary Mathematical Sciences, 4(1), 1-8.

[7] Baleanu, D., Wu, G. C., Zeng, S. D. 2017. Chaos analysis and asymptotic stability of generalized Caputo fractional differential equations. Chaos, Solitons & Fractals, 102, 99-105.

[8] Sweilam, N. H., Abou Hasan, M. M., Baleanu, D. 2017. New studies for general fractional financial models of awareness and trial advertising decisions. Chaos, Solitons & Fractals, 104, 772-784.

[9] Liu, D. Y., Gibaru, O., Perruquetti, W., Laleg-Kirati, T. M. 2015. Fractional order differentiation by integration and error analysis in noisy environment. *IEEE Transactions on Automatic Control*, *60(11)*, 2945-2960.

[10] Esen, A., Sulaiman, T. A., Bulut, H., Baskonus, H. M. 2018. Optical solitons to the space-time fractional (1+1)-dimensional coupled nonlinear Schrödinger equation. Optik, 167, 150-156.

[11] Veeresha, P., Prakasha, D. G., Baskonus, H. M. 2019. Novel simulations to the time-fractional Fisher's equation. Mathematical Sciences, 13(1), 33-42.

[12] Veeresha, P., Prakasha, D. G., Baskonus, H. M. 2019. New numerical surfaces to the mathematical model of cancer chemotherapy effect in Caputo fractional derivatives. Chaos: An Interdisciplinary Journal of Nonlinear Science, 29(1), 013119. https://doi.org/10.1063/1.5074099.

[13] Caponetto, R., Dongola, G., Fortuna, L., Gallo, A. 2010. New results on the synthesis of FO-PID controllers. Communications in Nonlinear Science and Numerical Simulation, 15(4), 997-1007.

[14] Mahgoub, M. A., & Mohand, M. (2019). The new integral transform "Sawi Transform". Advances in Theoretical and Applied Mathematics, 14(1), 81-87.

[15] Singh, G. P., & Aggarwal, S. (2019). Sawi transform for population growth and decay problems. *International Journal of Latest Technology in Engineering, Management & Applied Science*, *8*(8), 157-162.

[16] Higazy, M., Aggarwal, S., & Nofal, T. A. (2020). Sawi decomposition method for Volterra integral equation with application. *Journal of Mathematics*, *2020*, 1-13.

[17] Higazy, M., Aggarwal, S. (2021). Sawi transformation for system of ordinary differential equations with application. *Ain Shams Engineering Journal*, *12*(3), 3173-3182.

[18] Georgieva, A. T., & Pavlova, A. (2023). Application of the Double Fuzzy Sawi Transform for Solving a Telegraph Equation. *Symmetry*, *15*(4), 854.

[19] Gibbs, R. G. (1980). Traveling waves in the Belousov–Zhabotinskii reaction. *SIAM Journal on Applied Mathematics*, *38*(3), 422-444.

[20] Zhabotinsky Anatol M (2007) Scholarpedia 2(9):1435. https://doi.org/10.4249/scholarpedia

[21] Ray, S. S., & Bera, R. K. (2006). Analytical solution of a fractional diffusion equation by Adomian decomposition method. *Applied Mathematics and Computation*, *174*(1), 329-336.

[22] Adomian, G. (1994). Solving frontier problems of physics: the decomposition method, Springer. *Dordrecht*.

[23] Wazwaz, A. M., & Gorguis, A. (2004). An analytic study of Fisher's equation by using Adomian decomposition method. *Applied Mathematics and Computation*, *154*(3), 609-620.

[24] Das, S. (2009). Analytical solution of a fractional diffusion equation by variational iteration method. *Computers & Mathematics with Applications*, *57*(3), 483-487.

[25] Liao, S. J. (1995). An approximate solution technique not depending on small parameters: a special example. *International Journal of Non-Linear Mechanics*, *30*(3), 371-380.

[26] Shijun, L. (1998). Homotopy analysis method: a new analytic method for nonlinear problems. *Applied Mathematics and Mechanics*, *19*, 957-962.

[27] Liao, S. (2004). On the homotopy analysis method for nonlinear problems. *Applied mathematics and computation*, *147*(2), 499-513.

[28] Alkan, A. (2022). Improving homotopy analysis method with an optimal parameter for time-fractional Burgers equation. *Karamanoğlu Mehmetbey Üniversitesi Mühendislik ve Doğa Bilimleri Dergisi*, *4*(2), 117-134.

[29] Arikoglu, A., & Ozkol, I. (2007). Solution of fractional differential equations by using differential transform method. *Chaos, Solitons & Fractals*, *34*(5), 1473-1481.

[30] Merdan, M., Anaç, H., BEKİRYAZICI, Z., & Kesemen, T. (2019). Solving of Some Random Partial Differential Equations by Using Differential Transformation Method and Laplace-Padé Method. *Gümüshane Üniversitesi Fen Bilimleri Enstitüsü Dergisi*, *9*(1).

[31] He, J. H. (1998). Approximate analytical solution for seepage flow with fractional derivatives in porous media. *Computer Methods in Applied Mechanics and Engineering*, *167*(1-2), 57-68.

[32] He, J. H. (1999). Homotopy perturbation technique. *Computer methods in applied mechanics and engineering*, *178*(3-4), 257-262.

[33] He, J. H. (2003). Homotopy perturbation method: a new nonlinear analytical technique. *Applied and Mathematics Computation*, *135*(1), 73-79.

[34] Alquran, M., Al-Khaled, K., & Chattopadhyay, J. (2015). Analytical solutions of fractional population diffusion model: residual power series. *Nonlinear Stud*, *22*(1), 31-39.

[35] Kurt, A., Rezazadeh, H., Senol, M., Neirameh, A., Tasbozan, O., Eslami, M., & Mirzazadeh, M. (2019). Two effective approaches for solving fractional generalized Hirota-Satsuma coupled KdV system arising in interaction of long waves. *Journal of Ocean Engineering and Science*, *4*(1), 24-32.

[36] Şenol, M., Iyiola, O. S., Daei Kasmaei, H., & Akinyemi, L. (2019). Efficient analytical techniques for solving time-fractional nonlinear coupled Jaulent–Miodek system with energy-dependent Schrödinger potential. *Advances in Difference Equations*, *2019*(1), 1-21.

[37] Khuri, S. A. (2001). A Laplace decomposition algorithm applied to a class of nonlinear differential equations. *Journal of applied mathematics, 1,* 141-155.

[38] Akinyemi L (2019) q-Homotopy analysis method for solving the seventh-order time-fractional Lax's Korteweg–de Vries and Sawada–Kotera equations. Comput Appl Math 38(4):1–22.

[39] Akinyemi L, Iyiola OS, Akpan U (2020) Iterative methods for solving fourth- and sixth order time-fractional
Cahn–Hillard equation. Math Methods Appl Sci 43(7):4050–4074.

[40] El-Tawil, M. A., & Huseen, S. N. (2012). The q-homotopy analysis method (q-HAM). *Int. J. Appl. Math. Mech*, *8*(15), 51-75.

[41] El-Tawil, M. A., & Huseen, S. N. (2013). On convergence of the q-homotopy analysis method. *Int. J. Contemp. Math. Sci*, *8*(10), 481-497.

[42] Iyiola, O. S., Soh, M. E., & Enyi, C. D. (2013). Generalised homotopy analysis method (q-HAM) for solving foam drainage equation of time fractional type. *Mathematics in Engineering, Science & Aerospace (MESA)*, *4*(4).

[43] Iyiola, O. S. (2015). On the solutions of non-linear time-fractional gas dynamic equations: an analytical approach. *Int. J. Pure Appl. Math*, *98*(4), 491-502.

[44] Iyiola, O. S. (2016). Exact and approximate solutions of fractional diffusion equations with fractional reaction terms. *Progress in Fractional Differentiation and Applications*, *2*(1), 19-30.

[45] Akinyemi, L. (2020). A fractional analysis of Noyes–Field model for the nonlinear Belousov–Zhabotinsky reaction. *Computational and Applied Mathematics*, *39*(3), 175.

[46] Anaç, H. (2022). Conformable Fractional Elzaki Decomposition Method of Conformable Fractional Space-Time Fractional Telegraph Equations. *Ikonion Journal of Mathematics*, *4*(2), 42-55.

[47] Kartal, A., Anaç, H., Olgun, A. (2023). Numerical Solution of Conformable Time Fractional Generalized Burgers Equation with Proportional Delay by New Methods. *Karadeniz Fen Bilimleri Dergisi*, *13*(2), 310-335.

[48] Erol, A. S., Anaç, H., Olgun, A. (2023). Numerical Solutions of Conformable Time-Fractional Swift-Hohenberg Equation with Proportional Delay by the Novel Methods. *Karamanoğlu Mehmetbey Üniversitesi Mühendislik ve Doğa Bilimleri Dergisi*, *5*(1), 1-24.

[49] Khalil, R., Al Horani, M., Yousef, A., Sababheh, M. 2014. A new definition of fractional derivative. Journal of computational and applied mathematics, 264, 65-70.

[50] Abdeljawad, T. 2015. On conformable fractional calculus. Journal of computational and Applied Mathematics, 279, 57-66.

[51] Ala, V., Demirbilek, U., Mamedov, K. R. 2020. An application of improved Bernoulli sub-equation function method to the nonlinear conformable time-fractional SRLW equation. AIMS Mathematics, 5(4), 3751-3761.

[52] Gözütok, U., Çoban, H., Sağıroğlu, Y. 2019. Frenet frame with respect to conformable derivative. Filomat, 33(6), 1541-1550.